Electron Transfer and Supramolecular Studies of Amphiphilic Nickel(II)Pendant-Arm Polyazamacrocycles

A Thesis

Submitted to the Graduate Faculty

in Partial Fulfilment of the Requirements

for the Degree of

Master of Science

in the Department of Chemistry

Faculty of Science

University of Prince Edward Island

Jimmy E. Rowley

Charlottetown, P. E. I.

April, 2004

© 2004. J.E. Rowley

Reproduced with permission of the copyright owner. Further reproduction prohibited without permission.

National Library of Canada
Bibliothèque nationale du Canada

Acquisitions and Bibliographic Services
Acquisisitons et services bibliographiques

395 Wellington Street
Ottawa ON K1A 0N4
Canada

395, rue Wellington
Ottawa ON K1A 0N4
Canada

Your file Votre référence
ISBN: 0-612-93860-3
Our file Notre référence
ISBN: 0-612-93860-3

The author has granted a non-exclusive licence allowing the National Library of Canada to reproduce, loan, distribute or sell copies of this thesis in microform, paper or electronic formats.

L'auteur a accordé une licence non exclusive permettant à la Bibliothèque nationale du Canada de reproduire, prêter, distribuer ou vendre des copies de cette thèse sous la forme de microfiche/film, de reproduction sur papier ou sur format électronique.

The author retains ownership of the copyright in this thesis. Neither the thesis nor substantial extracts from it may be printed or otherwise reproduced without the author's permission.

L'auteur conserve la propriété du droit d'auteur qui protège cette thèse. Ni la thèse ni des extraits substantiels de celle-ci ne doivent être imprimés ou aturement reproduits sans son autorisation.

In compliance with the Canadian Privacy Act some supporting forms may have been removed from this dissertation.

Conformément à la loi canadienne sur la protection de la vie privée, quelques formulaires secondaires ont été enlevés de ce manuscrit.

While these forms may be included in the document page count, their removal does not represent any loss of content from the dissertation.

Bien que ces formulaires aient inclus dans la pagination, il n'y aura aucun contenu manquant.

Canada

Reproduced with permission of the copyright owner. Further reproduction prohibited without permission.

The author has agreed that the Library, University of Prince Edward Island, may make this thesis freely available for inspection. Moreover, the author has agreed that permission for extensive copying of this thesis for scholarly purposes may be granted by the professor or professors who supervised the thesis work recorded herein or, in their absence, by the Chair of the Department or the Dean of the Faculty in which the thesis work was done. It is understood that due recognition will be given to the author of this thesis and to the University of Prince Edward Island in any use of the material in this thesis. Copying or publication or any other use of the thesis for financial gain without approval by the University of Prince Edward Island and the author"s written permission is prohibited.

Requests for permission to copy or to make any other use of material in this thesis in whole or in part should be addressed to:

Chair of the Department of Chemistry

Faculty of Science

University of Prince Edward Island

Charlottetown, P. E. I.

Canada C1A 4P3

Reproduced with permission of the copyright owner. Further reproduction prohibited without permission.

SIGNATURE PAGE(S)

Not numbered in thesis

REMOVED

Table of Contents

Reproduced with permission of the copyright owner. Further reproduction prohibited without permission.

Reproduced with permission of the copyright owner. Further reproduction prohibited without permission.

Appendix D - X-Ray Crystallography Data

Reproduced with permission of the copyright owner. Further reproduction prohibited without permission.

Acknowledgements

I would especially like to thank Dr. Robert Haines for the incredible amount of time, effort, and guidance he has provided to me for this thesis and otherwise. I would like to thank the University of Prince Edward Island and its Chemistry Department for providing the program and facilities that enabled this project.

I would like to thank the chemistry department faculty for their patience. Thank you to the department technicians, Dawna Lund and Jill MacDonald, and secretary Sharon Martin for all their help.

I would like to thank Dr. Stan Cameron from Dalhousie University and Mr. Brian Moulton from the University of South Florida for the X-Ray crystal analysis and Mr. Tom Hunter for the electrospray mass spectrometry performed at Queen's University.

Finally, thanks to Diagnostic Chemicals Limited and NSERC for providing funding for this project.

Reproduced with permission of the copyright owner. Further reproduction prohibited without permission.

Glossary of Abbreviations

2,3,2-tet	1,4,8,11-tetraazaundezane
tacn	1,4,7-triazacyclononane
cyclam	1,4,8,11-tetraazacyclotetradecane
hmca	1-acetato-5,5,7,12,12,14-hexamethyl-1,4,8,11-tetraazacyclotetradecane
dap	1,3-diaminopropane
CD	Cyclodextrin
triflic acid	trifluromethanesulfonic acid
THF	tetrahydrofuran
ESMS	Electrospray Mass Spectrometry
BPI	Base Peak Intensity
L_n	n represents the number of carbons in the alkyl chain of the pendant-arm

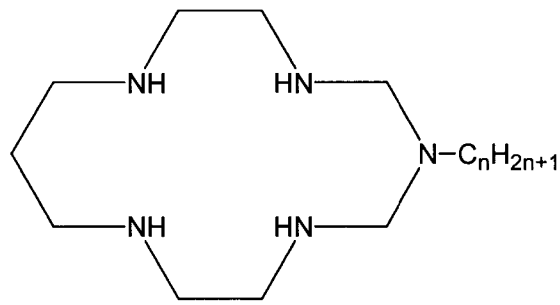

Reproduced with permission of the copyright owner. Further reproduction prohibited without permission.

Abstract

Three nickel(II) pentaazamacrocycles bearing pendant alkyl tails have been synthesized, and the crystal structure of one (bearing an octyl tail) is reported. The redox potentials of the complexes, for oxidation of the nickel(II) centre, is 0.72 V in all cases, indicating that the pendant alkyl tails have no effect on the redox site. The three compounds have been characterized by IR, CHN and ESMS. The kinetics of oxidation of the complexes by aqua(5,5,7, 12,12,14-hexamethyl-1,4,8,11-tetraazacyclotetradecane-1-acetato)nickel(III), $[Ni(hmca)(OH_2)]^{2+}$ have been studied. Only minimal differences in the rates for the three complexes are observed indicating that the tail length has only minimal effect.

The complexes have been studied with regard to their ability to form supramolecular complexes with α- and β-cyclodextrin. Results from ESMS and NMR show evidence of the formation of supramolecular complexes but cannot accurately quantify an association constant. The kinetics of oxidation of the complexes by the above oxidant in the presence of α- and β-cyclodextrin indicate that the rate is slowed by the presence of the cyclodextrins. A derived rate expression allows for association constants to be estimated from the oxidation kinetics.

The complexes are found to have unusual solvation properties in THF - water mixtures. The solubility of the complexes in various THF - water solution compositions have been studied.

The synthesis of a number of larger macrocycles (fifteen- and sixteen-membered) were attempted with little success. However, an attempt to synthesise a 16-membered macrocycle by a template method resulted in the formation of large crystals of *trans*-(bis-acetonitrilo)bis-(1,3-diaminopropane)nickel(II) perchlorate, $[Ni(dap)_2(MeCN)_2](ClO_4)_2$, which has been characterized

Reproduced with permission of the copyright owner. Further reproduction prohibited without permission.

cystallographically. The complex cation has two diaminopropane chelating ligands in a square planar arrangement about the nickel(II) ion, with two axially-coordinated acetonitrile ligands.

Reproduced with permission of the copyright owner. Further reproduction prohibited without permission.

Chapter 1 - Introduction

1.1 Macrocycles

Macrocyclic chemistry has become a major field of study over the past forty years. Macrocycles have been known and studied to some degree for one hundred years but it was not until the early 1960's that the work on macrocycles really intensified. It was in the 1960's that Neil Curtis in New Zealand and Darryl Busch in the U.S. took macrocyclic chemistry to the next level, especially in terms of their syntheses and that of their metal complexes.[1,2] Not coincidentally, the increase in macrocyclic study at this time was a result of the use of metal ions in the synthetic procedures. The use of a metal ion to aid in the synthesis of a macrocycle is commonly referred to as the template method[3] and will be discussed later.

Prior to 1960, there existed only a single well established category of synthetic macrocyclic ligands, that being the phthalocyanines. However, 1936 saw the production of the macrocyclic ligand 1,4,8,11-tetraazacyclotetradecane[4], commonly known as "cyclam", which is

Reproduced with permission of the copyright owner. Further reproduction prohibited without permission.

considered to be the matriarchal nitrogen donor macrocycle. The metal complexes of these compounds were not reported until the mid 1960's when Bosnich and Tobe formed complexes with nickel(II)[5] and cobalt(II)[6].

The phthalocyanines (Figure 1.1) have many of the characteristics that are common to macrocycles.[7] They are resistant to degradation, have high thermal stability, fastness to light and are stable in both acids and alkalis. They may act as catalysts for a variety of chemical transformations and have been used as models for a number of biochemical systems. Their copper(II) complexes have been used as blue and blue-green pigments and dyes. It is the wide range of interesting properties associated with the macrocycles and their metal complexes that make this field of study as large and diverse as it is. These characteristics will be discussed later.

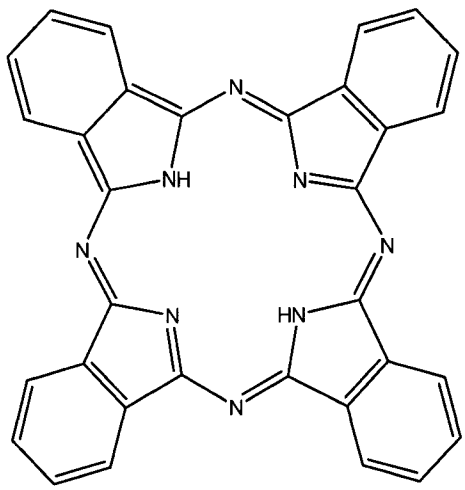

Figure1.1 Phthalocyanine

1.1.1 Definition of a Macrocycle

A macrocycle can be defined as a cyclic compound with a minimum of nine members, at least three of which are donor atoms. The donor atoms are usually nitrogen, oxygen, sulphur,

Reproduced with permission of the copyright owner. Further reproduction prohibited without permission.

phosphorus or arsenic, with oxygen and nitrogen being the most common. Macrocycles can consist of all the same donor atoms, for example the cyclam macrocycle has four nitrogen donor atoms, while the well known crown ethers contain only oxygen donor atoms. It is also possible for a macrocycle to possess a mixture of donor atoms. For example,1,4,7,10-tetraoxo-13-azacyclopentadecane has two nitrogens and two oxygen atoms.[8] The donor atoms can be divided into two categories. The first includes nitrogen, sulphur, phosphorus and arsenic donor atoms, which have shown themselves to strongly bind transition and heavy metals, but have less affinity for alkali and alkaline earth metal ions. The second group is comprised of the oxygen donor atom, such as those in crown ethers, whose ion affinities are the reverse of the first group.

There are many examples of macrocycles that can be found in nature whose function serve everyday purposes. Figure 1.2 below shows three such examples.

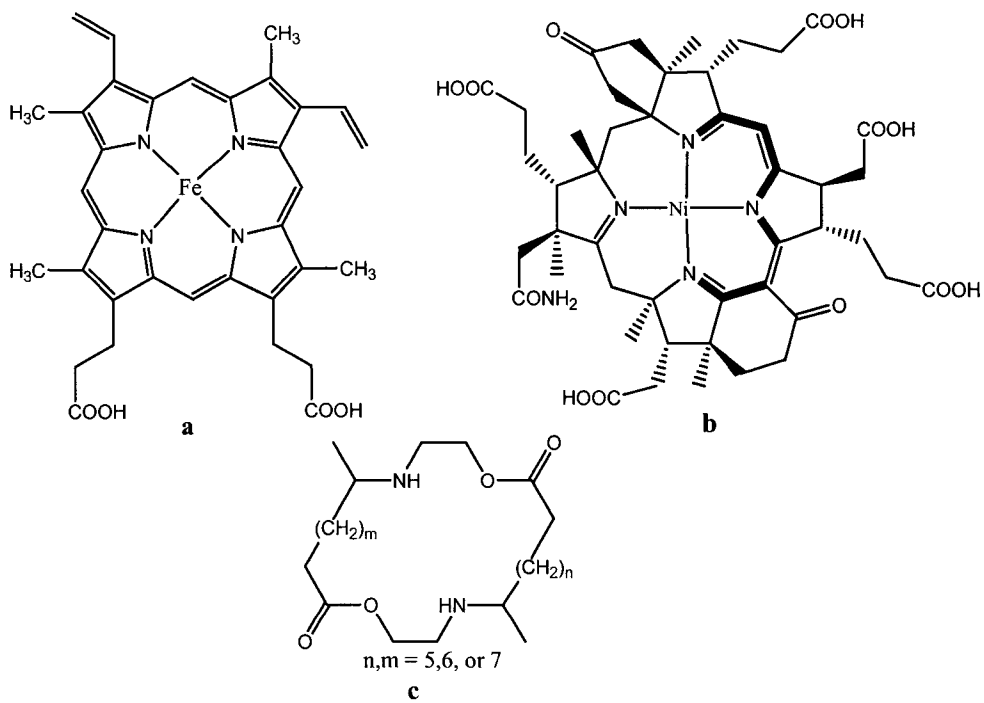

Figure 1.2 (a)Fe(II)protoporphyrin (b) Coenzyme F_{430} (c) Representative polyazamacrolide - one of a combination that constitute the pupal secretion of the *Epilachna borealis*

Reproduced with permission of the copyright owner. Further reproduction prohibited without permission.

Figure 1.2a shows Fe(II) protoporphryn IX,[9] which in association with its protein chains form haemoglobin and myoglobin, which are responsible for oxygen transport and storage in the body. Figure 1.2b shows coenzyme F_{430},[10] a key component of the enzyme methylcoenzyme reductase (MCR) which is involved in the methanogenesis cycle for the methanogens while Figure 1.2c shows one of the many polyazamacrolides that make up the pupal defensive secretions of the *Epilachna borealis* (Ladybird Beetle).[11]

1.1.2 Properties of Macrocycles and Their Metal Complexes

The study of macrocycles is broad because of the number of unique characteristics associated with macrocyclic ligands, especially regarding their complexation with metal ions. The spectral, electrochemical, structural, kinetic and thermodynamic aspects of macrocyclic complex formation have been well studied. Of particular interest is the high kinetic and thermodynamic stability associated with the metal ion - macrocycle complex. The reason for the increased stability is generally believed to be a result of the "macrocyclic effect".[12] The "macrocyclic effect" is an extension of the chelate effect which refers to the greater stability of complexes formed from multidentate ligands than from individual ligands. In the same manner, a metal ion - macrocycle complex offers greater stability than that of an analogous open chained multidentate ligand.

A macrocyclic ligand cannot dissociate from a metal ion in the stepwise manner that an acyclic ligand does. In a cyclic compound, there is no "end" of the chain at which the process commences as with acyclic ligands.

The term "macrocycle effect" was coined by Cabbiness and Margerum based on work on the enhanced stability of cyclic tetraamine ligands over their linear counterparts. Figure 1.3

Reproduced with permission of the copyright owner. Further reproduction prohibited without permission.

depicts the copper complexes of a macrocyclic ligand (Figure 1.3a) and a similar noncyclic ligand (Figure 1.3b).

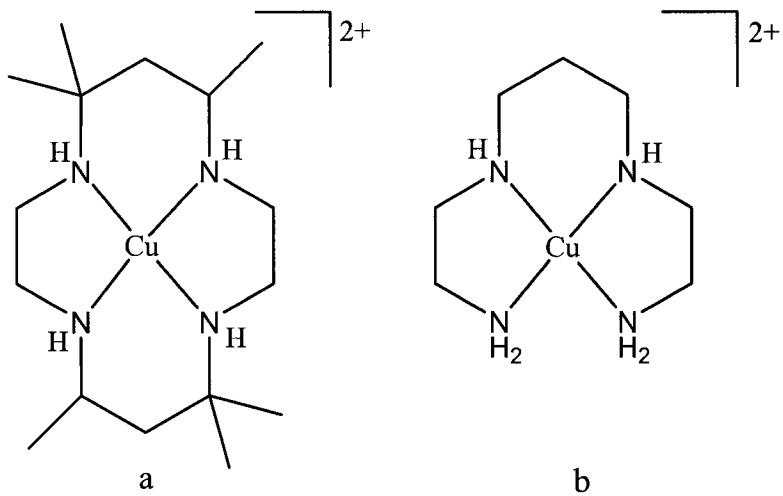

Figure 1.3 (a) 5,5,7,12,12,14-hexamethyl-1,4,8,11-tetraazacyclotetradecane nickel(II)
(b) 1,4,8,11-tetraazaundecane nickel(II)

The stability of the macrocyclic complex is approximately 10^4 times higher than the open chained complex. The chelate effect partially explains the difference as there are more chelate rings formed in the macrocyclic complex, but does not explain such a large difference. Similar results were also reported by Kodama and Kimura[13] with the copper(II) complexes of a smaller twelve-membered macrocycle (cyclen) and its open chained ligand (2,2,2-tet). Thus, the macrocyclic effect was the term used to describe the large increase in stability. This effect has also been observed in a number of nickel(II) complexes[14] and crown ethers.[15] The chelate effect is of entropic origin[16] but an enthalpic or entropic origin for the macrocyclic effect is not clear.

Macrocycles have been known to stabilize metals in higher oxidation states. For example, saturated tetraazamacrocycles[17] are often used to oxidize nickel(II) to nickel(III) as the nickel(III) complex is stabilized by the macrocyclic ligand. Generally, this does not occur for non-cyclic ligands although some work has been reported on the oxidation of nickel(II) to nickel(III) as a

Reproduced with permission of the copyright owner. Further reproduction prohibited without permission.

complex with the 2,3,2-tet ligand which is the open-chained analog to the cyclam ligand.[18] Lower oxidation states can also be stabilized with unsaturated macrocycles as they are able to accept electron density from the metal.[19]

1.1.3 Pendant-Arm Macrocycles

Apart from the range of macrocycles that exist based on just the size of the ring and the number of donor atoms, the ability to append side arms to the macrocycle can also change both the structure and functionality of the macrocycles. The pendant arms may be attached directly to the backbone chain or to the donor atoms. Figure 1.4 shows 1,4,7-triazacyclononane with pendant arms attached to the nitrogen donor atoms (a) or to both the donor atoms and non donor atoms (b).[20]

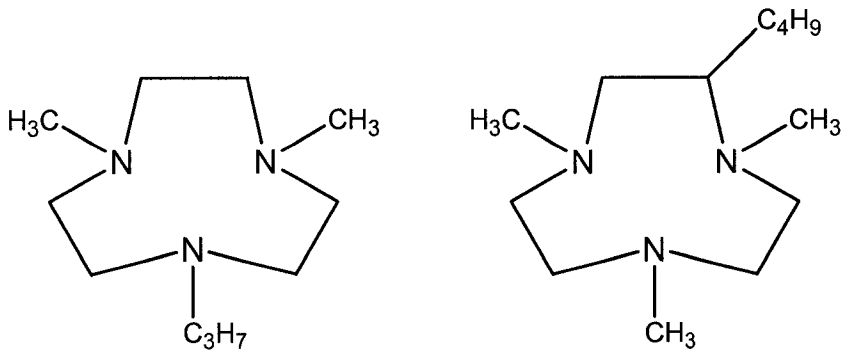

Figure 1.4 (a)1,4,-dimethyl-7-propyl-1,4,7-triazacyclononane (b) 2-butyl-1,4,7-trimethyl-1,4,7-butyltriazacyclononane

Pendant-arm macrocycles may be synthesized in two ways. The first is by modifying an already existing macrocycle and the second is directly from the non-cyclic precursors.[21] As mentioned, the functionality of a macrocycle can be altered by the addition of a pendant-arm, which can affect the nature of its metal ion coordination. Thus, macrocycles with functionalised

Reproduced with permission of the copyright owner. Further reproduction prohibited without permission.

pendant-arms have the possibility of having axial coordination with the metal ion, even in cases where the pendant-arms incorporate weak donor functions. This allows for greater stability in the complex. An example of this is the 5,5,7,12,12,14-hexamethyl-1,4,8,11-tetraazacyclotetradecane-1,8-*bis*-acetatonickel(II) where both carboxylate pendant-arms can coordinate to the nickel(II) centre forming a six-coordinate complex.[22]

The addition of pendant-arms to the macrocycle provides a great number of potential structures for the macrocyclic ring. Apart from the point of attachment of the pendant-arm to the ring, structural diversity stems from the size of the pendant-arm, in terms of both length and bulkiness, as well as the number of pendant-arms incorporated in the ring.

The macrocyclic pendant-arms may consist of flexible components such as alkyl chains or alkyl tails containing any number of functional groups including amines,[23] alcohols[24] and amides.[25] The macrocyclic ligand may also consist of more rigid pendant-arms including those with aromatic components.[26] In some cases the pendant-arms may actually attach in two places on the ring forming a bridge,[27] thus imparting greater rigidity to the ring.

Another common type of pendant-arm is one containing carboxylic acid functional groups which are often coordinated to the metal ion.[28] These systems are similar to a class of ligands known as complexones. The most common example of a complexone is EDTA (ethylenediaminetetraacetic acid). These macrocycles can complex with a wide variety of metal ions, forming complexes with both non-transition metal and transition metal ions, and are more stable than the corresponding EDTA complexes.

Reproduced with permission of the copyright owner. Further reproduction prohibited without permission.

1.1.4 Metal Ion Selectivity

The stability of a metal-ion macrocyclic complex is affected by a number of the macrocycle's structural characteristics. Therefore, it is possible to design macrocycles that fit better with one metal ion than another, making it possible for the macrocycle to selectively bind one metal over another. This provides the opportunity to develop specific metal ion sensors by manipulating the structure of the macrocycle.

There are a number of ring characteristics that will affect the complex stability with a specific metal ion. These include: the type and position of the donor atom; electronic and structural aspects associated with the ligand's backbone; formal charges and/or the presence/absence of dipoles; and the substitution of pendant-arms on the macrocycle.[29] The most important and obvious effect on stability arises from the size of the ring. The closer the fit between the metal ion and the size of the ring cavity, the better the fit, thus the higher the stability of the complex. If the ring is too big, the metal ion will "rattle" while a ring that is too small will not let the metal ion fit inside.

Another important characteristic of the macrocycle that greatly influences the stability of a metal ion complex is the nature of the donor atoms. It has been established that oxygen donor atoms favour alkali and alkaline earth metals over transition metal ions, while azamacrocycles generally form more stable complexes with the transition metal ions. Sulfur atoms have been shown to have a high affinity for silver(I) and mercury(II). However titanium and lead actually behave more like the alkali and alkaline earth metals.[30]

One option that has been used recently in the development of metal ion recognition is the use of mixed donor macrocycles. One reason for this is that macrocycles containing only nitrogen donor atoms generally have very high stability constants for most metal ions, whereas

Reproduced with permission of the copyright owner. Further reproduction prohibited without permission.

the mixed donor rings have lower overall stability, but high stability for select metal ions.

Another factor that can influence the stability of a metal ion macrocycle complex is the substitution on the ring. It is generally believed that N-alkylation of a macrocycle lowers the stability of the complex due to increased steric hindrance on complex formation.[31]

1.1.5 Synthesis of Macrocycles

The synthetic methods for macrocycles depend greatly upon a number of factors. These include mainly the size and structure of the desired macrocycle, but the nature of the donor atoms as well as the conjugation within the ring are also important. Another factor to be considered is whether it is the free macrocyclic ligand or the metal ion-macrocycle complex that is desired.

There are two basic methods for forming macrocycles. Macrocycles may be synthesized directly from their precursor and open chained components *via* standard organic reactions or they may use a metal ion as a template around which the ring is pieced together. Both methods have been well established and each have been used to produce a large number of synthetic macrocycles. However the path originally chosen does not limit the results as it is sometimes possible to remove or exchange the metal after synthesis,[32] and the addition of a metal to an already synthesized macrocycle is commonplace.

1.1.5.a Synthesis in the Absence of a Metal

The macrocycle ligand is in fact an organic moiety and can be considered as a cyclic version of its open-chained analogue. Thus, its synthesis without the use of a metal templating ion follows common organic reaction mechanisms. Often the synthesis of a macrocycle in this manner is comprised of a multi-step organic procedure including the use of protecting groups[33]

Reproduced with permission of the copyright owner. Further reproduction prohibited without permission.

that must be added prior to synthesis and removed after ring closure. As is often the case with multi-step processes, the yields tend to decrease from step to step, resulting in an overall less than desirable yield.

1.1.5.b Metal Directed Synthesis

It was previously stated that it was the introduction of the metal ion into the synthetic process that propelled synthetic macrocyclic chemistry to another level in the 1960's. During the synthetic procedure the metal ion acts as a foundation around which the macrocycle can be built. The reactions that occur to join the individual components are the general organic mechanisms and are not significantly altered by the presence of the metal.

The first synthetic macrocycle synthesized using the metal template occurred serendipidously in 1928 when an iron(II) complex with phthalimide was produced as a side product during a reaction to prepare phthalimide using phthalic anhydride and ammonia in an iron vessel.[34] However, it was a discovery by Curtis[35] in 1960 that led to the use of metal template procedures as commonplace for macrocycle synthesis and re-ignited an interest in macrocyclic ligand chemistry. The Curtis synthesis first occurred when a yellow crystalline product was observed to result from the reaction of $[Ni(1,2\text{-diaminoethane})_3]^{2+}$ and dry acetone. The product was shown to be a mixture of isomeric tetraazamacrocyclic complexes.[36,37]

There are two possible roles for the metal ion in the template synthesis.[38] The first is a thermodynamic template effect where the metal ion will remove the macrocyclic product from an equilibrium, for example, between reactants and products. The formation of the macrocycle is promoted as the metal complex and the ion act to shift the equilibrium. The second role is the kinetic template effect where the metal will direct the steric course of condensation such that the

Reproduced with permission of the copyright owner. Further reproduction prohibited without permission.

formation of the required cyclic product is facilitated. Often times the actual role of the metal ion is more complex than just one of the above and may involve aspects of both.

1.2 Cyclodextrins

Supramolecular chemistry is a field of study that has developed greatly in recent years to become a very diverse and intensly studied area of chemistry, drawing interest from many different disciplines. A variety of disciplines converge to study the chemical, physical and biological features of supramolecular complexes.

Supramolecular chemistry, in its simplest explanation, is the study of the interaction between two or more species that combine to form complexes without forming a covalent bond. Supramolecular chemistry was referred to as "chemistry beyond the molecule" by Jean Marie Lehn[39] as a definition phrase, but other definition phrases also include " the chemistry of the noncovalent bond" and "nonmolecular chemistry".[40] In supramolecular chemistry, molecules are to supramolecular complexes as atoms are to molecules in molecular chemistry.[41] In more technical terms, supramolecular chemistry is the study of chemical species of high complexity that are held together and organized by means of intermolecular or noncovalent binding interactions. The forces which hold the supramolecular complexes together typically include electrostatic interactions, hydrogen bonding, van der Waals interactions, ion pairing, π-acid to π-base interactions, metal to ligand binding, solvent reorganisation and partially-formed-and-broken covalent bonds (transition states).[39,42,48,49]

The roots and concepts of supramolecular chemistry can be traced back to almost the beginning of modern chemistry. However, it was truly in the late 1960's and early 1970's that the field of study, as it is known today, developed. The field started with selective binding of alkali

Reproduced with permission of the copyright owner. Further reproduction prohibited without permission.

metal cations by natural as well as synthetic macrocyclic and macropolycyclic ligands, the crown ethers and cryptands.[42] This time period corresponds to the earlier discussed developments in macrocyclic chemistry, in particular, macrocyclic ligands for metal cations, that occurred in the early to mid 1960's.

As mentioned, supramolecular chemistry has ties to a variety of disciplines. It has ties to organic chemistry and synthetic procedures for receptor construction, to coordination chemistry and metal ion-ligand complexes, to physical chemistry and the experimental and theoretical studies of interactions, to biochemistry with substrate binding and recognition.[39,42,48,49]

Some examples of supramolecular chemistry include substrate binding to enzymes, drugs that adhere to their targets and signals propagating between cells.[39] Chemically, examples of supramolecular complexes include host-guest complexes formed with host molecules such as cryptands,[43] crown ethers,[44] cucurbituril[45] and cyclodextrins.[46] It is the last that is of particular importance in the current work.

1.2.1 Structure and Properties of Cyclodextrins

The first reference to a cyclodextrin dates back well over a hundred years to 1891.[47] Cyclodextrins are cyclic oligosaccharides which are comprised of D(+)-glucopyranose subunits in the chair conformation. The glucopyranose subunits are linked by α-1,4 glycosidic bonds.[48] The number of subunits in the cyclodextrin can vary but the most common cyclodextrins are formed with six, seven and eight glucopyranose units which are named α-,β-, and γ- cyclodextrin respectively. Amongst these, it is the α- and β- cyclodextrins that have been the most studied. Figure 1.5 below provides a schematic representation of α-cyclodextrin. β-cyclodextrin has a similar but larger structure as it incorporates an additional glucose unit.

Reproduced with permission of the copyright owner. Further reproduction prohibited without permission.

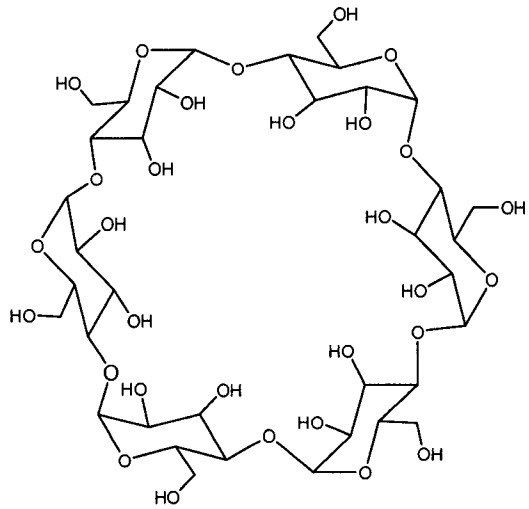

Figure 1.5 α-cyclodextrin

It is rare to form cyclodextrins consisting of less than six glucopyranose units because the steric hindrance is great. Cyclodextrins with greater than eight units are possible and have been studied[49], however, they provide little increase in size compared to the γ- cyclodextrin for reasons that will be discussed.

The individual units link in such a manner to provide the cyclodextrin with a structure that is often referred to as a truncated cone. From a visual standpoint, cyclodextrins resemble lamp shades in that they consist of a conic wall with openings at both ends, one opening being larger than the other. The narrower face or opening is the primary face consisting of primary hydroxyl groups while the wider secondary face consists of secondary 2- and 3- hydroxyl groups. It is the increased freedom of rotation allowed in the primary hydroxyl groups that produces the smaller opening. The linking of the glucopyranose units occurs edge-to-edge with all the units pointing inwards towards the cavity. The size of this cavity is influenced by the number of glucopyranose units. The figure below shows the diameter of the cavity for α-, β- and γ-cyclodextrin. As the

Reproduced with permission of the copyright owner. Further reproduction prohibited without permission.

number of units in the cyclodextrin increases, the diameter of the cavity increases correspondingly. However, for cyclodextrins with greater than eight units the cavity actually collapses or folds on itself producing an effective cavity that is smaller than that of the γ-cyclodextrin.[47]

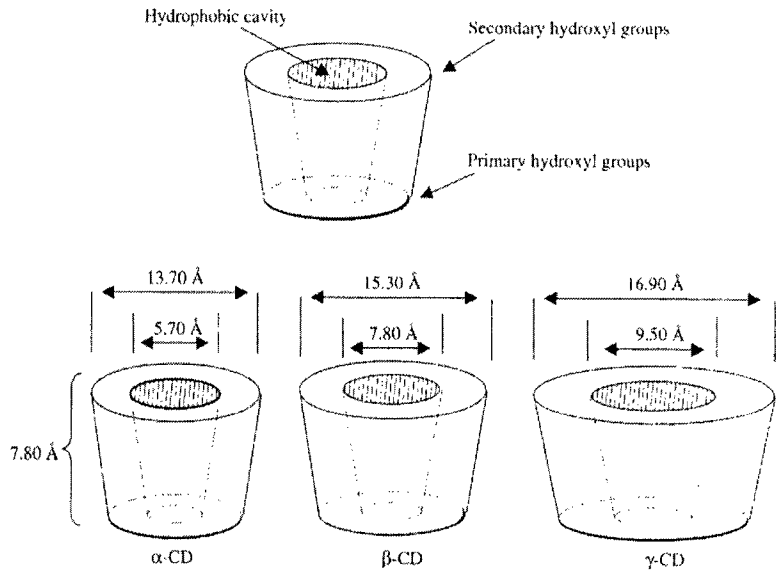

Figure 1.6 Dimensions and characteristics of α- β- and γ-cyclodextrin. Taken from "Supramolecular Chemistry"[50]

The cavity of the cyclodextrin is hydrophobic/lipophilic in nature while the exterior is hydrophilic as a result of the hydrophilic alcohol functionality. These opposing characteristics produce the unique complexation ability of cyclodextrins in aqueous solutions. The interior cavity, being hydrophobic, will attract other molecules of similar character to the inside of the cyclodextrin producing a host-guest complex.

Reproduced with permission of the copyright owner. Further reproduction prohibited without permission.

1.2.2 Uses of Cyclodextrins

As a result of the unique properties associated with cyclodextrins, in particular to the host-guest complexes they can form, there are numerous uses for cyclodextrins in the chemical, pharmaceutical, food and other industrial areas.

In the pharmaceutical industry, cyclodextrins are used as solubilizers, diluents or to improve the physical and chemical properties of the drugs. They are also used as drug carriers to increase the bioavailability of drugs with low solubilities.[51] They are used to stabilize flavours and fragrances in such industries as food, cosmetic, toiletry and tobacco. They can sometimes be used to help eliminate undesirable tastes, microbiological contaminants and other undesired components.[52,49]

In the chemical industry, it is their ability to form supramolecular complexes that is most exploited. They are used as catalysts to improve the selectivity of reactions as well as for the separation and purification of industrial scale products.[53] They can be used to increase the solubility of a guest molecule, to modify the reactivity of a compound or to change spectral properties and so may make particular measurements feasible for a compound when they would otherwise not be possible. They also have many uses in the field of analytical chemistry.[48]

1.2.3 Cyclodextrins as Hosts in Supramolecular Complexes

Cyclodextrins have become one of the most popular molecules used as host molecules in these host-guest complexes. Their use can be traced to a number of reasons. First, they are one of the cheapest commercially available hosts. More importantly though, they have a number of chemical properties which have already been discussed that make them attractive.

It is the ability to form the host-guest complexes that is probably the most characteristic

Reproduced with permission of the copyright owner. Further reproduction prohibited without permission.

property of cyclodextrins. They can form host-guest complexes with a wide range of molecules, from organic or inorganic compounds of neutral or ionic nature to noble gases.

Probably the most common host-guest complex formed with cyclodextrin is that where the guest is a smaller organic molecule. The stability of such a complex is dependent upon a number of variables. The strength of the interactions that hold the complex together, including van der Waals interactions, hydrogen bonding, and the release of water molecules from the cavity in the complex formation process will influence the stability of the complex. The polarity of the guest molecule plays an important role, since any guest that is more polar than water will not produce a favourable situation to displace the water molecules from the cyclodextrin cavity. However, with organic molecules as guests, this is rarely a concern. The obvious factor that influences complex stability is the size of the host and the guest. The better the fit between the two, the more stable the complex will be. Temperature can also play a role as increasing temperature will decrease the stability of a complex. Since host-guest complex formation is known to be exothemic,[49] the binding constant (K) will decrease with increasing temperature, according to the Van't Hoff equation ($\Delta G° = -RTlnK° = \Delta H° - T\Delta S°$). Also, there is an increase in the size of the cyclodextrin at elevated temperature, reducing the closeness of fit between the host and the guest. This principle is used in the synthesis of rotaxanes *via* the "slippage" method, where the solution is heated to allow the cyclodextrin to enlarge and pass over the stopper-group of the rotaxane.[54] The formation of the host-guest complex can have significant effects on the properties of both the host and the guest. The guest molecule can undergo changes to its solubility, chemical reactivity, pK_a value, diffusion, electrochemical properties, as well as its spectral properties.[48]

The changes to the spectral properties are of particular interest to many in the field as they

Reproduced with permission of the copyright owner. Further reproduction prohibited without permission.

are often used to measure the binding constant of a host-guest complex. It is the binding constant that indicates the stability of the supramolecular complex. In the simplest case, that of one guest molecule (G) and one host molecule (H) forming a 1:1 host-guest complex, the binding constant (K) can be expressed as follows:

$$G + H \rightleftharpoons G{:}H \qquad K = \frac{[G{:}H]}{[G][H]} \qquad \text{(Equation 1.1)}$$

This expression becomes increasingly more complex with the possibility of forming higher-ordered complexes such as 1:2, 2:1, 2:2 or even larger cluster complexes. As these complexes generally form simultaneously with the 1:1 complex, the resulting binding constant expression becomes large and complex. The complexity and nature of the binding constant expression may also be influenced by the method used to measure the constant. Some of the spectral methods commonly used include NMR,[55] UV-vis,[56] and fluorescence[57] spectroscopies. The ability of any of these methods relies on the complex having the necessary characteristics (e.g., to use fluorescence, the guest molecule must fluoresce).

1.3 Kinetics

Kinetics is a very powerful tool in the study of reactions and their mechanisms. Simply stated, kinetics is the study of reaction rates by the measurement of change in concentration of reactants or products as a function of time. However, it provides much more information than just the speed of the reaction. Kinetics can be divided into physical kinetics and chemical kinetics. Physical kinetics deals with physical phenomena such as diffusion and viscosity while chemical kinetics deals with chemical transformations. This includes both covalent and noncovalent bond changes.

Reproduced with permission of the copyright owner. Further reproduction prohibited without permission.

The use of chemical kinetics to study reaction mechanisms is probably one of its most important applications. The rate of a reaction is dependent on the concentration of the reactants, by studying the effect that concentration has on the rate, the rate law may be determined. While it is impossible to unequivocally prove any single mechanism, the mechanism can be shown to be true based on overwhelming evidence (data) supporting its case.[58]

While the above use is the most common application for chemical kinetics, there are many other applications. Kinetics can also be used to optimize process conditions. Examples include organic synthesis, analytical reactions or chemical manufacturing.[59] Kinetics can also be used for testing rate theories, measuring equilibrium constants, analysing of solutions including mixtures of solutes and the measurement of solvent properties that depend on rates.

Kinetics can be used to determine activation energy, enthalpy and entropy of chemical reactions. This can be achieved through the knowledge that a chemical reaction is affected by temperature. The most commonly observed behaviour is that observed by Arrhenius 100 years ago[60] and is expressed in the Arrhenius equation (equation 1.2) which relates the rate constant to the temperature and the activation energy, E_a.

$$k = Ae^{(-Ea/RT)} \qquad \text{(Equation 1.2)}$$

Plotting ln k *versus* 1/T produces a linear graph where the slope ($-E_a/R$) provides a measure of the activation energy for the reaction.

The activation enthalpy and entropy, $\Delta H^{\ddagger}$ and $\Delta S^{\ddagger}$ respectively, can be determined from an Eyring plot based on the equation below derived from transition state theory, where ln(k/T) is plotted against 1/T.

$$\ln (k/T) = \ln (\kappa /h) + \Delta S^{\ddagger}/R - \Delta H^{\ddagger}/RT \qquad \text{(Equation 1.3)}$$

Reproduced with permission of the copyright owner. Further reproduction prohibited without permission.

Kinetics is used to follow many types of chemical reactions, including ligand substitution reactions, equilibria, complex formation and redox. In a redox reaction, the oxidation state of at least two species changes. Redox mechanisms can be grouped into two categories, inner-sphere and outer-sphere. Outer-sphere electron transfer reactions are the simplest and most straightforward as the coordination shells of the reactants remain intact. Inner-sphere electron transfer reactions are characterized by changes in the coordination shells of the reactants, for example the reaction may require a bond to be formed between the two reactants *via* a bridging ligand[61] prior to electron transfer.

1.3.1 Kinetics Measurements

The method used in the kinetic study to determine a rate for a given reaction is completely dependent on the nature or the reaction. Specifically, the method depends on the speed at which the reaction occurs. Reactions can occur rapidly (milliseconds or less) or can take hours. Reactions that occur on the time scale of minutes to hours or longer can be measured using conventional batch methods. Reactants A and B are mixed and samples are taken from the solution and measured at different time intervals. The solution may be directly measured in the reaction vessel to save time which is important for reactions that occur in minutes.

This method becomes less favourable as the time scale decreases for several reasons. The shorter the timescale for the reaction the higher the amount of the reaction that is missed during the mixing and measuring. Secondly, batch methods ignore three stages of mixing that are negligible for longer time scales but become increasingly important as the time scale decreases. The three stages include the time it takes to add one reactant to the other, the time it takes to mix the solution to homogeneity and time that elapses from the point when solutions are completely

Reproduced with permission of the copyright owner. Further reproduction prohibited without permission.

mixed until the measurement begins. The most important problem though is that no kinetic data are gathered until the detection begins. This means that for very fast reactions, they may be complete or essentially complete before detection even starts. Reactions that occur on such time scales need a different method.

Flow methods are commonly used for very fast reaction as they operate in the time range of one millisecond to ten seconds and serve to extend the range of conventional batch mixing. In flow methods, the two reactants are forced under pressure to a mixing chamber where they are mixed and pushed along to a detection chamber. Here, the change in concentrations can be monitored as a function of time, often using UV-vis spectrometry. The most popular of the flow methods is stopped-flow. In stopped-flow kinetics, the reactants are mixed as described above. After the reactants are mixed and the solution is moved along to the detection chamber, the flow of the solution is stopped which then triggers the detection of the mixed solution. Figure 1.7 shows a simple schematic of a stopped flow system.

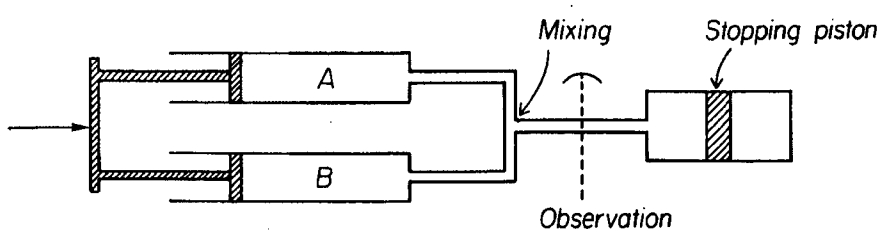

Figure 1.7 Simple schematic diagram of a stopped-flow apparatus. Taken from "Chemical Kinetics"[62]

The dead-time for this method, *i.e.* the time elapsed from mixing of the reactants until observation can begin, is typically 3-5 ms. In cases where this poses a problem, continuous flow may be used as it can measure reactions with half lives as short as 1 ms. The concept is similar to stopped-flow but the solution is not stopped and detection occurs as the solution passes through

Reproduced with permission of the copyright owner. Further reproduction prohibited without permission.

the observation chamber.

Kinetics have been studied over nearly all spectral regions and it represents the most powerful and utilized method of monitoring kinetic reactions. Fluorescence, NMR and IR have all been used to study kinetics, but the UV and visible regions are the most used, especially for transition metal complexes as the majority of such complexes undergo a spectral change in one or both of these regions during a reaction.[63]

1.3.2 Marcus Relationships

Marcus theory[64] can be a very useful tool in determining the mechanistic character of a redox reaction. It allows for the estimation of rate constants based on the theoretical self-exchange of each reactant as well as their cross-reaction. The theory requires that the activation process for each reactant be independent of the other, and that the self-exchange and cross-reactions have the same activated species. Thus, it follows that Marcus theory may only be applied to an outer-sphere electron transfer mechanism as an inner-sphere mechanism does not meet these requirements.

The Marcus equation is derived from the following three reactions which include the self-exchange reaction for each reactant, as well as the cross reactions.

$$A^- + B \xrightarrow{k_{AB}} A + B^- \qquad \text{(Equation 1.4)}$$

$$A^- + A \xrightarrow{k_{AA}} A + A^- \qquad \text{(Equation1.5)}$$

$$B^- + B \xrightarrow{k_{BB}} B + B^- \qquad \text{(Equation1.6)}$$

Reproduced with permission of the copyright owner. Further reproduction prohibited without permission.

From these reactions, Marcus theory states that for an outer-sphere electron transfer mechanism, the rate constant for the cross-reaction (k_{AB}) is related to the self-exchange rate constants for each of the components, k_{AA} and k_{BB}, and the equilibrium constant (K_{AB}) for the cross reaction according to the following expression:

$$k_{AB} = (k_{AA}k_{BB}K_{AB}f_{AB})^{½} \qquad \text{(Equation 1.7)}$$

where

$$\log f_{AB} = \frac{(\log K_{AB})^2}{4\log\left(\frac{k_{AA}k_{BB}}{Z^2}\right)} \qquad \text{(Equation 1.8)}$$

The Z term is a measure for the collision frequency for the ions in solution. Generally it is assumed that f_{AB} is approximately unity if the reactants are not of opposite charges and the K_{AB} term is not large.[65] When these assumptions are made the equation reduces to what is commonly known as the simplified Marcus equation:

$$k_{AB} = (k_{AA}k_{BB}K_{AB})^{½} \qquad \text{(Equation 1.9)}$$

1.4 Objectives of Present Work

The work presented in this thesis focuses on the synthesis and study of pendant-arm-macrocyclic complexes with the potential for use as heavy metal sensors as well as guests in supramolecular complex formation. The synthesis of a range of macrocycles are attempted with the idea of complexing different metals. The pendant-arms can be used in two ways. First, they

Reproduced with permission of the copyright owner. Further reproduction prohibited without permission.

are able to change the metal binding properties of the macrocycles. Second, the pendant-arm is required to form the supramolecular complexes with the cyclodextrins as the macrocyclic ring is itself too large.

Macrocycles with nickel(II) centres are prepared to allow for the oxidation study of the macrocyclic complexes. The kinetic studies along with NMR, electrochemistry and electrospray mass spectrometry are used to probe the interaction between the pendant-arm macrocycles and both α-and β-cyclodextrin.

1.4.1 Macrocycle Synthesis

The size of a macrocycle and the nature of its donor atoms are important factors influencing the ability of a macrocycle to form a stable complex with a metal ion. The fourteen-membered macrocycles are known to be a good fit for the first row transition metals while the late transition and heavy metals prefer a larger ring cavity. As well, the heavier metals form more stable complexes when the donor atoms are oxygen or sulphur compared to the first row-transition metals which prefer nitrogen.

The (attempted) synthesis of the macrocycles was carried out with the goal of being able to complex a number of metal ions including the larger second and third row transition metals and to be used as guest in the formation of supramolecular complexes with cylcodextrins. The fourteen-membered tetraaza pendant-arm macrocycles were a possibility with modifications, as were the larger fifteen- and sixteen-membered macrocycles that were attempted. The fourteen-membered macrocycle can have additional pendant-arms attached at the nitrogen atoms of the ring. When these pendant-arms bear chelating atoms, the effective size of the ring cavity can be increased as the metal can be positioned slightly out of the plane of the ring and be chelated to the

Reproduced with permission of the copyright owner. Further reproduction prohibited without permission.

ring nitrogens as well as the chelating atoms of the pendant-arms. The addition of pendant-arms with carboxylate groups should also vary the affinity of the macrocyclic ligand for different metals. The presence of non-coordinating pendant-arms is important as they are needed to interact with the cyclodextrin molecules.

Synthesis of azamacrocycles that bear pendant-arms or can be modified to have pendant-arms attached have been attempted. The addition of pendant-arms to the nitrogen atom of the macrocyclic backbone has been well established[66] and those methods have been used in this lab. It is possible to add a pendant-arm that can coordinate to the metal or one that is hydrophobic in nature and will function as a guest in the supramolecular complexes.

The macrocycle itself is too large to fit inside the cyclodextrin but the pendant-arm allows for the complex formation. The formation of supramolecular complexes between cyclodextrins and alkyl chains has been established but the present system, with the alkyl chain attached to a nickel macrocyclic complex is novel.

The complex formation is studied *via* a number of the typical methods used for studying supramolecular systems. Electrochemistry, NMR and ESMS all provide useful information about the complex formation but it is the study of the redox kinetics of the nickel(II/III) metal centre that is the main tool used here to determine the association constants for the formed complexes.

Reproduced with permission of the copyright owner. Further reproduction prohibited without permission.

1.4.2 Kinetics to Probe $[NiL_{4,8,12}]^{2+}$ - Cyclodextrin Interaction

As previously discussed, the study of electron transfer kinetics is very useful in determining the parameters of a reaction mechanism. In particular, the redox kinetics of transition metals have been widely studied. The nickel(II/III) redox couple[67] is one of the most explored examples. In most cases, the nickel(II/III) couple is present as part of a metal-macrocycle complex, because the increased stability imparted by the macrocycle is required to stabilize the nickel(III) form. It is for this reason that the nickel(II/III) redox couple, as part of an azamacrocyclic complex, was chosen to for use in this study. It is important to have a well understood system to act as a probe to study the interaction that occurs between these macrocyclic complexes and the cyclodextrin molecules.

The work on the supramolecular complexes formed between the nickel(II) pendant-arm macrocycles and cyclodextrins stems from supposedly simple oxidation study of the nickel(II) bibracchial macrocycles with peroxodisulfate.[68] The nickel(II) complexes with pendant-arms in excess of a few carbon atoms in length were insoluble in aqueous media. The cyclodextrins were used to increase the solubility of the nickel(II) compounds to allow for the kinetic study. However, the cyclodextrins proved to have a significant effect on the reaction rates. The presence of the cyclodextrin had the effect of making the relationship between the rate constant and the oxidant concentration linear for the oxidation kinetics with the peroxodisulfate. This is a departure from the accepted curved relationship between the observed rate and the oxidant concentration that occurs in transition metal systems that are oxidized by peroxodisulfate.[69]

This phenomenon lead to an interest in studying the interaction that occurs between the nickel pendant-arm complexes and the cyclodextrin. While there has been some work done using kinetics for the study of binding constants,[70] the use of the nickel(II/III) redox couple of a metal-

Reproduced with permission of the copyright owner. Further reproduction prohibited without permission.

macrocycle complex is a novel approach.

Previous work[71] developed a reaction mechanism that could be used to approximate the binding constant from the system involving the nickel(II) macrocycle appended with two alkyl tails and cyclodextrins using peroxodisulfate as the oxidant. This is an extremely cumbersome system, producing a complex rate law as seen below:

$$k_{obs} = 2\left[\frac{k_1K'_{ip} + k_2K''_{ip}K_1[CD] + k_3K'''_{ip}K_1K_2[CD]^2}{(1+K_1[CD]+K_1K_2[CD]^2)(1+K'_{ip}[S])(1+K''_{ip}[S])(1+K'''_{ip}[S])}\right][S] \qquad \text{(Equation 1.10)}$$

where $S = S_2O_8^{2-}$.

This mechanism is too cumbrous to be used to estimate the binding association constants between the nickel(II) complex and the cyclodextrin. The complexity of the system stems from two main factors. First, the reductant is of negative charge. This results in ion-pairing between the oxidant and reductant. Second, the presence of two pendant-arms on the macrocycle requires that approximations must be made that include the complex forming supramolecular complexes with one or two cyclodextrin molecules.

Previously, the system was simplified by removing one of the pendant arms which reduced the complexity of the system by simplifying the cyclodextrin - macrocycle interactions. However the resulting rate law (Equation 1.11) still required significant approximations to produce an expression that could reasonably be used to estimate an association constant.

$$k_{obs} = \frac{2K_{ip}[S_2O_8^{2-}]}{1+K_{ip}[S_2O_8^{2-}]}\left[\frac{k_1+k_2K[CD]}{1+K[CD]}\right] \qquad \text{(Equation 1.11)}$$

This work further reduces the system to a point where the complexity of the system is

Reproduced with permission of the copyright owner. Further reproduction prohibited without permission.

minimized. The use of an oxidant of positive charge removes the ion-pairing component of the previously discussed systems. This leaves a supramolecular system that will have the interaction between only one alkyl chain pendant-arm and cyclodextrin. The rate expression for this case is far more manageable, and will be derived later (see equation 3.21).

Reproduced with permission of the copyright owner. Further reproduction prohibited without permission.

Chapter 2 - Experimental

2.1 Synthesis of Nickel(II) Complexes

The synthesis of all of the nickel(II) compounds reported here were carried out *via* the template method.

2.1.1 Synthesis of $[NiL_{4,8,12}](ClO_4)_2$

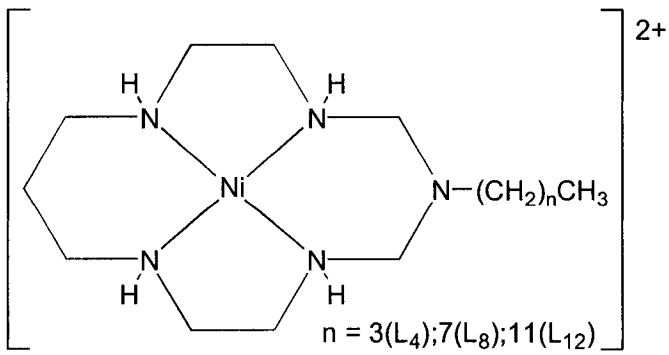

Figure 2.1 1-butyl/octyl/dodecyl-1,3,6,9,12-pentaazacyclotetradecane nickel(II) cation

Reproduced with permission of the copyright owner. Further reproduction prohibited without permission.

The synthesis of these compounds is an adaptation of a literature method.[72] A common procedure was used for all three complexes, described as follows:

2,3,2-Tetraazaaundecane (2,3,2-tet) (1.61 g, 0.0100 mol, 1 eq.) was weighed into a 100 mL round bottom flask and 15 - 20mL of methanol was added along with 3 mL of 37% HCHO. (**Note:** it is important that there is methanol present before adding the HCHO. Without the methanol, the HCHO reacts immediately with the 2,3,2-tet to form a polymeric substance.) The solution was then set up to reflux.

After approximately 10 minutes of refluxing (solution now had a yellow colour), $NiCl_2 \cdot 6H_2O$ (2.38 g, 0.0100 mol, 1 eq.), dissolved in 15 mL methanol, and n-butyl/octyl/dodecyl amine (0.73 g for the NiL_4 complex, 0.0100 mol, 1 eq.) were added to the refluxing solution along with an additional 5-10 mL of methanol. This solution was then refluxed overnight. The dark green/brown solution was cooled to room temperature and vacuum filtered. To the filtrate, approximately 3 mL of 60% $HClO_4$ was added to precipitate the desired compound.

The solution was placed in the fridge for several hours to enhance precipitation. The solution containing orange precipitate was suction filtered and washed with ice cold ethanol and diethyl ether and allowed to dry.

On occasion, the first yield actually produced a purple precipitate corresponding to the complex with chlorides coordinated in the axial positions. The purple powder was dissolved in warm methanol and an additional 2-3 mL 60 % $HClO_4$ was added to precipitate the desired compound. The same method as above was then continued from this point.

The $[NiL_4](ClO_4)_2$ was recrystallized from hot methanol while the $[NiL_8](ClO_4)_2$ and $[NiL_{12}](ClO_4)_2$ were recrystallized from an 80 - 90 % (weight by weight) THF-water solution. The yields for these compounds were: $[NiL_4](ClO_4)_2$ - 0.5750 g (11.1 %); $[NiL_8](ClO_4)_2$ -

Reproduced with permission of the copyright owner. Further reproduction prohibited without permission.

0.5989 g (10.5 %); $[NiL_{12}](ClO_4)_2$ - 0.6522 g (10.4 %).

Elemental analysis calculated for $[NiL_4](ClO_4)_2$: C 30.32%, H 6.07%, and N 13.60%; found C 30.19%, H 5.94%, and N 13.39%. For $[NiL_8](ClO_4)_2$: C 35.75%, H 6.88%, and N 12.16%; found C 34.81%, H 6.66%, and N 12.16%. For $[NiL_{12}](ClO_4)_2$: C 40.21%, H 7.55%, and N 11.17%; found C 40.15%, H 7.59%, and 11.05%.

Caution ! Compounds containing perchlorate anions must be regarded as potentially explosive and should be handled with caution.

2.1.2 Synthesis of trans-$[Ni(dap)_2(MeCN)_2](ClO_4)_2$

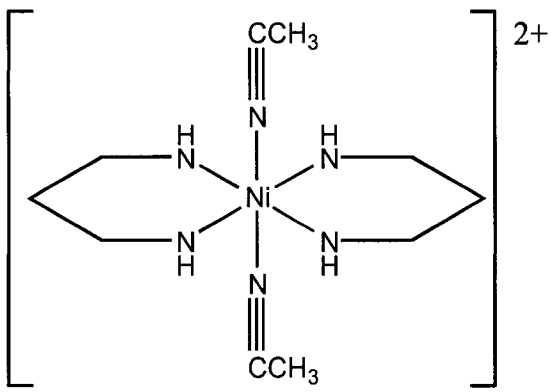

Figure 2.2 *trans*-(*bis*-acetonitrilo)*bis*-(1-3-diaminopropane)nickel(II) cation

Tris-(1,3-diaminopropane)nickel(II) perchlorate (2.50g, 0.00521 mol, 1 eq.) was mixed with approximately 50 mL (excess) of butylmethyl ketone and left in a covered round bottom flask. The mixture was stirred overnight to help the solid dissolve. As not all the solid dissolved, the liquid was decanted and the solid left to dry. Once dry, a minimum amount of acetonitrile was used to dissolve the solid. Once dissolved, the previously decanted liquid was slowly returned into the solution, producing a brownish colour. The solution was allowed to stand and

Reproduced with permission of the copyright owner. Further reproduction prohibited without permission.

crystals began to form on the bottom of the flask after several days. The solution was then left for a further two days to induce further precipitation. The resulting solution was vacuum filtered and washed with diethyl ether and left on suction to dry. The product was recrystallized from acetonitrile. The yield for this product was 0.8241g (32.8%).

2.1.3 Synthesis of $[Ni(dap)_3](ClO_4)_2$

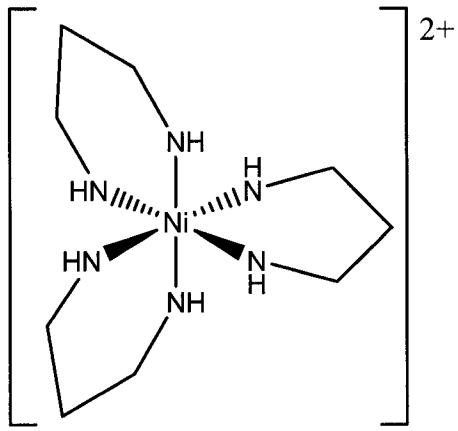

Figure 2.3 *Tris*-(1,3-diaminopropane) nickel(II) cation

1,3-diaminopropane, "dap", (2.23g, 0.0300 mol, 3 eq.) was weighed into a round bottom flask and 15 mL of methanol was added to dissolve the solid. Nickel(II) perchlorate hexahydrate (3.66g, 0.0100 mol, 1eq.), dissolved in 15 mL of methanol was added dropwise over a period of 45 - 60 minutes to the stirring solution of 1,3-diaminopropane. The addition of the nickel(II) perchlorate immediately produced a purple coloured solution. By the time that the last of the nickel(II)perchlorate was added, a purple precipitate was already formed on the bottom of the flask. This solution was placed in the fridge to maximize the precipitation. The solution was then filtered under reduced pressure and the precipitate washed with ice cold ethanol and diethyl

Reproduced with permission of the copyright owner. Further reproduction prohibited without permission.

ether and left to dry. The final product was a light purple powder. The synthesis produced a high yield of 4.177 g (88.1 %).

2.2 Attempted Synthesis of Larger Azamacrocycles for Larger Metals

There were a number of attempts made to synthesize macrocyclic ligands with larger cavity sizes to better fit the larger heavy metal ions. Attempts were made using both the template method as well as direct synthesis. The following outlines a number of the synthetic attempts made.

2.2.1 Synthesis of 2,2,4,10,10,12-hexamethyl-1,5,9,13-tetraazacyclohexadecane

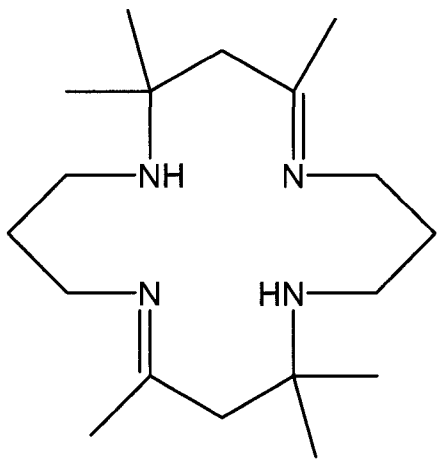

Figure 2.4 2,2,4,10,10,12-hexamethyl-1,5,9,13-tetraazacyclohexadecane

1,3-diaminopropane (25.1 g, 0.331mol) was weighed into a large round bottom flask. To this 500 mL of HPLC grade acetone was added to dissolve the 1,3-diaminopropane. Once dissolved, 60 % $HClO_4$ (53.0 g 0.316 mol) was added dropwise to the reaction. Upon addition of the $HClO_4$ the solution began to darken. Once all the $HClO_4$ was added, the solution was placed

Reproduced with permission of the copyright owner. Further reproduction prohibited without permission.

in the fridge to induce precipitation. The solution turned dark brown in colour, unfortunately no precipitate formed. Removal of the solvent did not produce a finite nickel(II) macrocycle complex.

2.2.2 Synthesis of 1-butyl-1,3,6,9,13-pentaazacyclopentadecane nickel(II)perchlorate

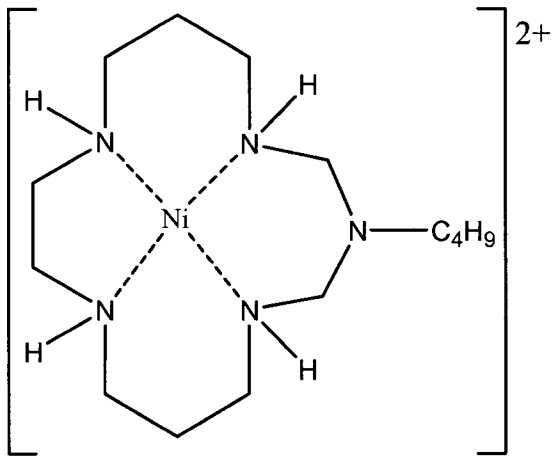

Figure 2.5 1-butyl-1,3,6,9,13-pentaazacyclopentadecane nickel(II) cation

3,2,3-Tetraazadodecane (3,2,3-tet) (1.77 g, 0.0100 mol, 1 eq.) was weighed into a round bottom flask and 15 mL of methanol was added. Approximately 3 mL (excess) of 37% HCHO was added to this solution which was then set to reflux. After refluxing for approximately 10 - 15 minutes, a brownish tint could be observed for the solution. At this point the $NiCl_2 \cdot 6H_2O$ (2.39 g, 0.010 mol, 1 eq), dissolved in about 20 mL of methanol, was added along with *n*-butylamine (0.73 g, 0.010 mol, 1 eq). This resulted in a greenish-blue colour. After approximately one hour of refluxing, the solution appeared to be a cloudy green colour. An additional 10 mL of methanol was added and the solution was left to reflux overnight.

After a day of refluxing, the solution was a cloudy brownish colour with light green

Reproduced with permission of the copyright owner. Further reproduction prohibited without permission.

deposits on the surface and bottom of the flask. The solution was left to reflux for a further 24 hours.

The reflux was stopped and the solution left to cool. Once at room temperature, the solution was suction filtered to remove the green precipitate. Approximately 3 mL of $HClO_4$ was added to the filtrate which was placed in the fridge overnight to induce precipitation. When removed from the fridge, there was some precipitate present consisting of a heterogenous white material. No definitive nickel(II) macrocycle could be isolated from the precipitate.

2.2.3 Synthesis of 2,2,4,10,10,12-hexamethyl-1,5,9,13-tetraazacyclohexadecane nickel(II)perchlorate

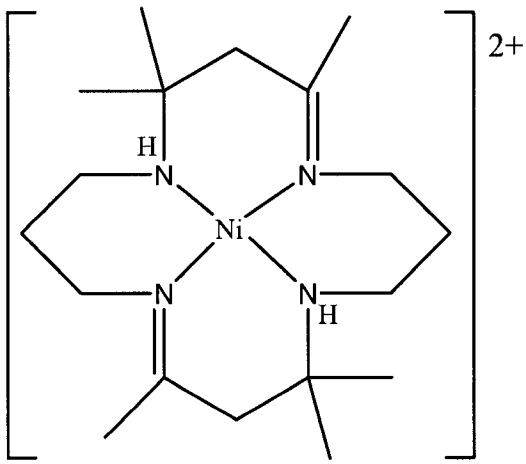

Figure 2.6 2,2,4,10,10,12-hexamethyl-1,5,9,13-tetraazacyclohexadecane nickel(II) cation

Tris-(1,3-diaminopropane) nickel(II) perchlorate (5.01g, 0.0100 mol, 1 eq.) was dissolved in HPLC grade acetone (100 mL) and left in a stoppered flask. This solution was left sitting for several weeks. At this point there were only a few small specks of precipitate detectable. The cover was removed in order to reduce the volume of the solution. The solution was a very dark

Reproduced with permission of the copyright owner. Further reproduction prohibited without permission.

yellow/brownish colour.

After sitting for a further two weeks, there appeared to be some crystalline precipitate on the bottom of the flask. The solution was suction filtered and washed with ice-cold diethyl ether.

The resulting solid was brown with a yellow tint, The solution was washed with acetone and left to dry overnight in hopes that this would remove the brownish colour (presumably from the polymeric substance that commonly forms in such procedures).

The dried solid now appeared to have more of a yellow colour to it but there was still significant brownish colour.

This time the solid was washed with dichloromethane and left to dry to remove the brown colour, which was unsuccessful. Other solvents were attempted to remove the brownish colour but unfortunately nothing appeared effective. No definitive nickel macrocycle could be isolated from the reaction mixture.

2.3 Kinetics

Stock solutions of $NaClO_4$, $HClO_4$, and trifluoromethanesulfonic acid (triflic acid) were prepared for kinetic runs. The concentration of the $NaClO_4$ solution was determined by passing the solution through a Dowex-50W-X8 cation exchange column and titrating the eluent with 0.1000 $mol \cdot dm^{-3}$ NaOH (Acculute). The concentrations of the $HClO_4$ and triflic acid were analysed by standard titration methods with 0.1000 $mol \cdot dm^{-3}$ NaOH (Acculute).

All the kinetic runs were carried out using pseudo-first order conditions. This is achieved by having one of the reactants in a minimum ten-fold excess over the other. This allows for one of the reactants (that held in excess) to maintain an approximately "constant" concentration. In all kinetic runs conducted, the $[NiL_{4,8,12}]^{2+}$ reductant was held in excess.

Reproduced with permission of the copyright owner. Further reproduction prohibited without permission.

All UV-vis spectra were collected using a Hewlett Packard 8453 Diode Array UV-vis spectrometer on a Pentium 75 MHz computer. A 1-cm pathlength quartz cuvette was used, thermostated using a Haake circulating water bath. Data were collected and fitted using the UV-vis Chemstation Rev.A.06.04 software package.

The stopped-flow kinetics measurements were made using a HI-TECH Scientific SF-61 DX2 Double Mixing Stopped-Flow spectrophotometer, thermostated with an RM6 LAUDA refrigerated recirculating water bath. The data were collected and fitted using HI TECH Scientific's "KinetAsyst" software on a Dell 466MHz Pentium III computer.

2.3.1 Preparation of Oxidizing Agent ($[Ni(hmca)(OH_2)]^+ \rightarrow [Ni(hmca)(OH_2)]^{2+}$)

The oxidizing agent used for the outer-sphere kinetic runs was aqua-5,5,7,12,12,14-hexamethyl-1,4,8,11-tetraazacyclotetradecane-1-acetatonickel(III) perchlorate, $[Ni(hmca)(OH_2)]^{2+}$ which can be seen in figure 3.6 (section 3.3.1).

The nickel(II) form of the oxidant used in these kinetic studies was previously synthesized and available in our laboratory.

The $[Ni(hmca)(OH_2)]^+$ was oxidized from nickel(II) to nickel(III) using a stoichiometrically deficient solution of $[Co(OH_2)_6]^{3+}$ (or $Co^{3+}_{(aq)}$). The $[Ni(hmca)(OH_2)]^+$ was held in slight excess (5 - 10%) to ensure that all the $Co^{3+}_{(aq)}$ was consumed, leaving none remaining in solution to oxidize $[NiL_{4,8,12}]^{2+}$ in a spurious side reaction.

The $Co^{3+}_{(aq)}$ solution was prepared by electrolytic oxidation of a 0.075 $mol \cdot dm^{-3}$ solution of $Co(ClO_4)_2 \cdot 6H_2O$ in a solution of 5 $mol \cdot dm^{-3}$ $HClO_4$. (In the absence of the $HClO_4$ the cobalt complex is unstable and can undergo hydrolysis in water to form $[Co(OH_2)_5OH]^{2+}$, which oxidizes the solvent). The $Co^{3+}_{(aq)}$ solution was stored in a freezer until needed to keep solution

Reproduced with permission of the copyright owner. Further reproduction prohibited without permission.

decomposition to a minimum. The exact $HClO_4$ concentration in the $Co^{3+}_{(aq)}$ solution was determined by standard titration methods with 0.1000 mol·dm^{-3} NaOH(Acculute). The concentration of the $Co^{3+}_{(aq)}$ was determined by UV-vis spectroscopy prior to each experiment using its known molar absorptivity of 35.3 dm^3·mol^{-1}·cm^{-1} at 605 nm.[73]

2.3.2 Concentration Dependence Kinetics

For the concentration dependence of $[NiL_{4,8}]^{2+}$, the concentration of the $[Ni(hmca)(OH_2)]^{2+}$ oxidant was held constant at 1.00 x 10^{-5} mol·dm^{-3} while the concentration of $[NiL_{4,8}]^{2+}$ was varied from 1.00 x 10^{-4} to 5.00x10^{-4} mol·dm^{-3}. The rate was determined by the growth of a peak at 300 nm. The runs were carried out at least three times and the results averaged. All runs were done at 25.0 ± 0.1°C. Ionic strength was held constant at 0.100 mol·dm^{-3} using $NaClO_4/HClO_4$.

2.3.3 Temperature Dependence Kinetics

For the temperature dependence, the concentration of the $[NiL_4]^{2+}$ was held constant at 2.00 x 10^{-4} mol·dm^{-3} while the concentration of $[Ni(hmca)(OH_2)]^{2+}$ was held constant at 2.00 x 10^{-5} mol·dm^{-3}. The temperature was varied from 285.2 - 305.2 K with rates determined at six separate temperatures. Again the runs were carried out in at least triplicate and within each separate temperature, the temperatures were measured to within ± 0.1°C. The ionic strength was held constant at 0.100 mol·dm^{-3} using $NaClO_4/HClO_4$.

2.3.4 Cyclodextrin Dependent Kinetics

The kinetics involving the cyclodextrins were carried out using constant concentrations of both the oxidant and the reductant. The concentration of the α- or β- cyclodextrin was varied.

Reproduced with permission of the copyright owner. Further reproduction prohibited without permission.

The concentration of the cyclodextrin was constant in the solution of both the oxidant and the reductant prior to mixing to ensure that there was no change when mixed. All of these runs were conducted at a temperature of 25.0 ± 0.1 °C with a constant ionic strength of 0.100 $mol \cdot dm^{-3}$ using $NaClO_4/HClO_4$.

2.4 Other Methods and Instrumentation

2.4.1 Electrochemistry

Cyclic voltammograms were measured using a Princeton Applied Research model 482 fast scanning electrochemical apparatus. A 3mm diameter Pt disk was used for the working electrode and platinum wire was used for the counter electrode. The reference electrode was an Ag/AgCl/saturated NaCl electrode. The measured solutions were prepared in concentrations of $1.00 \times 10^{-3} mol \cdot dm^{-3}$ $[NiL_{4,8,12}]^{2+}$ and 0.100 $mol \cdot dm^{-3}$ background electrolyte. Triflic acid was used for the background electrolyte. All measured solutions were purged with argon for 15 minutes and then left under argon atmosphere during scanning. Each cyclic voltammogram was collected at multiple scan speeds and multiple voltage cycles for each speed were carried out to produce the most accurate results.

2.4.2 Electrospray Mass Spectrometry and Elemental Analysis

All electrospray mass spectrometry was carried out by Mr. Tom Hunter at Queens University. The mass spectroscopy measurements were obtained on a VG quadrupole mass spectrometer with an atmospheric pressure electrospray source. Samples, in distilled water, were introduced into the source at flow rate of 5 $mL \cdot min^{-1}$.

Reproduced with permission of the copyright owner. Further reproduction prohibited without permission.

The CHN analyses were conducted by Canadian Microanalytical Services Ltd. in Delta, British Columbia.

2.4.3 NMR and IR Spectra Collection

All NMR spectra were measured using a Bruker Avance 300 MHz NMR spectrometer, in deuterated solvents. The NMR titrations for $[NiL_{4,8,12}]^{2+}$ with cyclodextrins were carried out two ways. The first method involved varying the ratio[74] of cyclodextrin to complex, both greater than and less than one. The second method had the concentration of the $[NiL_{4,8,12}]^{2+}$ held constant and the cyclodextrin concentration (in excess) varied. This was achieved by preparing two solutions with equal concentrations of $[NiL_{4,8,12}]^{2+}$ but having cyclodextrin present in only one of the solutions. By mixing different ratios of each solution, the $[NiL_{4,8,12}]^{2+}$ concentrations remains constant while the cyclodextrin concentration changes.[75]

All IR spectra were collected using a Perkin Elmer 1600 series FTIR, using the KBr pellet method.

2.4.4 Water Content of α- and β- Cyclodextrin

The water content of both α- and β-cyclodextrin were measured by drying to constant weight in a vacuum oven. A number of samples of varying weight (0.15 to 0.50 g) were measured into small beakers and placed in the vacuum oven and dried for a period of between three and four hours. The dried samples were then cooled in a desiccator and weighed. The percent mass of the water in the samples was then calculated. This was carried out on a minimum of four samples for each cyclodextrin. The percent by mass water was found to be 9.18% in α-cyclodextrin and 13.0 % in β-cyclodextrin. These correction factors were applied to the

Reproduced with permission of the copyright owner. Further reproduction prohibited without permission.

concentrations of all α- and β-cyclodextrin solutions.

2.5 X-Ray Crystallography

Numerous attempts were made at growing crystals for X-Ray analysis including effusion from: water; water/THF mixed solutions; acetone; acetonitrile; and methanol. Diffusion methods using water and methanol, acetone and ether, and acetonitrile and ether were also used. Only the diffusion method with acetonitrile and ether proved successful.

The diffusion method involves using two solvents that are miscible, where the compound is soluble in one but not the other, as seen below. Solvent 1 contains the compound, as Solvent 2 diffuses into Solvent 1, the compound becomes less soluble and begins to crystallize out of solution.

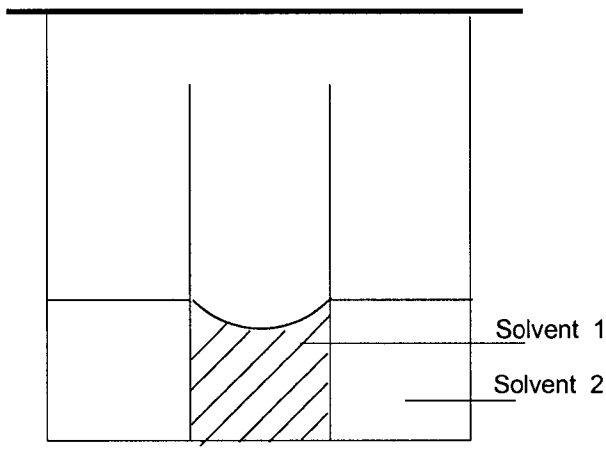

Figure 2.7 Setup for the diffusion method of growing crystals

The crystals of $[NiL_8](ClO_4)_2$ and $[Ni(dap)_2(MeCN)_2](ClO_4)_2$ for X-Ray crystallography were grown *via* the diffusion method with acetonitrile (Solvent 1) and diethyl ether (Solvent 2).

Reproduced with permission of the copyright owner. Further reproduction prohibited without permission.

2.5.1 Crystal Structure of $[NiL_8](ClO_4)_2$

The X-Ray crystallographic data for the $[NiL_8](ClO_4)_2$ complex were collected by Dr. Stan Cameron of Dalhousie University. The X-Ray structure determination was performed on a Mercury CCD area detector coupled with a Rigaku AFC8 diffractometer, using graphite monochromated MoK_α radiation (λ= 0.71073 Å). The orange plate crystal was mounted on a glass fibre. Further details are listed in Appendix D.

2.5.2 Crystal Structure of $[Ni(dap)_2(MeCN)_2](ClO_4)_2$

The X-Ray crystallographic data for the *trans*-$[Ni(dap)_2(MeCN)_2](ClO_4)_2$ complex were collected by Mr. Brian Moulton at the University of South Florida. Single-crystal X-ray diffraction data for the compounds were collected on a Bruker-AXS SMART APEX/CCD diffractometer using $Mo\kappa_\alpha$ radiation (λ = 0.7107 Å). Diffracted data were corrected for Lorentz and polarization effects and for absorption using the SADABS[76] program package. The structure was solved by direct methods and the structure solution and refinement was based on $|F|^2$. All non-hydrogen atoms were refined with anisotropic displacement parameters whereas hydrogen atoms were placed in calculated positions when possible and given isotropic U values 1.2 times that of the atom to which they bonded. All crystallographic calculations were conducted with the SHELXTL v.6.1[77] program package. The blue crystal was mounted in a sealed glass capillary tube, under acetonitrile liquor.

Reproduced with permission of the copyright owner. Further reproduction prohibited without permission.

2.6 THF-Water Solubility of $[NiL_{8,12}]^{2+}$

Solvent mixture of varying THF-water compositions were prepared with mole fractions of THF ranging from 0 to 1. In centrifuge tubes, solid $[NiL_{8,12}]^{2+}$ was added to the mixed solvent solutions. Enough solid was added to produce saturated solutions. After equilibration for twenty-four hours the mixtures were then centrifuged for 15 - 20 minutes and the supernatant liquid was decanted to separate the excess solid from the saturated solution. The supernatant liquids were then diluted by a factor of ten and their absorbances at 450 nm were measured using UV-vis spectrometry. This procedure was followed for all the different THF - water compositions.

2.7 Solvents and Reagents

A complete list of all Solvents and reagents used in the experimental procedures is tabulated in Appendix A.

Reproduced with permission of the copyright owner. Further reproduction prohibited without permission.

Chapter 3 - Results and Discussion

3.1 Characterization of $[NiL_{4,8,12}]^{2+}$

The $[NiL_{4,8,12}]^{2+}$ complexes synthesized are all orange in colour in the solid form. The crystals grown appear as bright orange shiny plates. The IR data show peaks present at 2850 - 3000 cm^{-1} and 1465 - 1475 cm^{-1} which represent C-H bond stretching and bending modes. Also present are single peaks at approximately 3200 cm^{-1} representing secondary amines. NMR does not provide useful characteristic data for reasons that will be explained in section 3.2.2.

The CHN analysis performed on each of the three compounds provided results (section 2.1.1) that corresponded very well with the calculated percentages for each compound. This is indicative of the high purity of the compounds.

Reproduced with permission of the copyright owner. Further reproduction prohibited without permission.

3.1.1 Crystal Structure for $[NiL_8](ClO_4)_2$

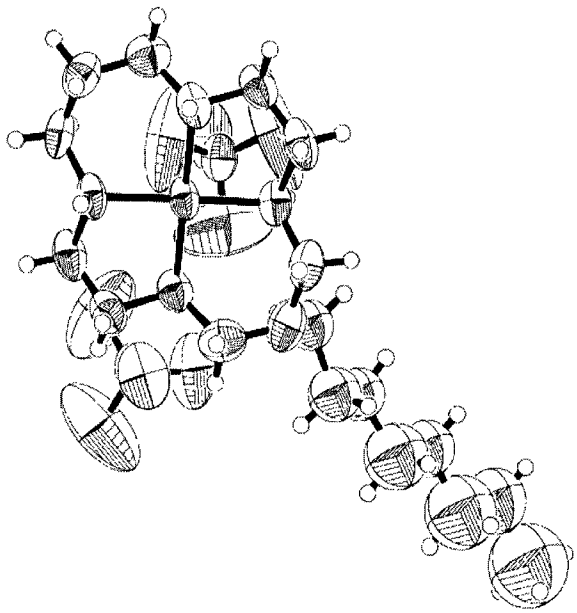

Figure 3.1 ORTEP diagram for $[NiL_8](ClO_4)_2$. (To view a ball and stick diagram with the atoms numbered, see Appendix B.)

The crystal structure for $[NiL_8](ClO_4)_2$, depicted in Figure 3.1, consists of monomeric $[NiL_8]^{2+}$ cations with two non-interacting perchlorate ions. The cyclic ligand is coordinated to the nickel in a square-planar manner through four nitrogen atoms with an eight-carbon alkyl chain attached to the complex at a fifth, non-coordinating nitrogen which directs the octyl chain away from the metal centre. Figure 3.2 shows the packing diagram for the crystal and shows that the alkyl tails are all pointed away from the metal centre and that they align themselves with the tails from adjacent complexes, *via* strong van der Waal interactions, for optimum packing. Similar packing was observed[78] in $[Ni(C_{25}H_{55}N_5)]^{2+}$ (or $[NiL_{16}]^{2+}$) which is essentially the same complex but with a hexadecyl chain pendant-arm in place of the octyl chain in our system. The macrocyclic ligand assumes the more thermodynamically favourable chair configuration

Reproduced with permission of the copyright owner. Further reproduction prohibited without permission.

(designated *trans-III* conformation) around the metal centre as is common for similar transition metal-tetraazamacrocyclic ligand complexes.[79] For example, the transition metal complexes of 1,4,8,11-tetraazacyclotetradecane assume this *trans-III* conformation.

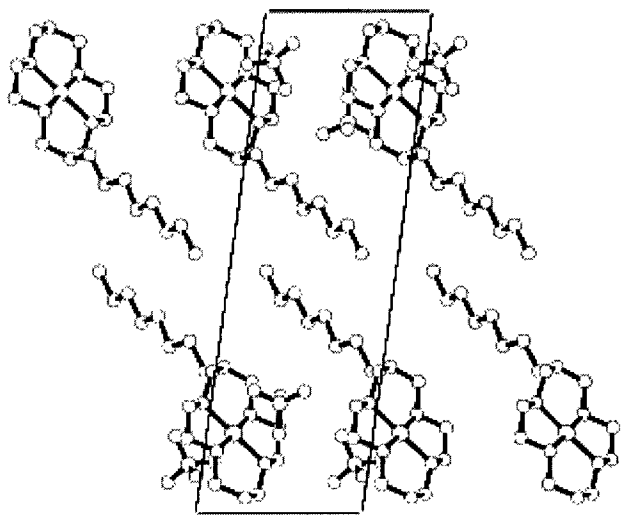

Figure 3.2 Packing diagram for $[NiL_8](ClO_4)_2$

The two perchlorate ions associated with the $[NiL_8]^{2+}$ cation both have approximately equal Cl-O bond lengths. The Cl-O bond lengths all range from 1.39(1)Å to 1.399(10)Å and there appears to be no significant difference between the two perchlorate anions. The average Ni-O distance is approximately 3.18Å which is evidence of their non-coordination to the nickel as Ni-O bond lengths have been reported as 2.089 - 2.301Å for octahedral nickel(II) tetraaza ligand complexes.[78]

The O-Cl-O bond angles in the perchlorate anions also indicate very little difference in either of the two anions as all the bond angles are close to the 109.5° expected for tetrahedral geometries. The O-Cl-O bond angles range from 109.24(14)° to 109.77(14)° within the two

Reproduced with permission of the copyright owner. Further reproduction prohibited without permission.

anions.

The bond lengths between the nickel centre and the four coordinating nitrogen atoms are all approximately equal with lengths of 1.951(5)Å, 1.957(6)Å, 1.963(6)Å, and 1.936(5)Å. These values are typical for similar nickel(II) polyazamacrocycles.[50] Comparing the bond lengths of the $[NiL_8]^{2+}$ cation with those seen for the $[Ni(2,3,2\text{-tet})]^{2+}$ complex[18] cation shows that the bond lengths are almost identical. The average of the four Ni-N (1.952Å) bonds present in this complex compares extremely well to the average bond length (1.946Å) of the similar $[NiL_{16}]^{2+}$ macrocycle complex.

Looking at the bond angles about the nickel atom, the two angles from N(1)-Ni-N(3) and N(2)-Ni-N(4) should theoretically be 180° but the actual measured angles are slightly offset at 179.3(2)° and 178.8(3)° respectively.

The ORTEP diagram shows that within the molecule, there are four chelate rings formed about the central nickel atom. There are two five-membered rings and two six-membered rings with each of the four nickel coordinated nitrogen participating in both a five-membered ring as well as a six-membered one.

The two five-membered rings are essentially similar while the two six-membered rings differ at the four position (assuming Ni as position one). In one case there is a carbon atom while the other ring has a non-coordinating nitrogen with the octyl chain attached at that ring position.

The bite angles associated with the four chelate rings indicate that as expected, the two five-membered rings have similar angles to each other. This is also the case for the two six-membered rings. The bite angles of the two five-membered rings are 86.8(2)° and 86.3(2)° for N(1)-Ni-N(2) and N(3)-Ni-N(4) respectively. These compare well with other five-membered chelate rings formed about transition metal centres. The two five-membered rings in [Ni(2,3,2-

Reproduced with permission of the copyright owner. Further reproduction prohibited without permission.

tet)]$^{2+}$ formed bite angles of 86.3(2)° and 86.4(2)° while similar rings in [Cu(2,3,2-tet)]$^{2+}$ formed angles of 85.3(2)° and 85.2(2)° while a bite angle of 86.0(2)° was observed for the five-membered rings in [Cu(cyclam)]$^{2+}$.[81] The bite angles for what would be the [NiL$_{16}$]$^{2+}$ complex were 85.6(4)° and 86.6(4)°. All of these reported bond angles compare well with the angles observed for the [NiL$_8$]$^{2+}$ complex cation.

The two six-membered chelate rings form bite angles of 92.7(2)° and 94.2(2)° about the N(1)-Ni-N(4) and N(2)-Ni-N(3) bonds respectively. Such a difference in the two angles is not surprising considering the different composition of the two rings. Again, the bite angle observed in this complex compares favourably to other systems with similar six-membered chelate rings. The six-membered chelate ring in [Ni(2,3,2-tet)]$^{2+}$ has a reported bite angle of 94.5(2)° while that of the similar copper complex is 93.9(2)°. [Cu(cyclam)]$^{2+}$ has a reported bite angle of 94.0(2)° which, along with the two [Ni/Cu(2,3,2-tet)]$^{2+}$ complexes, are very close to the observed angle of the six-membered rings of the [NiL$_8$]$^{2+}$ complex. The [NiL$_{16}$]$^{2+}$ complex, which like the [NiL$_8$]$^{2+}$, has one of its six-membered ring with a nitrogen in place of a carbon, had corresponding bite angles of 92.5(4)° and 95.3(4)° which are very close to the observed angles for the [NiL$_8$]$^{2+}$ complex.

Comparing the bond angles about the carbon atoms in each of the rings, it appears as though there is increased strain in the larger six-membered rings. The N-C-C bond angles for the five-membered ring range from 105.8(7)° to 108.2(7)° and, with the exception of the 105.8(7)° angle, are all relatively close to the 109.5 ° angle expected around tetrahedral carbon atoms. The six-membered rings have increased N-C-C and C-C-C bond angles ranging from 111.7(6)° to 116.0(6)° which indicates greater ring strain.

Reproduced with permission of the copyright owner. Further reproduction prohibited without permission.

3.1.2 ESMS for $[NiL_{4,8,12}]^{2+}$

Figure 3.3 shows the electrospray mass spectrum obtained for a solution of 10^{-4} mol·dm^{-3} $[NiL_4](ClO_4)_2$ in the presence of 10^{-3} mol·dm^{-3} α-cyclodextrin.

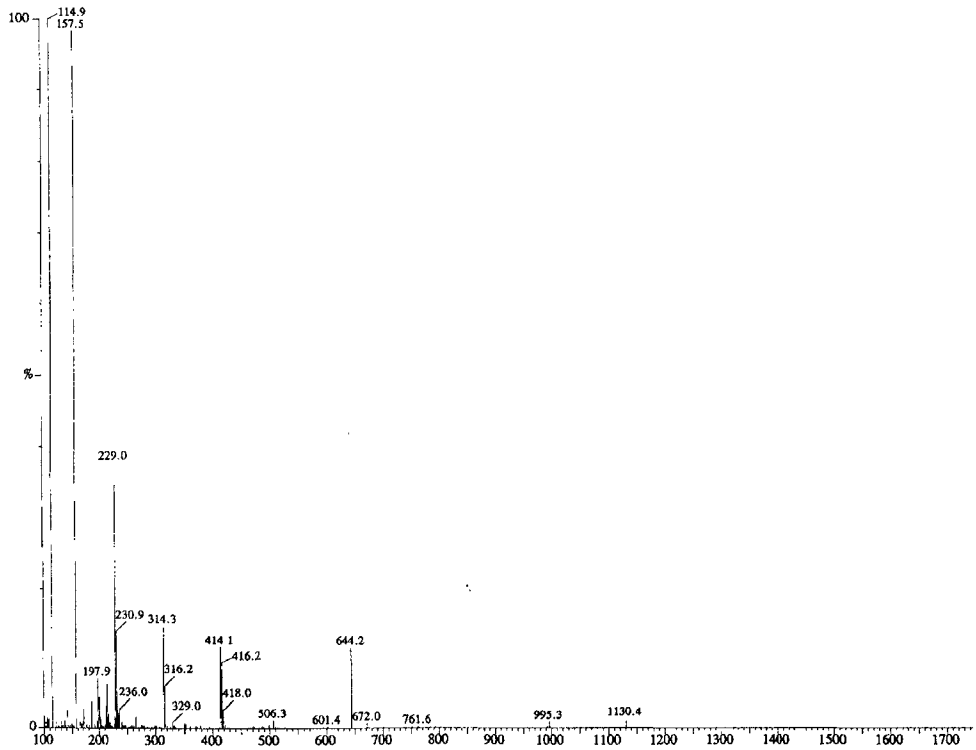

Figure 3.3 ESMS for 10^{-4} mol·dm^{-3} $[NiL_4]^{2+}$ in 10^{-3} mol·dm^{-3} α-cyclodextrin.

The spectrum shows that there are fragmentation patterns representing the parent ion peak for the $[NiL_{4,8,12}]^{2+}$ compounds as well as evidence of the formation of guest host complexes with the cyclodextrins in solution. The latter will be discussed in section 3.2.1. The spectrum is typical of those obtained for the three $[NiL_{4,8,12}]^{2+}$ complexes in the presence of both α- and β-cyclodextrin with similar concentrations to that detailed above. Table 3.1 summarizes the peaks corresponding to the free compounds.

Reproduced with permission of the copyright owner. Further reproduction prohibited without permission.

Species	Calculated m/e	Actual m/e	% BPI
$[NiL_4]^{2+}$	158.5	157.5 (major)	100
$[NiL_4](ClO_4)^+$	416	416	5.99 - 11.59
$[NiL_8]^{2+}$	186.5	185.6 (major)	100
$[NiL_8](ClO_4)^+$	472	470.3	2.17 - 5.19
$[NiL_{12}]^{2+}$	215	213.8 (major)	100
$[NiL_{12}](ClO_4)^+$	528.5	528.3	0.48 - 3.22

Table 3.1 ESMS data for 1.00×10^{-4} mol·dm^{-3} solutions of $[NiL_{4,8,12}]^{2+}$ in 1.00×10^{-3} mol·dm^{-3} α- and β-cyclodextrin.(BPI = Base Peak Intensity)

In each spectrum, the major peak represents the parent mononuclear complex ion $[NiL_{4,8,12}]^{2+}$. There are also peaks present for each complex that represent the monoperchlorate ion pair, $\{[NiL_{4,8,12}](ClO_4)\}^+$, which is common for multiply-charged complex ions. The major m/e peak positions obtained for the three complexes are: 157.5 for $[NiL_4]^{2+}$; 185.6 for $[NiL_8]^{2+}$; and 213.8 for $[NiL_{12}]^{2+}$ correspond very well with the calculated values of 158.5, 186.5, and 215 respectively. These data are further characteristic evidence for the three $[NiL_{4,8,12}]^{2+}$ macrocyclic complexes and show that complexes remain intact in solution.

3.1.3 Electrochemistry

The results for the electrochemical measurements in the presence of cyclodextrins will be summarized later in Table 3.4. Of importance here are the results obtained in the absence of cyclodextrin. Figure 3.4 shows the observed cyclic voltammogram for a solution of 1.00×10^{-3} mol·dm^{-3} $[NiL_4]^{2+}$ complex at an ionic strength of 0.100 mol·dm^{-3}. The cyclic voltammogram is representative of that obtained for all $[NiL_{4,8,12}]^{2+}$ complexes. The cyclic voltammogram shows that there is a reversible one-electron transfer which was common to each of the systems studied.

Reproduced with permission of the copyright owner. Further reproduction prohibited without permission.

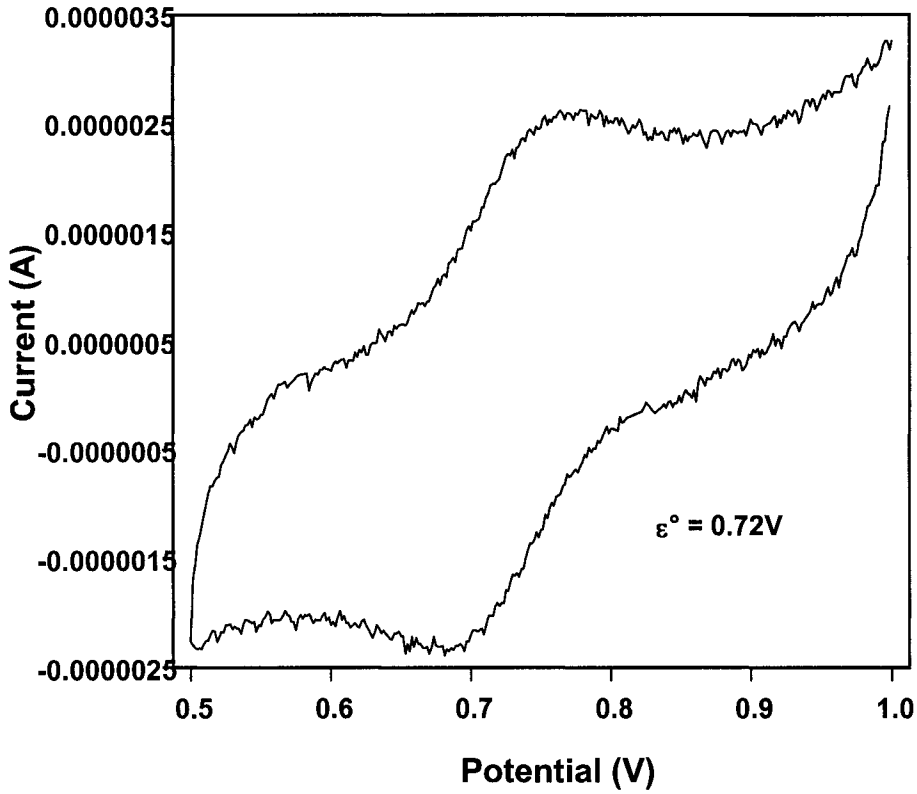

Figure 3.4 Cyclic voltammogram of 1.00 x 10^{-3} mol·dm^{-3} $[NiL_4]^{2+}$ at 298K.

The data indicate that the half-wave potential ($E_{1/2}$) does not change with the different tail lengths of the $[NiL_{4,8,12}]^{2+}$ complexes. It was found that the $E_{1/2}$ value remained at 0.72 ± 0.01V versus the Ag/AgCl electrode with a peak separation of 60 mV over the series of tail lengths which indicates that the redox potential is independent of tail length. The redox potential found here is similar to one electron transfers of other nickel(II/III) systems.[82]

The X-ray crystal structure for the $[NiL_8]^{2+}$ complex shows unequivocal evidence as to the structure of the compound. While there is no X-ray structure for the $[NiL_{4,12}]^{2+}$ compounds, the similarities in the data suggest that they are similar in nature. The presence of the ESMS peaks

Reproduced with permission of the copyright owner. Further reproduction prohibited without permission.

are strong evidence for the structure and while the IR and electrochemical data do not by themselves prove the structure, the data are essentially identical to that for the $[NiL_8]^{2+}$, suggesting similar structures with only the length of the alkyl chain changing. This is expected as the length of the alkyl chain should not have a great effect on the formation of the macrocyclic complex. Thus, the structures for all three of the compounds are strongly supported either directly or indirectly.

3.2 Interaction Between the $[NiL_{4,8,12}]^{2+}$ Complexes and Cyclodextrin

As discussed in section 1.2, there is a great deal of interest in the study of supramolecular complexes, especially relating to the determination of their association or binding constants. The long alkyl chain of the $[NiL_{4,8,12}]^{2+}$ compounds would seem to be a good fit for the cyclodextrin molecule which is known to often form supramolecular complexes with smaller organic molecules. First, it must be established that there is in fact a supramolecular complex formed between the $[NiL_{4,8,12}]^{2+}$ compounds and the cyclodextrin molecules. There are a number of methods that may be employed and those relevant to this study are discussed in the following sections.

3.2.1 ESMS for $[NiL_{4,8,12}]^{2+}$ with α- and β- cyclodextrin

Electrospray mass spectrometry is not necessarily a common method of determining binding constants. However, important information about the interaction between the $[NiL_{4,8,12}]^{2+}$ complexes and both α- and β- cyclodextrin may be gained from the ESMS data. The peaks of interest, in terms of cyclodextrin interaction, from the ESMS are displayed in Table 3.2.

Reproduced with permission of the copyright owner. Further reproduction prohibited without permission.

Species	Calculated m/e	Actual m/e	% BPI
$[NiL_4(\alpha\text{-CD})]^{2+}$	645	644 (strong)	11.50
$[NiL_4(\alpha\text{-CD})_2]^{2+}$	1132	1130.4	1.34
$[NiL_4(\beta\text{-CD})]^{2+}$	726	724.5	1.54
$[NiL_4(\beta\text{-CD})_2]^{2+}$	1294	1293	0.01
$[NiL_8(\alpha\text{-CD})]^{2+}$	673	672.2 (strong)	29.75
$[NiL_8(\alpha\text{-CD})_2]^{2+}$	1160	1158.4	3.77
$[NiL_8(\beta\text{-CD})]^{2+}$	754	753.2 (strong)	9.49
$[NiL_8(\beta\text{-CD})_2]^{2+}$	1321.5	1320.9	0.48
$[NiL_{12}(\alpha\text{-CD})]^{2+}$	701	700.3 (strong)	7.82
$[NiL_{12}(\alpha\text{-CD})_2]^{2+}$	1188	1186	0.81
$[NiL_{12}(\beta\text{-CD})]^{2+}$	782	781 (strong)	6.29
$[NiL_{12}(\beta\text{-CD})_2]^{2+}$	1350	1349 (weak)	0.29

Table 3.2 ESMS data for 1.00×10^{-4} mol·dm^{-3} solutions of $[NiL_{4,8,12}]^{2+}$ in 1.00×10^{-3} mol·dm^{-3} α- *and* β-*cyclodextrin. Only peaks representing* $[NiL_{4,8,12}]^{2+}$ *- CD interaction are listed.*

For the $[NiL_4]^{2+}$ complex, there are m/e peaks at 644 and 724.5 representing the $[NiL_4]^{2+}$ complex associated with a single cyclodextrin unit for both α- and β- cyclodextrin respectively. Both of these values agree with the calculated m/e values of 645 and 726. The mono-cyclodextrin complex with α-cyclodextrin has a peak intensity that is approximately ten-fold stronger than that formed with β- cyclodextrin. This should be the case for such a short tail length as the α- cyclodextrin has a smaller cavity than that of β- cyclodextrin. This provides a "tighter fit" with the α-cyclodextrin and thus a more stable complex. Also present is a peak at m/e= 1130.4 representing a 2:1 α- cyclodextrin to $[NiL_4]^{2+}$ complex. This is not a function of the tail interacting with a two cyclodextrin units. Rather, cyclodextrins can associate with one another in solution forming complexes where the two cyclodextrins are associated end-to-end *via*

Reproduced with permission of the copyright owner. Further reproduction prohibited without permission.

their hydrophobic/hydrophilic character at the top and bottom of the cyclodextrin. Such observations are known.[83]

The four-carbon tail present on the $[NiL_4]^{2+}$ complex is much too short to interact with two separate cyclodextrin molecules as it would be required to thread completely through one cyclodextrin molecule and at least partially through a second. As a result, the cyclodextrin-cyclodextrin association is the most probable explanation for the presence of supramolecular complexes greater than 1:1 for $[NiL_4]^{2+}$. A corresponding m/e peak can be found for the analogous β- cyclodextrin complex at 1293, but its relative intensity is extremely low.

From the $[NiL_8]^{2+}$ ESMS, it appears that the $[NiL_8]^{2+}$ complex association properties with α- and β- cyclodextrin are similar to those found for the $[NiL_4]^{2+}$ compound. There appears to be a stronger association for $[NiL_8]^{2+}$ with α-cyclodextrin (m/e = 672.2) than with β- cyclodextrin (m/e = 753.2), as was the case for $[NiL_4]^{2+}$. The eight-carbon chain is similar in length to the cavity depth of a cyclodextrin (both α- and β- cyclodextrin have equal depths as only cavity width increases with the additional glycopyranose unit present in the β-cyclodextrin). Once again, the smaller cavity size of the α-cyclodextrin proves more conducive to a tighter fit with the tail. However, there is only an approximate three-fold increase in peak intensity for the α-cyclodextrin complex compared to the β- cyclodextrin one for $[NiL_8]^{2+}$, compared to a ten-fold increase for the $[NiL_4]^{2+}$ compound. There is also evidence for the formation of the 2:1 cyclodextrin to $[NiL_8]^{2+}$ complex with both α- (m/e = 1158.4) and β- (m/e = 1320.9) cyclodextrins. Since such species were present for the $[NiL_4]^{2+}$ complex, it is reasonable that they should also be present for the $[NiL_8]^{2+}$ complex. Again, the tail is most likely not completely threading through both cyclodextrins although the tail may be long enough to have a slight interaction with a second cyclodextrin molecule. The most likely explanation is again the

Reproduced with permission of the copyright owner. Further reproduction prohibited without permission.

presence of cyclodextrin-cyclodextrin association. As was the case for $[NiL_4]^{2+}$, the 2:1 complex is more significant with the α-cyclodextrin than with the β- cyclodextrin.

The mass spectral data for $[NiL_{12}]^{2+}$ with α- and β- cyclodextrin provide evidence of similar cyclodextrin- $[NiL_{12}]^{2+}$ complexes as those formed with the shorter four- and eight-carbon chained macrocyclic complexes. There is evidence of the formation of 1:1 complexes between the $[NiL_{12}]^{2+}$ and both α- and β- cyclodextrin with m/e peaks at 700.3 and 781 respectively. Unlike the $[NiL_4]^{2+}$ and $[NiL_8]^{2+}$ complexes, there does not appear to be much difference between the ability of the α- and β- cyclodextrin to form these 1:1 complexes with the $[NiL_{12}]^{2+}$. This also appears to be the case with the 2:1 complex formation.

3.2.2 NMR Titrations

The results of the electrospray mass spectral studies indicate that there is in fact an interaction between the $[NiL_{4,8,12}]^{2+}$ compounds and both α- and β- cyclodextrin indicating the presence of a supramolecular complex in solution.

In our system, standard methods cannot be used, as the guest molecule does not possess any fluorescent markers, which excludes the use of fluorescence to measure binding constants. There is documented work in which NMR techniques have been used to measure binding constants between cyclodextrins and alkyl chains.[84] From this knowledge, attempts were made to use NMR titrations to determine the binding constants of the supramolecular complexes formed between $[NiL_{4,8,12}]^{2+}$ and both α- and β-cyclodextrin.

NMR spectroscopy is a viable method for determining binding constants between cyclodextrins and organic molecules as a result of the changing of the proton environment upon complexation between the cyclodextrin and the guest molecule. Depending on the guest, it is

Reproduced with permission of the copyright owner. Further reproduction prohibited without permission.

possible to study the binding constants by observing the change in chemical shift from both the protons within the cyclodextrin cavity as well as the protons belonging to the guest molecule.

In our case, it was hoped that the binding constants could be measured from both the change in chemical shift of the cyclodextrin protons as well as the protons on the alkyl tails of the pendant-arm macrocyclic compounds. Based on the cavity diameter size of the cyclodextrins (5.3 and 6.5 Å for α-and β-CD respectively) and an estimated size of the metal-complexed macrocycles[78] (9.4 x 8.8 $Å^2$ for the head group), it appears that the interaction can only occur between the alkyl tail of the complex and the cyclodextrin, as the macrocyclic ring is too large to fit within the cyclodextrin. As a result, the protons on the macrocyclic ring backbone should not be significantly affected by the presence of cyclodextrins.

The titrations are carried out by keeping the concentration of either the host or the guest constant and varying the other in excess. Unfortunately there are a number of limits that make this method difficult for this particular host-guest system. First, the $[NiL_{4,8,12}]^{2+}$ compounds are not very soluble in water, limiting the range of concentrations possible. Second, paramagnetic line broadening was observed in the NMR spectra. The latter is a result of the high-spin low-spin equilibrium that exists for the $[NiL_{4,8,12}]^{2+}$ compounds in aqueous solutions. The solid $[NiL_{4,8,12}](ClO_4)_2$ complex exists as a low-spin square-planar complex. However, in aqueous media the following equilibrium is established:[85]

$$[NiL_{4,8,12}]^{2+} + H_2O \rightleftarrows [NiL_{4,8,12}(OH_2)_2]^{2+} \qquad \text{(Equation 3.1)}$$

It is the addition of the solvent water molecule that results in the change to the high-spin state for the $[NiL_{4,8,12}]^{2+}$ complexes and it is the high-spin state of the metal complex that is known to produce paramagnetic line broadening in the NMR.

Reproduced with permission of the copyright owner. Further reproduction prohibited without permission.

The line broadening that occurs reduces the definition in the proton peaks, making it difficult to accurately measure a change in chemical shift. This indicates that the cyclodextrin protons would provide the optimal peak shifts to study. For the titrations however, if the chemical shift of the cyclodextrin protons are to be observed, the $[NiL_{4,8,12}]^{2+}$ complex must be in excess. The low solubility of the complexes make this unfeasible. Thus, the only option is to hold the cyclodextrin in excess and follow the chemical shift of the protons from the alkyl tail of the complex.

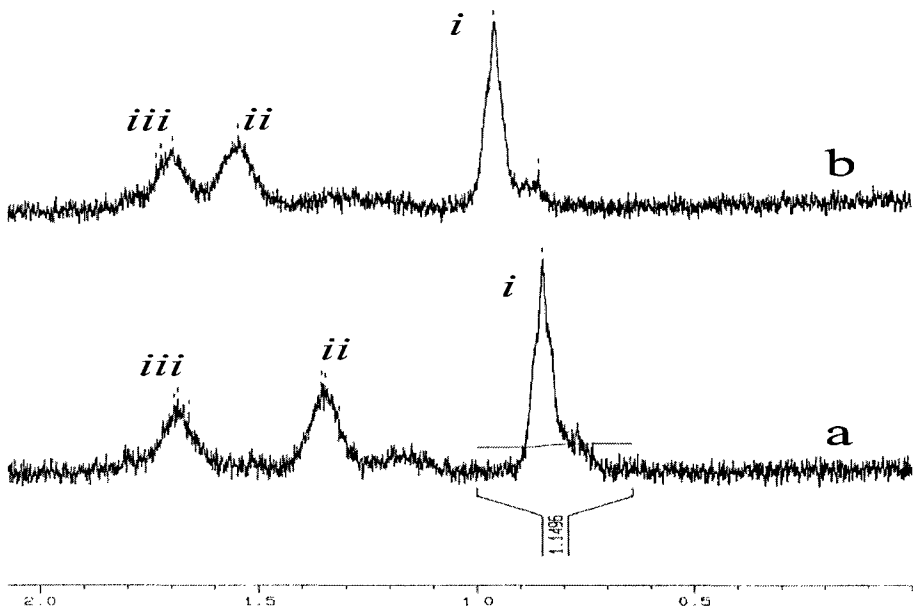

Figure 3.5 NMR spectra for 1.00×10^{-3} mol·dm^{-3} $[NiL_4]^{2+}$ in (a) the absence of α-CD and in (b) 2.50×10^{-2} mol·dm^{-3} α-CD. Both (a) and (b)solutions prepared in D_2O at 298K.

Figure 3.5 shows the effect of adding α-cyclodextrin to an $[NiL_4]^{2+}$ solution. Peaks (*i*) and (*ii*) are both shifted downfield while peak (*iii*) remains unchanged. This supports the assumption that only the pendant-arm of the complex interacts with the cyclodextrin as peaks (*i*) and (*ii*) represent protons from the alkyl tail while the further downfield peak (*iii*) is due to the protons of

Reproduced with permission of the copyright owner. Further reproduction prohibited without permission.

the ring backbone. The figure shows the maximum observed change in chemical shift. While the overall shift is not great, it is measurable. Table 3.3 shows the observed chemical shifts for peaks (*i*) and (*ii*) over a range of [α-CD] from spectrum (a) to spectrum (b).

	Peak (*i*)		Peak (*ii*)	
10^2[α-CD]/M	δ/ppm	Δ/ppm	δ/ppm	Δ/ppm
0	0.85		1.36	
0.83	0.94	0.09	1.51	0.15
1.43	0.95	0.10	1.53	0.18
1.88	0.95	0.10	1.54	0.18
2.22	0.96	0.11	1.55	0.19
2.50	0.96	0.11	1.55	0.19
K_{CD}/mol^{-1}·dm^3	220 ± 42		180 ± 50	

Table 3.3 Change in chemical shift for the protons on the alkyl tail of $[NiL_4]^{2+}$ as [α-CD] is increased. $[NiL_4]^{2+}$ was held constant at 1.00 x 10^{-3} mol·dm^{-3}.

This data can then be fit to the Scatchard[86] equation below.

$$\frac{\Delta}{[CD]} = -K_{CD}\Delta + \Delta_o K_{CD} \qquad \text{(Equation 3.2)}$$

Where Δ is the observed change in chemical shift and Δ_o is the maximum change in chemical shift. Linear regression of the data to this equation produces the K_{CD} as the negative of the slope.

The estimated equilibrium constant of 180 - 220 mol^{-1}·dm^3 is relatively weak indicating only slight interaction between $[NiL_4]^{2+}$ and α-cyclodextrin. Similar experiments with β-cyclodextrin showed no observable change in chemical shift indicating very weak interaction if any. The greater interaction with the α-cyclodextrin is reasonable considering that its cavity is

Reproduced with permission of the copyright owner. Further reproduction prohibited without permission.

smaller and will have a tighter fit with the pendant-arm of the complex. This will be discussed in greater detail in section 3.4.3.

With only slight changes in the chemical shift, the paramagnetic line broadening of the peaks makes it difficult to accurately follow the chemical shift during the titrations. The longer tailed compounds would be expected to have a greater chemical shift as they bind more strongly with the cyclodextrins. Unfortunately, the low solubility of the $[NiL_8]^{2+}$ and $[NiL_{12}]^{2+}$ complexes makes it very difficult to make solutions concentrated enough to produce signals that have enough amplitude where line broadening effects are somewhat minimized. As a result, using NMR techniques to determine the binding constants between the $[NiL_{8,12}]^{2+}$ complexes and α- and β- cyclodextrin is not practical. While the results with the more soluble $[NiL_4]^{2+}$ are evidence of interaction with cyclodextrin, low solubility of the $[NiL_{8,12}]^{2+}$ compounds does not allow measurement of a binding constant.

3.2.3 Electrochemistry

The results of the ESMS indicates that there is interaction between the $[NiL_{4,8,12}]^{2+}$ compounds and the cyclodextrins. This is confirmed by NMR but cannot be quantified *via* NMR techniques. As stated, electrochemistry has been known to be a potential method of determining binding constants, again depending on the nature of the individual species involved. At the very least, the electrochemical data will provide information about the nickel(II/III) redox centre of the compound. It will be possible to determine the effect, if any, that the presence of cyclodextrin has on the redox centre.

The results for the electrochemical study are summarized in Table 3.4. The redox potentials for the $[NiL_{4,8,12}]^{2+}$ complexes are shown to be 0.72 ± 0.01 V versus the Ag/AgCl

Reproduced with permission of the copyright owner. Further reproduction prohibited without permission.

electrode with a peak separation of 60 mV which was also the case for the $[NiL_{4,8,12}]^{2+}$ in the absence of cyclodextrin.

Sample	E° (V)
0.001M $[NiL_4]^{2+}$	0.72
0.001M $[NiL_8]^{2+}$	0.72
0.001M $[NiL_{12}]^{2+}$ + 0.002M α-CD	0.71
0.001M $[NiL_4]^{2+}$ + 0.002M α-CD	0.72
0.001M $[NiL_8]^{2+}$ + 0.001M α-CD	0.73
0.001M $[NiL_8]^{2+}$ + 0.002M α-CD	0.72

Table 3.4 Electrochemical data for $[NiL_{4,8,12}]^{2+}$ in both the presence and absence of cyclodextrin. E° values are reported versus the Ag/AgCl electrode at 298K

The data show that the half-wave potential ($E_{1/2}$) does not change with the different tail lengths of the $[NiL_{4,8,12}]^{2+}$ complexes nor does the addition of either α- or β- cyclodextrin affect the $E_{1/2}$ value. From Table 3.4, it can be seen that the $E_{1/2}$ value remains at 0.72 ± 0.01 V over the series of chain lengths and cyclodextrin concentrations which indicates that the redox potential is independent of both tail length and cyclodextrin concentration. The lack of a change in redox potential in the presence of cyclodextrins suggests that any interaction between the complex and cyclodextrin occurs only with the alkyl tail of the complex, thus leaving the active nickel(II) redox centre unaffected. This supports the assumption made previously for the NMR titrations. This is important for the kinetic studies. It indicates that any effect the cyclodextrin has on the rate must occur *via* a steric effect where the cyclodextrin-macrocycle host-guest complexation limits access of the oxidant to the nickel(II) centre.

It has been shown that cyclic voltammetry can be used to study host-guest complexes in which cyclodextrins are hosts. A supramolecular system comprised of β-cyclodextrin as the host

Reproduced with permission of the copyright owner. Further reproduction prohibited without permission.

and substituted viologens as the guest, to form [2]pseudorotaxanes has been studied.[87] In that case the oxidation occurs *via* two, one-electron transfers, one at each of the pyridyl rings. The viologens will only interact with the cyclodextrin when they are in the reduced state. Thus, the cyclodextrin will only encapsulate part of the viologen if it is only singularly reduced to the monocation form but will fully complex the viologen when the latter is completely reduced to the neutral state. In the cyclic voltammogram for this system, it is seen that the presence of cyclodextrin will only slightly affect the first reduction wave but the second reduction wave is shifted significantly. The second wave $E_{1/2}$ is shifted by approximately 160 mV to more positive potentials. The move to a more positive potential is the result of the complex stabilization with the cyclodextrin.

A similar example of this can be seen with the cobaltocenium/cobaltocene redox couple.[88] In this case the positively charged cobaltocenium does not interact with β-cyclodextrin while its reduced counterpart – the neutral, hydrophobic cobaltocene does form a supramolecular complex with β-cyclodextrin. Similar behaviour can be observed in the carboxy derivatives of the compounds. In acidic conditions, with the carboxyl group deprotonated, the $E_{1/2}$ value is stabilized by 57 mV in the presence of β-cyclodextrin. This is a result of the inclusion complex formed between the reduced carboxycobaltocene and β-cyclodextrin. The cobaltocene/cobaltocenium couple also shows similar characteristics in a case where they are part of dendrimers.[89] Again cyclic voltammetry indicates that the oxidized cobaltocenium form does not appear to interact with β-cyclodextrin but the reduced form does. While it has been shown that cyclic voltammetry may be used to study the binding interactions within a host-guest complex, it requires that there be a change in the complexing ability of the guest and host depending on the oxidation/reduction of the guest. There is no such change in the case of the

Reproduced with permission of the copyright owner. Further reproduction prohibited without permission.

$[NiL_{4,8,12}]^{2+}$ complexes as the $E_{1/2}$ value remains constant in the absence and presence of α- and β-cyclodextrin. While this eliminates the possibility of studying the binding constant using cyclic voltammetry, it does provide useful information that any change in the rate cannot be a function of a changing redox potential of the $[NiL_{4,8,12}]^{2+/3+}$ centre. Again, this indicates that any interaction between the $[NiL_{4,8,12}]^{2+}$ complexes and cyclodextrins occurs with the alkyl tail of the complex.

The results of the electrochemical experiments are very important in that the information learned simplifies the use of kinetics for binding constant determination. The lack of any effect from the cyclodextrin on the redox potential indicates that the redox centre is unchanged in the presence/absence of cyclodextrin. Hence, any change in rate observed with or without cyclodextrin present must be a direct result of the cyclodextrin inhibiting the ability of the oxidant to oxidize the $[NiL_{4,8,12}]^{2+}$ compounds.

3.3 Kinetics

As previously discussed, the study of electron transfer kinetics is very useful in determining the parameters of a reaction mechanism. In particular, the redox kinetics of transition metals have been widely studied[67] with the nickel(II/III) redox couple being an obvious example. In most cases, the nickel(II/III) couple is present as part of a metal-macrocycle complex, because the increased stability imparted by the macrocycle is required to stabilize the nickel(III) form. It is for this reason that the nickel(II/III) redox couple, as part of an azamacrocyclic complex, was chosen for use in this study. It was important to have a well understood system to act as a probe to study the interaction between these complexes and the cyclodextrin molecules.

Reproduced with permission of the copyright owner. Further reproduction prohibited without permission.

The $L_{4,8,12}$ series of macrocyclic ligands used to complex the nickel ions are well suited for this study. First, while they actually have five nitrogen atoms in the ring, only four of these are donor atoms. They are essentially tetraazamacrocycles and the benefits of this with regard to the oxidation of nickel were outlined in section 1.5.1. Also, as seen from previous probing experiments, the pendant-arm of the macrocycle is available to interact with cyclodextrin molecules forming host-guest complexes.

Originally, $[Ni(1,4,7\text{-triazacyclononane})_2]^{3+}$ (commonly abbreviated as $[Ni(tacn)_2]^{3+}$) was to be used as the oxidant. The $[Ni(tacn)_2]^{2+}$ complex is well know in transition metal chemistry and its oxidized form $[Ni(tacn)_2]^{3+}$ is often used as an oxidant for transition metal complexes.[90] It is well known to undergo a one electron outer-sphere redox process that is acid-independent.

Unfortunately, the $[Ni(tacn)_2]^{3+}$ compound was not a good choice for the current system. All attempts to oxidize $[NiL_{4,8,12}]^{2+}$ using $[Ni(tacn)_2]^{3+}$ proved unsuccessful as no changes in the UV-vis spectrum were observed.

The lack of a significant change in the UV-vis spectrum when the $[NiL_{4,8,12}]^{2+}$ and $[Ni(tacn)_2]^{3+}$ species were mixed was somewhat surprising because, as mentioned, the $[Ni(tacn)_2]^{3+}$ is a very common oxidant for similar transition metal macrocycles. An understanding of the reasons for the inability of the $[Ni(tacn)_2]^{3+}$ to oxidize the $[NiL_{4,8,12}]^{2+}$ was gained through the results from the electrochemical studies. As discussed earlier, all of the $[NiL_{4,8,12}]^{2+}$ complexes have redox potentials of approximately 0.72 V *versus* an Ag/AgCl electrode. In order for one compound to oxidize another, there is requirement for a difference in the redox potential of the two compounds. The redox potential for the $[Ni(tacn)_2]^{3+}$ complex is known to be 0.940 V[91] *versus* the S.H.E.. This redox potential becomes 0.746 V *versus* the Ag/AgCl electrode when accounting for the 0.194 V correction factor required when comparing

Reproduced with permission of the copyright owner. Further reproduction prohibited without permission.

results between these two different electrodes. The results make it clear that there is only a very small difference in the redox potential between the $[NiL_{4,8,12}]^{2+}$ and $[Ni(tacn)_2]^{3+}$ compounds. The differential of only about 0.02 - 0.03 V results in only slight changes to the UV-vis spectrum making measurements impractical and the requirement for a stronger oxidant.

Hence, a different oxidant must be used for the oxidation of $[NiL_{4,8,12}]^{2+}$. One option was the use of the $Co^{3+}_{(aq)}$ solution, however, the low stability of the $Co^{3+}_{(aq)}$ made this a less than desirable option. However, it was used indirectly in the oxidation process.

3.3.1 Oxidation with $[Ni(hmca)(OH_2)]^{2+}$ in the Absence of Cyclodextrin

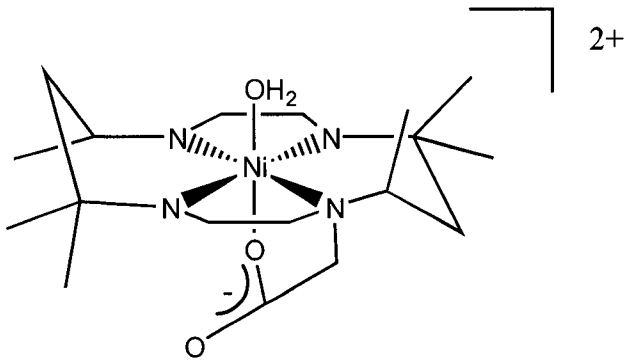

Figure 3.6 Diagram of $[Ni(hmca)(OH_2)]^{2+}$ which was used as an oxidant in the kinetic runs with $[NiL_{4,8,12}]^{2+}$

The compound chosen as oxidant for use in these kinetic studies was $[Ni(hmca)(OH_2)]^{2+}$ which can be seen in Figure 3.6. The electron transfer kinetics using $[Ni(hmca)(OH_2)]^{2+}$ have previously been studied within this group.[92] The complex is known to undergo outer-sphere electron transfer with $[Ni(tacn)_2]^{2+}$ and has a measured redox potential of 0.845 V *versus* the Ag/AgCl electrode. This is approximately a 0.12 - 0.13 V difference between the species in this case and therefore the $[Ni(hmca)(OH_2)]^{2+}$ is sufficiently strong enough to oxidize the $[NiL_{4,8,12}]^{2+}$

Reproduced with permission of the copyright owner. Further reproduction prohibited without permission.

complexes. The reaction of $[NiL_{4,8,12}]^{2+}$ with $[Ni(hmca)(OH_2)]^{2+}$ was found to be independent of acid and obeys an overall second order rate law. The reaction scheme for the oxidation of $[NiL_{4,8,12}]^{2+}$ with $[Ni(hmca)(OH_2)]^{2+}$ is shown in equation 3.3.

$$[NiL_{4,8,12}]^{2+} + [Ni(hmca)(OH_2)]^{2+} \xrightarrow{k_1} [NiL_{4,8,12}]^{3+} + [Ni(hmca)(OH_2)]^{+} \qquad \text{(Equation 3.3)}$$

From this reaction expression the rate expression may be obtained from:

$$\text{Rate} = \frac{d[NiL_{4,8,12}^{2+}]}{dt} = k_1[NiL_{4,8,12}^{2+}][Ni(hmca)(OH_2)^{2+}] \qquad \text{(Equation 3.4)}$$

Under pseudo first-order conditions with $[NiL_{4,8,12}]^{2+}$ in excess, we can say that

$$\text{Rate} = k_{obs}[Ni(hmca)(OH_2)^{2+}] \qquad \text{(Equation 3.5)}$$

Therefore

$$\text{Rate} = k_1[NiL_{4,8,12}^{2+}][Ni(hmca)(OH_2)^{2+}] = k_{obs}[Ni(hmca)(OH_2)^{2+}] \qquad \text{(Equation 3.6)}$$

From this we can say that:

$$k_{obs} = k_1[NiL_{4,8,12}^{2+}] \qquad \text{(Equation 3.7)}$$

This expression can then be rearranged to give

$$k_1 = \frac{k_{obs}}{[NiL_{4,8,12}^{2+}]} \qquad \text{(Equation 3.8)}$$

From this expression, a plot of k_{obs} versus the concentration of the $[NiL_{4,8,12}]^{2+}$ complex will produce a straight line through the origin with a positive slope of k_1 which is the second-order rate constant.

Figure 3.7 shows (a) the growth of an absorbance peak at 300 nm corresponding to the oxidation of $[NiL_4]^{2+}$ to $[NiL_4]^{3+}$ and (b) first-order growth of the peak during the oxidation of the $[NiL_4]^{2+}$ at 300 nm which was observed throughout the series of oxidation experiments.

Reproduced with permission of the copyright owner. Further reproduction prohibited without permission.

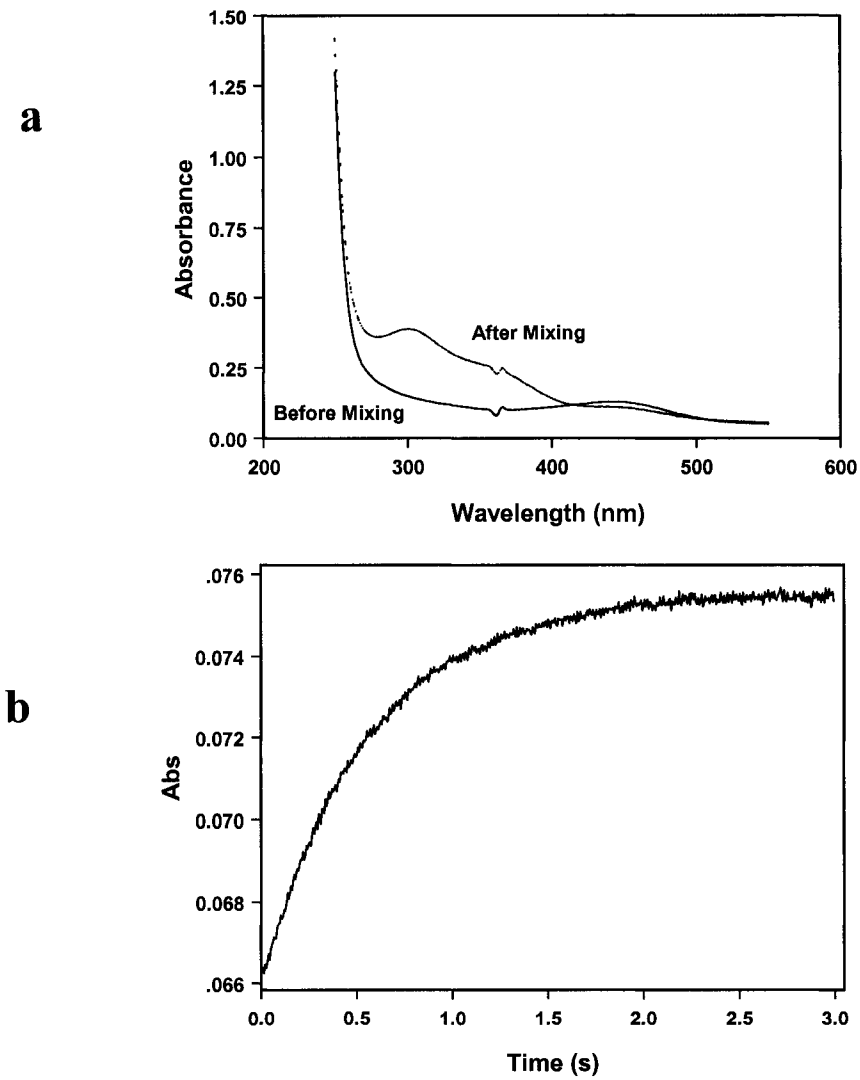

Figure 3.7 (a) Spectrum of 5.00 x 10^{-4} mol·dm^{-3} $[NiL_4]^{2+}$ and 5.00 x 10^{-5} mol·dm^{-3} $[Ni(hmca)(OH_2)]^{2+}$ before and after mixing. (b) First-order growth at 300 nm for oxidation of 1.00 x 10^{-4} mol·dm^{-3} $[NiL_{4,8,12}]^{2+}$ by 1.00 x 10^{-5} mol·dm^{-3} $[Ni(hmca)(OH_2)]^{2+}$ at 298K.

The data obtained from the oxidation of $[NiL_{4,8}]^{2+}$ by $[Ni(hmca)(OH_2)]^{2+}$ as a function of reductant concentration are summarized in Table 3.5. For a first pseudo-order-reaction, it is expected that a linear relationship exists between the observed rate constant and the concentration. Figure 3.8 shows this relationship and indicates that the graph for each of $[NiL_{4,8}]^{2+}$ is similar indicating only a small difference in the k_{obs}.

Reproduced with permission of the copyright owner. Further reproduction prohibited without permission.

	k_{obs} / s^{-1}	
$10^4[NiL_{4,8}]^{2+}$/(mol·dm^{-3})	$[NiL_4]^{2+}$	$[NiL_8]^{2+}$
1.00	0.794	0.756
2.00	1.59	1.44
3.00	2.40	2.35
4.00	3.20	2.86
5.00	3.95	3.58
k_1 / mol^{-1}·dm^3·s^{-1}	7960 ± 70	7080 ± 310

Table 3.5 Observed first-order rate constants, k_{obs} and calculated second-order rate constants, k_1 for the oxidation of $[NiL_4]^{2+}$ and $[NiL_8]^{2+}$ by $[Ni(hmca)(OH_2)]^{2+}$ as a function of reductant concentration at 298K

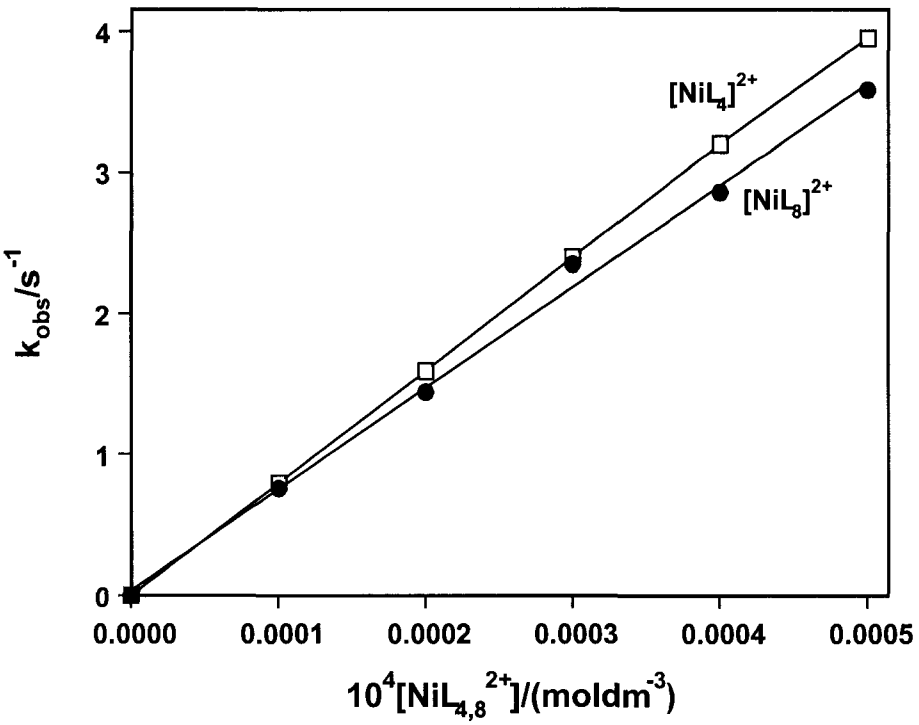

Figure 3.8 First-order dependence for the oxidation of $[NiL_4]^{2+}$ and $[NiL_8]^{2+}$ by $[Ni(hmca)(OH_2)]^{2+}$ as a function of reductant concentration at 298K

Reproduced with permission of the copyright owner. Further reproduction prohibited without permission.

From fitting the data identified in Figure 3.8 to equation 3.7, the pseudo first-order kinetics with the $[NiL_{4,8,12}]^{2+}$ in excess produced second-order rate constants of 7960 ± 70 $mol^{-1}\cdot dm^3 s^{-1}$ and 7080 ± 310 $mol^{-1}\cdot dm^3 s^{-1}$ for $[NiL_4]^{2+}$ and $[NiL_8]^{2+}$ respectively. The first-order rate constant for $[NiL_{12}]^{2+}$ was not determined due to the low solubility of the compound in water. While it would appear that the low solubility of the $[NiL_{4,8,12}]^{2+}$ compounds, in particular the $[NiL_{12}]^{2+}$, would favour using the $[Ni(hmca)(OH_2)]^{2+}$ as the excess reagent, this is not the optimal condition.

In this case it is better to have the $[NiL_{4,8,12}]^{2+}$ in excess because it minimizes the importance of knowing the exact concentration of the $[Ni(hmca)(OH_2)]^{2+}$. Under normal conditions, the $[Ni(hmca)(OH_2)]^{2+}$ compound will actually be in the nickel(II) state. For it to be used as an oxidant it must first be oxidized. This is done using a $Co^{3+}_{(aq)}$ in acid solution. The $Co^{3+}_{(aq)}$ solution oxidizes the $[Ni(hmca)(OH_2)]^{+}$ in a one-to-one ratio which allows for the theoretical concentration of the $[Ni(hmca)(OH_2)]^{2+}$ to be known.

As the $Co^{3+}_{(aq)}$ is unstable, its concentration does not remain constant and therefore must be determined prior to each use. The absorbance of the $Co^{3+}_{(aq)}$ solution is first measured using UV-vis spectroscopy to determine its concentration. The $Co^{3+}_{(aq)}$ solution is then used to oxidize the $[Ni(hmca)(OH_2)]^{2+}$ to $[Ni(hmca)(OH_2)]^{3+}$ stoichiometrically based on its determined concentration. This solution is then used as the oxidant with the $[NiL_{4,8,12}]^{2+}$ compounds. Because the $Co^{3+}_{(aq)}$ is not stable, the delay in the time from determining its concentration until it is used to oxidize the $[Ni(hmca)(OH_2)]^{+}$ will result in some small error as some of the $Co^{3+}_{(aq)}$ solution will have decomposed. The resulting $[Ni(hmca)(OH_2)]^{2+}$ solution is more stable than the $Co^{3+}_{(aq)}$ solution but there are still concerns with its stability and thus the actual concentration of the $[Ni(hmca)(OH_2)]^{2+}$ solution is never accurately known.

Reproduced with permission of the copyright owner. Further reproduction prohibited without permission.

Under pseudo first-order conditions, it is not required that the concentration of the non-excess reactant be accurately known. Thus, optimum results are achieved using $[NiL_{4,8}]^{2+}$ as the excess reagent. Unfortunately, these conditions are impractical for the $[NiL_{12}]^{2+}$ kinetics to be obtained, due to solubility limitations.

3.3.2 Temperature Dependence

The temperature dependence data for the rate constant for $[NiL_4]^{2+}$ with $[Ni(hmca)(OH_2)]^{2+}$ are given in Table 3.6 while the Eyring plot can be seen as Figure 3.9. The enthalpy and entropy of activation were calculated to be 11 ± 1 kJ·mol^{-1} and -130 ± 10 J·mol^{-1} K^{-1} respectively. These values are in line with the expected activation parameters for outer-sphere electron transfer reactions. The low enthalpy value is consistent with redox reactions where there is no bond breaking and the negative entropy value is a result of the increased ordering of the solvent shell that occurs when two water molecules coordinate to the $[NiL_4]^{2+}$ complex.

T/K	Replicate observed first-order rate constants k_{obs}/s^{-1}					k_1/mol^{-1} dm^3 s^{-1}
285	0.610	0.590	0.619	0.618	0.591	6000 ± 250
289	0.687	0.669	0.669	0.658	0.697	6760 ± 160
293	0.742	0.737	0.736	0.733	0.750	7400 ± 70
297	0.787	0.787	0.771	0.8001		7880 ± 90
302	0.840	0.823	0.826	0.821	0.820	8260 ± 80
306	0.855	0.872	0.855	0.863	0.897	8680 ± 180

Table 3.6 Observed first-order rate constants, k_{obs} for the oxidation of $[NiL_4]^{2+}$ by $[Ni(hmca)(OH_2)]^{2+}$ and calculated second-order rate constants, k_1 as a function of temperature. Concentrations of $[NiL_4]^{2+}$ and $[Ni(hmca)(OH_2)]^{2+}$ were 1.00 x 10^{-4} mol·dm^{-3} and 1.00 x 10^{-5} mol·dm^{-3} respectively.

Reproduced with permission of the copyright owner. Further reproduction prohibited without permission.

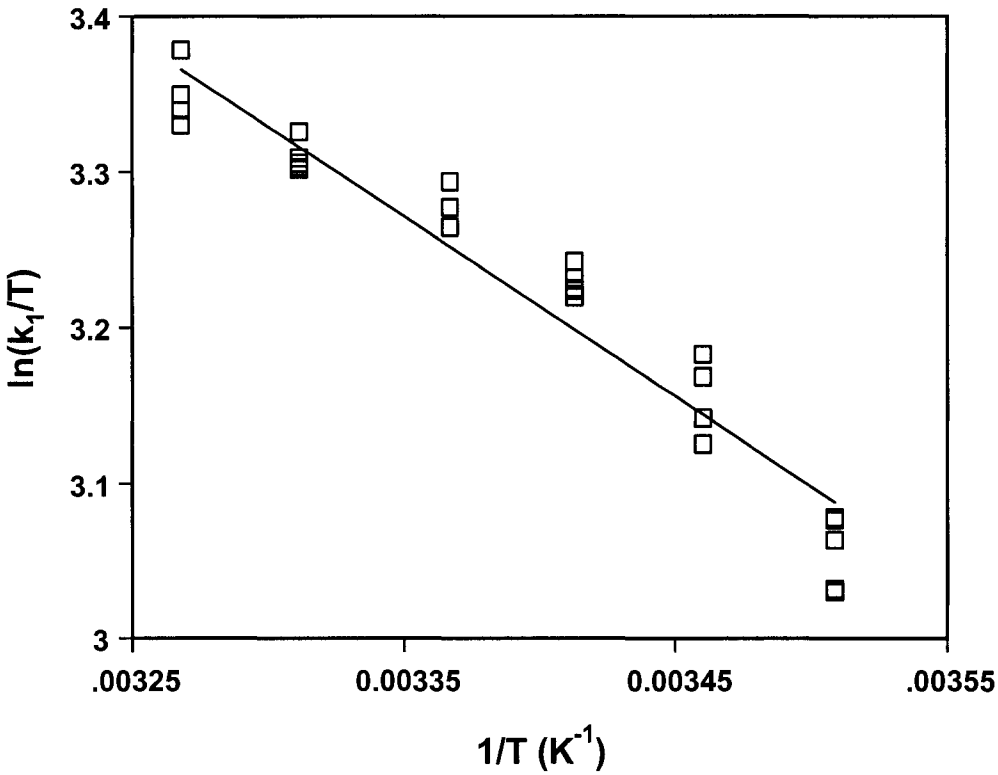

Figure 3.9 Eyring diagram for the oxidation of $[NiL_4]^{2+}$ by $[Ni(hmca)(OH_2)]^{2+}$over a temperature range of 285K to 306K.

3.3.3 Marcus Correlation

Marcus relationships are used here to determine the self-exchange rates for the $[NiL_{4,8,12}]^{2+}$ compounds. This will provide further information on the effect that the length of the pendant-arm has on the rate of oxidation. As the results from the concentration dependence studies for $[NiL_{4,8}]^{2+}$ showed that there was little difference in the k_{obs} observed for the compounds, it should be expected that the self-exchange rates for the complexes would also be similar. For the oxidation of $[NiL_{4,8,12}]^{2+}$ with $[Ni(hmca)(OH_2)]^{2+}$, the self-exchange reactions and cross reactions are as follows:

Reproduced with permission of the copyright owner. Further reproduction prohibited without permission.

$$[NiL_{4,8,12}]^{2+} + [Ni(hmca)(OH_2)]^{2+} \xrightarrow{k_{AB}} [NiL_{4,8,12}]^{3+} + [Ni(hmca)(OH_2)]^{+} \quad \text{(Equation 3.9)}$$

$$[NiL_{4,8,12}]^{2+} + [NiL_{4,8,12}]^{3+} \xrightarrow{k_{AA}} [NiL_{4,8,12}]^{3+} + [NiL_{4,8,12}]^{2+} \quad \text{(Equation 3.10)}$$

$$[Ni(hmca)(OH_2)]^{2+} + [Ni(hmca)(OH_2)]^{+} \xrightarrow{k_{BB}} [Ni(hmca)(OH_2)]^{+} + [Ni(hmca)(OH_2)]^{2+} \quad \text{(Eq 3.11)}$$

Using the relationships in the above equations and the simplified Marcus equation (equation 1.9), k_{AB} represents the cross reaction rate for the $[NiL_{4,8,12}]^{2+}$ cation with $[Ni(hmca)(OH_2)]^{2+}$, which is taken from the observed kinetic data. The k_{AA} and k_{BB} values are the self-exchange rates for $[NiL_{4,8,12}]^{2+}$ and $[Ni(hmca)(OH_2)]^{2+}$ respectively where k_{BB} has been taken from the literature[92] and k_{AA} is the value to be calculated. The K_{AB} value is determined from the electrochemical data of the two reactants using the following equation.

$$K = e^{\frac{nF\Delta E^{\circ}}{RT}} \quad \text{(Equation 3.12)}$$

This expression can also be written as

$$\ln K = \frac{nF\Delta E^{\circ}}{RT} \quad \text{(Equation 3.13)}$$

where ΔE° is the difference in redox potential between the $[NiL_{4,8,12}]^{2+}$ and the $[Ni(hmca)(OH_2)]^{2+}$ species. Thus:

$$\ln K = \frac{(1)(96500\ C/mol)(.845V-.720V)}{(8.314J\cdot mol^{-1}\cdot K^{-1})(298.2K)}$$

Hence $K = 130$

Reproduced with permission of the copyright owner. Further reproduction prohibited without permission.

As mentioned above, the simplified Marcus equation where f_{AB} is assumed to be unity can be used when the equilibrium constant is not large, which is the case here. It can be rearranged to solve for the self-exchange rate (k_{AA}).

$$k_{AA} = \frac{(k_{AB})^2}{(k_{BB})(K_{AB})} \qquad \text{(Equation 3.14)}$$

These values can now be substituted into equation 3.14 to determine k_{AA} for $[NiL_4]^{2+}$ and $[NiL_8]^{2+}$ at 298K. For $[NiL_4]^{2+}$:

$$k_{AA} = \frac{(7950\ mol^{-1}dm^3s^{-1})^2}{(870\ mol^{-1}dm^3s^{-1})(130)}$$

$$k_{AA} = 560\ mol^{-1}dm^3s^{-1}$$

The equation yields a k_{AA} value for $[NiL_8]^{2+}$ of 440 $mol^{-1}dm^3s^{-1}$. A second-order rate constant could not be determined for the $[NiL_{12}]^{2+}$ in the absence of cyclodextrin. However, using the estimated second-order rate constant obtained with cyclodextrin present (section 3.3.4), a second-order rate constant (k_{AA}) of 375 $mol^{-1}dm^3s^{-1}$ can be estimated. While self-exchange rates do appear to decrease slightly as the chain length is increased, the values of k_{AA} obtained for $[NiL_{4,8,12}]^{2+}$ are all very similar to one another indicating that the length of the appended alkyl chain has only a small effect, if any on the self-exchange rates of the complexes. This is not unexpected based on the previous determination from the kinetic data, that the length of the appended alkyl tail has little effect on the rate of oxidation. The estimate of the k_{AA} values are in good agreement with the self-exchange rates of other nickel(II/III) tetraazamacrocyclic systems,[93] which have self-exchange rates in the region of 1500 $mol^{-1}\ dm^3\ s^{-1}$. For example, $[Ni(cyclam)]^{2+}$ has a self-exchange rate of 2000 $mol^{-1}\ dm^3\ s^{-1}$.

Reproduced with permission of the copyright owner. Further reproduction prohibited without permission.

3.3.4 Oxidation Kinetics in the presence of Cyclodextrin

From our understanding of the redox kinetics of the $[NiL_{4,8,12}]^{2+}$ macrocycles it is now possible to use the oxidation kinetics to probe the interaction between the $[NiL_{4,8,12}]^{2+}$ and the cyclodextrins. For this to be true though, it is necessary for the presence of cyclodextrin to have a measurable effect on the rate of the reaction. For an example of this, the presence of cyclodextrin is often known to increase the fluorescence of many organic molecules or, as was discussed earlier, the presence of cyclodextrin may shift the electrochemical waves in the cyclic voltammogram. Association constants are often measured based on the change in proton shift of one of the molecules. Regardless, by comparing what occurs in the absence and presence of the cyclodextrin it is possible to mathematically determine the binding constant.

We have shown through the ESMS results that there is in fact an association, this was supported by the limited NMR data. From electrochemical measurements, we have shown that the presence of the cyclodextrin does not affect the redox potential of the metal center which means that any observed change in the rate of reaction in the presence of cyclodextrin must be a steric effect that hinders the bringing together of the oxidant and reductant. The kinetic study for the oxidation of $[NiL_{4,8,12}]^{2+}$ by $[Ni(hmca)(OH_2)]^{2+}$ shows that the system is a well behaved outer-sphere oxidation that is typical of similar transition metal complexes. This information allows for the association constant to be determined on a kinetic basis, based on the effect that cyclodextrin has on the rate of oxidation. By understanding how the oxidation reaction occurs, we can derive an expression that will include rate for the oxidation with and without cyclodextrin and will take into account the formation of the supramolecular complex between $[NiL_{4,8,12}]^{2+}$ and the cyclodextrin. This expression can provide the association constant between the $[NiL_{4,8,12}]^{2+}$ and the cyclodextrin molecule.

Reproduced with permission of the copyright owner. Further reproduction prohibited without permission.

It is known that the equilibrium formation of the supramolecular complex will occur rapidly[94] which means that the first step of the overall reaction mechanism will be the formation of the supramolecular complex between the $[NiL_{4,8,12}]^{2+}$ and the cyclodextrin molecule. The amount of the $[NiL_{4,8,12}]^{2+}$ that will participate in the supramolecular complex will depend on the association constant. Thence, the $[NiL_{4,8,12}]^{2+}$ and $[NiL_{4,8,12}(CD)]^{2+}$ species will be oxidized by $[Ni(hmca)(OH_2)]^{2+}$ in parallel pathways. The overall reaction scheme is seen below:

$$[NiL_{4,8,12}]^{2+} + [CD] \overset{K_{CD}}{\rightleftarrows} [NiL_{4,8,12}(CD)]^{2+} \qquad \text{(Equation 3.15)}$$

$$[NiL_{4,8,12}]^{2+} + [Ni(hmca)(OH_2)]^{2+} \overset{k_1}{\rightarrow} [NiL_{4,8,12}]^{3+} + [Ni(hmca)(OH_2)]^{+} \qquad \text{(Equation 3.16)}$$

$$[NiL_{4,8,12}(CD)]^{2+} + [Ni(hmca)(OH_2)]^{2+} \overset{k_2}{\rightarrow} [NiL_{4,8,12}(CD)]^{3+} + [Ni(hmca)(OH_2)]^{+} \qquad \text{(Eq 3.17)}$$

From the overall reaction scheme the rate expression may be obtained from the knowledge that for parallel pathways, the overall rate is the sum of the rates for the individual pathways.

$$\text{Rate} = \frac{-d[NiL_{4,8,12}{}^{2+}]}{dt} = \left(k_1[NiL_{4,8,12}{}^{2+}] + k_2[NiL_{4,8,12}(CD)^{2+}]\right)[Ni(hmca)(OH_2)^{2+}] \qquad \text{(Equation 3.18)}$$

The concentrations of free $[NiL_{4,8,12}]^{2+}$ and complexed $[NiL_{4,8,12}(CD)]^{2+}$ are not known and therefore must be expressed in terms of the total $[NiL_{4,8,12}]^{2+}$ present in solution $[NiL_{tot}]$. This is done using the law of mass balance which provides the following terms (see Appendix B for complete mass balance derivation):

Reproduced with permission of the copyright owner. Further reproduction prohibited without permission.

$$[NiL_{4,8,12}{}^{2+}] = \left(\frac{1}{1+K_{CD}[CD]}\right)[NiL_{tot}] \qquad [NiL_{4,8,12}(CD)^{2+}] = \left(\frac{K_{CD}[CD]}{1+K_{CD}[CD]}\right)[NiL_{tot}] \qquad \text{(Eq 3.19a,b)}$$

Substituting these into equation 3.18 produces

$$\text{Rate} = \left(\frac{k_1}{1+K[CD]} + \frac{k_2 K[CD]}{1+K[CD]}\right)[NiL_{tot}][Ni(hmca)(OH_2)^{2+}] \qquad \text{(Equation 3.20)}$$

From the pseudo first-order conditions with $[NiL_{4,8,12}]^{2+}$ in excess, we can say that:

$$\text{Rate} = k_{obs}[Ni(hmca)(OH_2)^{2+}] \qquad \text{(Equation 3.21)}$$

By combining equations 3.20 and 3.21 we obtain:

$$k_{obs} = \left(\frac{k_1 + k_2 K_{CD}[CD]}{1+K_{CD}[CD]}\right)[NiL_{tot}] \qquad \text{(Equation3.22)}$$

This expression can then be written as:

$$\frac{k_{obs}}{[NiL_{tot}]} = \frac{k_1 + k_2 K_{CD}[CD]}{1+K_{CD}[CD]} \qquad \text{(Equation 3.23)}$$

This is the derived rate expression and is used to fit the data. From this expression, the oxidation kinetics for $[NiL_{4,8,12}]^{2+}$ with $[Ni(hmca)(OH_2)]^{2+}$ can be graphed as a plot of $k_{obs}/[NiL_{tot}]$ *versus* cyclodextrin concentration. This will produce a non-linear graph that can be fit to the rate expression using non-linear least- squares fitting with the FigP software program.

Inspection of the rate expression explains the observed curvature of the data. At zero cyclodextrin concentration, the rate expression simplifies to

$$\frac{k_{obs}}{[NiL_{tot}]} = \frac{(k_1 + 0)}{(1+0)}$$

$$= k_1$$

Reproduced with permission of the copyright owner. Further reproduction prohibited without permission.

where k_1 is the second-order rate constant in the absence of cyclodextrin. This simplification remains true for low [CD] as well, where it can be assumed that $k_1 >>> k_2K_{CD}[CD]$ and $1 >>> K_{CD}[CD]$.

At the other extreme, when high [CD] is present, the assumptions can be made that $k_2K_{CD}[CD] >>> k_1$ and $K_{CD}[CD] >>> 1$. The rate expression thus becomes:

$$\frac{k_{obs}}{[NiL_{tot}]} = \frac{k_2K_{CD}[CD]}{K_{CD}[CD]} \qquad \text{(Equation 3.24)}$$

$$= k_2$$

where k_2 is the second-order constant for the oxidation when saturation of the $[NiL_{4,8,12}(CD)]^{2+}$ complex has occurred. These two values can be estimated visually from the plot as k_1 will be the y-intercept and the k_2 is the extrapolated limiting value of k_{obs}.

The results obtained for the effect of α- and β-cyclodextrin on the rate of oxidation for $[NiL_{4,8,12}]^{2+}$ can be seen in Table 3.7. Following the table, the plot of the data for β-cyclodextrin with $[NiL_{4,8,12}]^{2+}$ is shown as Figure 3.10. The plot demonstrates the large difference in effect that β-cyclodextrin has on the three compounds, based on the length of the attached alkyl chain pendant-arm.

Reproduced with permission of the copyright owner. Further reproduction prohibited without permission.

	α-CD		β-CD	
Complex	10^3[CD]/M	$(k_{obs}/[NiL_{tot}])/M^{-1}s^{-1}$	10^3[CD]/M	$(k_{obs}/[NiL_{tot}])/M^{-1}s^{-1}$
$[NiL_4]^{2+}$	0	8287	0	8391
	0.908	8435	1.74	8505
	1.82	7929	3.48	8480
	3.63	8514	5.22	8474
	2.73	7958	6.58	8565
	4.54	8300		
	5.45	8380		
	6.36	8213		
$[NiL_8]^{2+}$	0.907	8410	0	8000
	1.81	7700	0.435	7850
	2.72	7430	0.870	7695
	3.63	7040	1.74	7605
	4.54	6970	2.61	7540
			3.48	7485
			4.35	7295
			5.22	7230
			6.09	6975
$[NiL_{12}]^{2+}$			0.348	4873
			0.783	4642
			1.22	4337
			1.65	4273
			2.09	4236
			2.96	4171

Table 3.7 Second-order rate constants $(k_{obs}/[NiL_{4,8,12}])$, as a function of increasing [CD] at 298K. Constant concentrations of 1.00×10^{-4} mol·dm^{-3} and 1.00×10^{-5} mol·dm^{-3} were maintained for $[NiL_{4,8,12}]^{2+}$ and $[Ni(hmca)(OH_2)]^{2+}$ respectively.

Reproduced with permission of the copyright owner. Further reproduction prohibited without permission.

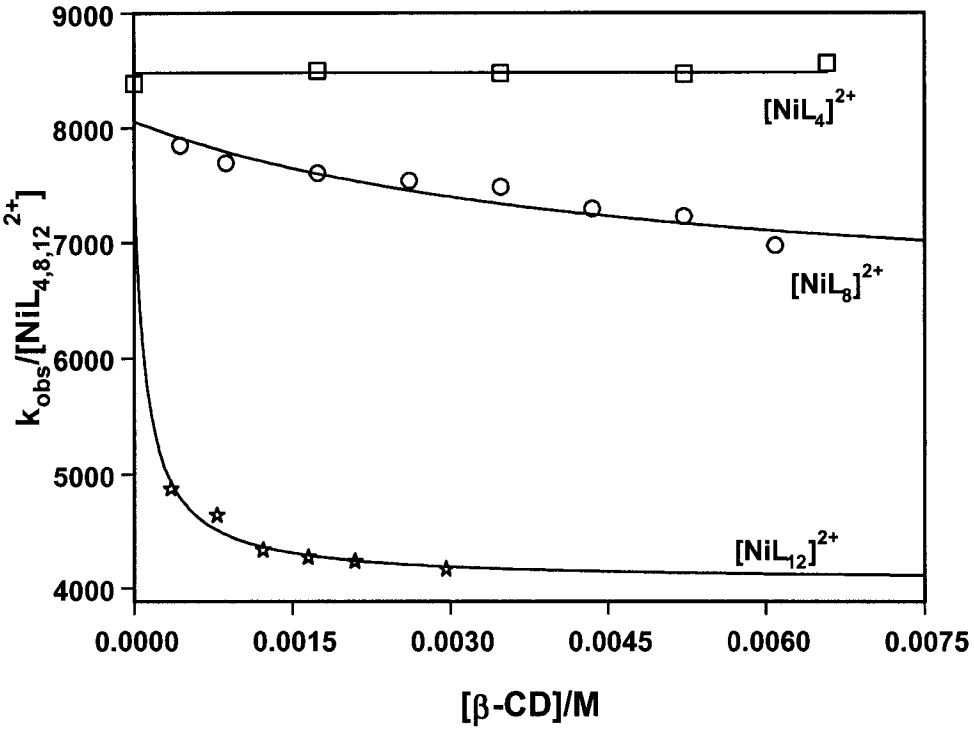

Figure 3.10 Plot of the second-order rate constants ($k_{obs}/[NiL_{4,8,12}^{2+}]$), as a function of increasing [β-CD] at 298K. Constant concentrations of 1.00 x 10^{-4} mol·dm^{-3} and 1.00 x 10^{-5} mol·dm^{-3} were maintained for $[NiL_{4,8,12}]^{2+}$ and $[Ni(hmca)(OH_2)]^{2+}$ respectively.

The plot in Figure 3.10 shows that as the length of the pendant-arm is increased, the effect that cyclodextrin has on the rate of oxidation of $[NiL_{4,8,12}]^{2+}$ is also increased. The results show that the $[NiL_4]^{2+}$ is essentially unaffected by the increasing [β-CD] while there is a slow decrease in rate with increasing [β-CD] for $[NiL_8]^{2+}$. In fact, the data for the $[NiL_4]^{2+}$ do not really fit the rate expression suggesting that there is little or no measurable association with β-cyclodextrin. The rate for the $[NiL_{12}]^{2+}$ appears to be significantly affected by the presence of [β-CD]. There is a large drop in the rate as [β-CD] is increased, even at low concentrations.

Table 3.8 provides a summary of the estimated k_1, k_2, and K_{CD} values obtained from non-linear least-squares fitting of the data in Table 3.7 to the derived rate expression (equation 3.23).

Reproduced with permission of the copyright owner. Further reproduction prohibited without permission.

Complex	CD	k_1/mol^{-1}dm^{3}s^{-1}	k_2/mol^{-1}dm^{3}s^{-1}	K_{CD}/mol^{-1}·dm^3
$[NiL_4]^{2+}$	α	8250 ± 210	NA	–
	β	8480 ± 60	NA	–
$[NiL_8]^{2+}$	α	9800 ± 500	6000 ± 400	1200 ± 200
	β	8100 ± 150	6400 ± 500	200 ± 100
$[NiL_{12}]^{2+}$	β	7500 ± 215	4060 ± 30	8500 ± 650

Table 3.8 Estimated values for k_1, k_2, and K_{CD} obtained from fitting of the data in table 3.7 for the change in $k_{obs}/[NiL_{4,8,12}]$ as a function of [CD] to equation 3.22.

The k_1 values obtained from fitting the data indicates that the length of the pendant-arm of each complex does not have a large effect as the k_1 is the rate in the absence of cyclodextrin. The earlier second-order rate constants and self-exchange values calculated indicated that the tail length had little or no effect. While the k_1 obtained here for the $[NiL_8]^{2+}$ and α-cyclodextrin system is slightly higher than the rest, the k_1 values are all approximately 8000 mol^{-1}dm^{3}s^{-1} which is similar to the previous second-order rate constants obtained for $[NiL_4]^{2+}$ and $[NiL_8]^{2+}$.

The results show that there is a significant decrease in the k_2 value from the k_1 values. It is reasonable that the rate will be reduced for the $[NiL_{4,8,12}(CD)]^{2+}$ complex compared to the free $[NiL_{4,8,12}]^{2+}$ compound. As mentioned earlier, this will be a steric effect as the cyclodextrin has been shown to not affect the redox potential of the nickel center. The access of the oxidant cation to the nickel center of the $[NiL_{4,8,12}]^{2+}$ complex will be partly inhibited by the cyclodextrin that is associated with the molecule. The assumption made when discussing the NMR titrations (section 3.2.2) was that the macrocyclic head-groups of the $[NiL_{4,8,12}]^{2+}$ compounds were too large to enter the cyclodextrin cavity, resulting in the cyclodextrin interaction with only the alkyl chain pendant-arm of the $[NiL_{4,8,12}]^{2+}$ compounds. This was supported by the estimated sizes of the

Reproduced with permission of the copyright owner. Further reproduction prohibited without permission.

head-groups and by the electrochemistry results. The rate reduction from the non-complexed $[NiL_{4,8,12}]^{2+}$ to the complexed $[NiL_{4,8,12}]^{2+}$ is also supportive of this assumption. It can be assumed that if the nickel centre was itself inside the cyclodextrin molecule that it would essentially be inaccessible to the oxidant and would result in a much larger reduction in the k values or even cessation of the reaction. In this case there is a reduction of about 20 - 50 % which is significant. Electron transfer will occur most easily when the oxidant can closely approach the reductant centre, which would be the axial positions of the compound as the macrocycle ring will block access to the sides of the nickel. In the case of the $[NiL_{4,8,12}(CD)]^{2+}$ complexes, access to the top and the bottom of $[NiL_{4,8,12}]^{2+}$ will only be slightly impeded by the cyclodextrin molecule as it is mostly peripheral to the site of electron transfer.

It should be remembered that the difference in the k_1 and the k_2 is not a measure of the binding constant. K_{CD} is a measure of the affinity between the $[NiL_{4,8,12}]^{2+}$ and the cyclodextrin. Recall that the formation of the $[NiL_{4,8,12}(CD)]^{2+}$ complex occurs before the oxidation of either species, thus the equilibrium constant (K_{CD}) and both rate constants (k_1 and k_2) are components of the composite k_{obs}.

While the individual rate constants provide insightful information about the effect the cyclodextrin has on the oxidation of $[NiL_{4,8,12}]^{2+}$, it is the binding constants that are of particular interest.

In comparing the binding constants there are a few factors to consider. First, the value for K_{CD} will be determined by the nature of both the host and the guest. In this case, the stability of the supramolecular complex will be influenced by the length of the alkyl chain pendant-arm as well as the cavity size of each cyclodextrin. Generally, the longer the alkyl tail, the stronger the association with the cyclodextrin molecules.

Reproduced with permission of the copyright owner. Further reproduction prohibited without permission.

The lack of measurable binding constants for the $[NiL_4]^{2+}$ complex is a result of the very small amount of association between the short four-carbon chain and the cyclodextrin molecule. While the K_{CD} values cannot be estimated, there is probably some association between the $[NiL_4]^{2+}$ but this method may not be sufficiently sensitive to quantify it. It would require the presence of very high [CD] which cannot be obtained due to the solubility limitations of the cyclodextrins. With such a short chain, there are several factors that work to prevent the formation of a strong supramolecular complex. These factors include the formation of the complex as well as the ability of any formed complex to remain intact.

First, the short chain means that the penetration of the tail into the cyclodextrin cavity will not be complete which results in the easy dissociation of any complex that does initially form. This is mostly a steric effect. The closer the size of the guest is to the cavity size of the cyclodextrin, the better the fit. This is important for both the length as well as the width. The short alkyl chain can only associate with part of the cyclodextrin cavity as it is much too short to thread completely through and it is known that the width of the short alkyl tail will not produce an ideal fit as the cyclodextrins are capable of enclosing compounds containing aromatic backbones which are much broader than the alkyl chain pendant-arm. However, it should be assumed that the alkyl chains have thermal motion in solution which will increase to some degree their effective cross-section but not to a large enough extent. From this it could be assumed that any interaction between the cyclodextrin and the $[NiL_4]^{2+}$ compounds would be stronger in the case of α-cyclodextrin as it has a reduced cavity size compared to the β-cyclodextrin which should increase the goodness-of-fit and thus strengthen the association.

The second factor is the lack of a driving force to form the complex. Recalling that the interior of the cyclodextrin molecule is hydrophobic it is going to attract molecules of similar

Reproduced with permission of the copyright owner. Further reproduction prohibited without permission.

character in aqueous solutions. The hydrophobic character of the $[NiL_{4,8,12}]^{2+}$ compounds is derived from the alkyl chain pendant arm while the head group is mostly hydrophilic. For the $[NiL_4]^{2+}$ compound there is little hydrophobic character associated with it. Therefore, the hydrophobic attraction with the cyclodextrin molecule will be small and results in an inability of the two species to form a supramolecular complex. This would also be a likely factor in the ability of a formed complex to remain intact. Considering that there is very little that will either drive the formation or hold the complex together it is not surprising that the binding constants would be extremely low.

The estimated K_{CD} values for the $[NiL_8]^{2+}$ complex are 1200 $mol^{-1}\cdot dm^3$ and 200 $mol^{-1}\cdot dm^3$ for α- and β-cyclodextrin respectively. As expected, these values indicate that the $[NiL_8]^{2+}$ forms significantly more stable complexes with the cyclodextrins than does $[NiL_4]^{2+}$, especially for α-cyclodextrin. Unlike the $[NiL_4]^{2+}$ compounds, the alkyl chain of the $[NiL_8]^{2+}$ is sufficiently long to thread completely through the cyclodextrin. As well, the longer chain increases the hydrophobic character of the $[NiL_8]^{2+}$ and results in more hydrophobic-hydrophobic interaction with the cyclodextrin. The binding constant for α-cyclodextrin is significantly larger than for β-cyclodextrin indicating that there is a stronger association with the α-cyclodextrin. This is most likely due to the smaller cavity size. As discussed, the smaller cavity size of the cyclodextrin will allow for a tighter fit with an alkyl chain, as a result the $[NiL_8]^{2+}$ favors the closer fit of the α-cyclodextrin.

For $[NiL_{12}]^{2+}$ the binding constant could only be estimated in the β-cyclodextrin case. It was determined to be 8500 $mol^{-1}\cdot dm^3$ which is much larger than any of the other observed binding constants and is indicative of the greater stability of the $[NiL_{12}(CD)]^{2+}$ complex. The increased magnitude for the K_{CD} value of $[NiL_{12}]^{2+}$ is a result of the tail length of the compound. First, the

Reproduced with permission of the copyright owner. Further reproduction prohibited without permission.

increased tail length will increase the hydrophobic character which will increase the interaction with the hydrophobic interior of the cyclodextrin similar to the $[NiL_8]^{2+}$ complex. However, this alone is probably not a great enough effect to justify the large difference in the binding constants. This is most likely due to the better fit achieved with the dodecyl chain by folding up inside the cyclodextrin molecule. A depiction of this is shown in figure 3.11. The increased length of the chain allows it to do so more freely than the shorter chains. The curling of the alkyl chain gives it a significantly greater width and is therefore better able to interact with the interior of the cyclodextrin as it will be closer in proximity. This has previously been seen for long chain sodium carboxylates with β-cyclodextrin.[74,95]

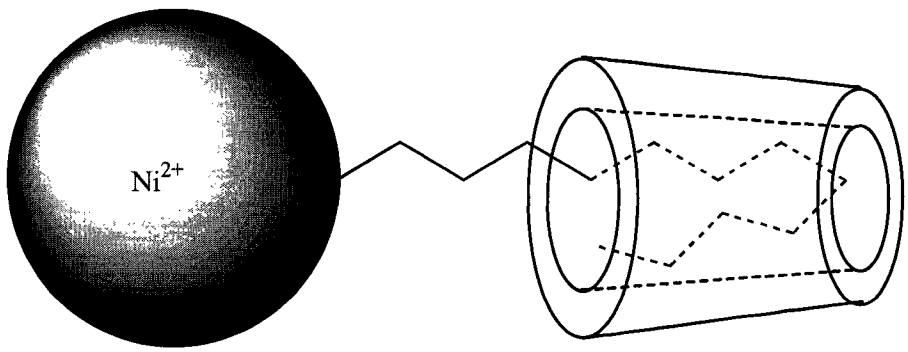

Figure 3.11 Proposed curling of the alkyl chain pendant-arm of the $[NiL_{12}]^{2+}$ inside the cavity of the cyclodextrin molecule.

Unfortunately, the binding constant for the α-cyclodextrin was not determined. The $[NiL_{12}]^{2+}$ had to be prepared in cyclodextrin solution as it was insoluble in pure water. While this was also true with β-cyclodextrin, there was an increased concentration required with α-cyclodextrin to solubilize the $[NiL_{12}]^{2+}$. This resulted in only a small range of practical α-cyclodextrin concentrations. As a result, the change in concentration did not have any effect on the rate of oxidation and thus did not provide data that fit the rate expression. Any data obtained

Reproduced with permission of the copyright owner. Further reproduction prohibited without permission.

showed the rate constant to be approximately 3800 $mol^{-1}dm^3s^{-1}$, including that for the solution with the minimum amount of cyclodextrin. Comparing this to the results for [β-CD], this would seem to be the limiting rate (k_2).

To compare the results obtained here with comparable systems[74,96-100] is very difficult as there are few to be found. As well, other reported binding constants for alkyl chains with cyclodextrins vary significantly depending on the method use. Also, small differences in the guest often have large effects on the binding constants. For example the binding constants for β-cyclodextrin with the sodium salts of $C_8H_{17}SO_3^-$ and $C_8H_{17}CO_2^-$ have been reported as 900 ± 110 and 2200 ± 300 $mol^{-1}\cdot dm^3$. In general these results are generally similar to other results which indicate that the binding constants for four-carbon tails are close to zero, the eight-carbon tails have binding constants in the range of 500 - 1000 $mol^{-1}\cdot dm^3$ and the binding constants for twelve-carbon chains can be ≥4000 $mol^{-1}\cdot dm^3$. It should be noted that the much larger K_{CD} value for α-cyclodextrin over β-cyclodextrin is almost unique to this study and that the binding constants presented here are usually smaller but comparable to other work.

To understand this it must be understood that the system studied here is significantly different from most other systems found. Most of the alkyl chains in other work will have a relatively small group such as CO_2^-, SO_4^-, or $[(CH_3CH_2\text{-})_3N]^+$. In this case the head group is much larger and will result in interference in the formation of the complex between the alkyl chain and the cyclodextrin. It is reasonable that the small head groups will have little or no steric hindrance compared to the very bulky macrocycle in this case. This is the most likely explanation for the generally lower binding constants as the more difficult it is to form or hold together the supramolecular complex, the lower the resulting association constant.

Reproduced with permission of the copyright owner. Further reproduction prohibited without permission.

3.4 Unsuccessful Synthesis of Azamacrocycles for Larger Metal Ions.

As was discussed in the introduction, it is possible to design macrocycles that are specific to a particular metal ion or a small group of metal ions. One part of this work was to try and develop macrocycles that would bind to different sized metal ions, including the larger second and third row metals. Presented here are the attempts to synthesize macrocyclic compounds that had potential to bind to larger transition metal ions.

The fourteen-membered tetraazamacrocycles are known to form very stable complexes with the first row transition metals. This is a result of both the nitrogen affinity for these metal ions, as well as the closeness of fit between the metal ion and the cavity of the fourteen-membered ring. It has previously been explained that it is these two characteristics, fit and nature of the donor atoms that are most important in designing a macrocyclic ligand to fit a specific metal ion. Larger metal ions generally require an increased cavity size within the macrocycle as they have larger ionic radii compared to nickel(II) which, as a first row transition metal, forms its most stable complexes with the fourteen- membered tetraazamacrocycles.

Several attempts were made to synthesize a tetraazamacrocycle that could be altered to increase its ability to form complexes with larger metal ions. This could be done by increasing the ring size and/or adding pendant-arms that include oxygen donor atoms in the form of carboxylic acids. The addition of carboxylic acid pendant-arms to an azamacrocycle has been carried out in this laboratory.[22,92] The addition of the carboxylic acid groups to the macrocyclic backbone provide additional coordinating atoms and can increase the macrocycle's metal-binding ability.

Reproduced with permission of the copyright owner. Further reproduction prohibited without permission.

3.4.1 Fourteen- and Fifteen-Membered Macrocycles

It was hoped that the $[NiL_{4,8,12}]^{2+}$ complexes could be altered to form complexes with larger metal ions. They already possessed the aliphatic tail that can be used to form supramolecular complexes with cyclodextrins and they contain four nitrogen atoms to which carboxylic acids could be appended. Unfortunately, these particular complexes are only attainable using the metal template synthetic method. This is a concern as it requires that the complex be demetallated to remove the metal ion and leave the free ligand which would be required to bind another metal. Demetallation of metal ion macrocyclic complexes is not uncommon but in this case the fifth nitrogen in the ring, although not coordinated to the metal ion, results in decreased stability of the ligand to dissociate from the metal and from a free ligand.[101] Attempts to demetalate such complexes results in decomposition of the macrocycle.

This discovery was problematic for several of the macrocyclic complexes. First, the $[NiL_{4,8,12}]^{2+}$ complexes could not be demetalated to produce the required free ligand. Also, attempts were made to synthesize a larger analog to the $[NiL_{4,8,12}]^{2+}$ complexes. The synthesis of the fifteen-membered analog, based on the adapted procedure for that of the fourteen-membered rings, proved unsuccessful. The only variance in procedure was the use of 3,2,3-tetraazadodecane in place of 2,3,2-tetraazaundecane. This would have produced a similar nickel(II) macrocyclic complex in that it would have had the hydrophobic chain attached to the macrocyclic backbone, but would have been slightly larger. It would have also had four potential nitrogens to which pendant-arms may have been attached and it would have had a larger cavity even if the carboxylic pendant-arms were not attached. Unfortunately, the use of nickel appears to be inappropriate in this case as the larger ring size is too large to allow the metal ion to act as a template. The results

Reproduced with permission of the copyright owner. Further reproduction prohibited without permission.

of this attempted synthesis produce a brownish-yellow coloured precipitate. However, this solid could not be purified as it was insoluble in all common solvents including methanol, ethanol, acetonitrile, dichloromethane, and THF - water mixtures. Regardless of the lack of success of this attempted synthesis, the end product would not have been useful as it also would have had the additional nitrogen in the ring and could not have been demetallated.

3.4.2 Sixteen-Membered Macrocycles

Attempts were made to synthesize 2,2,4,10,10,12-hexamethyl-1,5,9,13-tetraaza-cyclohexadecane *via* both the metal template and direct synthesis methods. The direct synthesis method was unsuccessful. The synthesis of its fourteen-membered analog, 2,2,4,9,9,11-hexamethyl-1,5,8,12-tetraazacyclotetradecane, is known to occur rapidly but the synthesis of the larger macrocycle did not work even with an extended reaction time. This is probably a result of the larger ring size making its synthesis too unstable without the aid of a templating metal ion.

Nickel(II) was used as a templating ion based on the known synthesis for the fourteen-membered analog. This also proved to be unsuccessful. The reaction time was prolonged up to three weeks at which point there was some precipitate but no solvent was able to dissolve the brown solid. Methanol, ethanol, acetonitrile, diethyl ether, dicloromethane and THF - water mixtures were all attempted. Considering that the nickel was too small to use with the fifteen-membered macrocycle, it is probably too small to be a template for the larger sixteen-membered macrocycle.

The larger ring cavity may have increased its ability to complex larger metal ions, but it would not have had the hydrophobic character associated with the $[NiL_{4,8,12}]^{2+}$ macrocycles. This

Reproduced with permission of the copyright owner. Further reproduction prohibited without permission.

would have excluded it from being used to form supramolecular complexes with the cyclodextrins. An attempt was made to synthesize a similar sixteen-membered complex with four of the six methyl substituents replaced with longer alkyl chains as depicted in figure 3.12. Butyl pendant-arms were the first group attempted. The result was not the desired compound but it did produce a new compound.

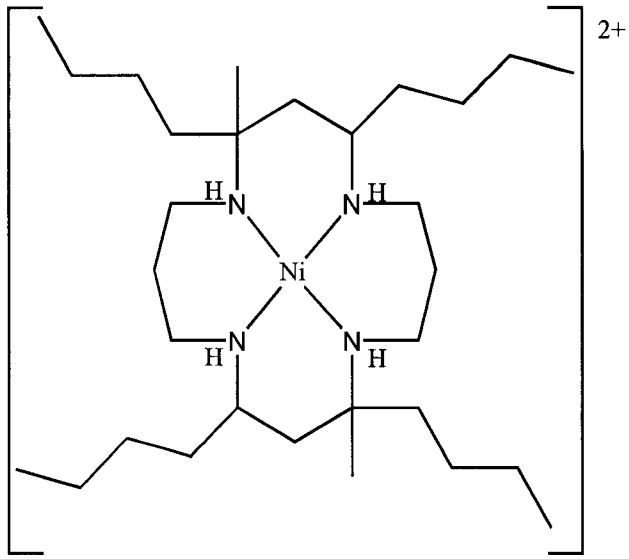

Figure 3.12 Proposed structure of 2,4,10,12-hexabutyl-2,10-dimethyl-1,5,9,13-tetraazacyclohexadecane.

3.4.3 $[Ni(dap)_2(MeCN)_2](ClO_4)_2$

The synthesis of the $[Ni(dap)_2(MeCN)_2](ClO_4)_2$ complex produced a purple coloured solid, characteristic of high-spin nickel(II) octahedral complexes.[102] The synthesized complex was achieved serendipitously as the goal of the procedure was the synthesis of the macrocycle with four butyl chains. The product was characterized by X-ray crystallography as well as UV-vis spectroscopy.

Reproduced with permission of the copyright owner. Further reproduction prohibited without permission.

The UV-vis spectrum of $[Ni(dap)_2(MeCN)_2](ClO_4)_2$ complex, Figure 3.13, in acetonitrile is typical of high-spin, octahedral nickel(II) compounds. The spectrum shows a maximum in the UV range at 342 nm and a maximum in the visible region at 549 nm. The respective molar absorptivities are 34.9 ± 0.3 $mol^{-1} \cdot dm^3 \cdot cm^{-1}$ and 10.9 ± 0.1 $mol^{-1} \cdot dm^3 \cdot cm^{-1}$. UV-Vis spectra could not be obtained in water as the complex is unstable in water. The addition of water caused decomposition of the complex resulting in the precipitation of pale green nickel(II) hydroxide.

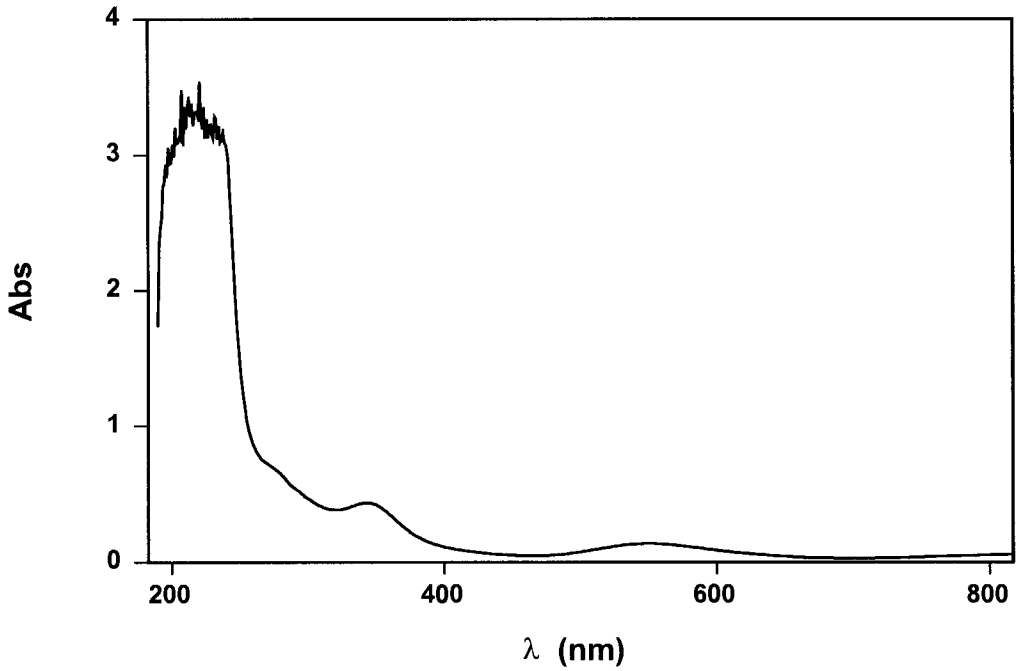

Figure 3.13 UV-vis spectrum of 1.24×10^{-2} $mol \cdot dm^{-3}$ $[Ni(dap)_2(MeCN)_2]^{2+}$ in MeCN at 298K.

The synthesis of the complex produced a purple colour which is well known for nickel(II) octahedral complexes. However, exposure to air caused desolvation of the complex and produced a yellow powder. This process was found to be easily reversible by reintroducing the

Reproduced with permission of the copyright owner. Further reproduction prohibited without permission.

desolvated complex to acetonitrile which returned the complex to its purple high-spin octahedral form after slow evaporation of liquid solvent. This behaviour is similar to that seen in the case of bis(2,6-dimethylpyrazine)copper(II) nitrate[103] where crystallization of the complex from THF solvent produced a complex with a THF solvent molecule coordinated to the copper ion. The same reversible behaviour occurs as the THF molecule is lost when dried but re-coordinates on dissolution in THF. Nickel(II) is known to have similar reversible coordination of solvent molecules. It is well know that for nickel(II) tetraazamacrocycles there exists an equilibrium in solution between the yellow square-planar complex $[NiL_{4,8,12}]^{2+}$ and the blue, octahedral solvated complex $[NiL_{4,8,12}S_2]^{2+}$ (where S = solvent). For 1,4,8,11-tetraazacyclotetradecane nickel(II), the ratio of the yellow to blue mixture in aqueous solution at room temperature is known to be 60:40.[104] This equilibrium is known to produce nickel complexes that are unsuitable for NMR analysis as the octahedral complex formed in aqueous solution is high-spin resulting in paramagnetic line broadening. This problem has previously been discussed in section 3.2.2.

3.4.3.a. Crystal structure of $[Ni(dap)_2(MeCN)_2](ClO_4)_2$

The crystal structure for $[Ni(dap)_2(MeCN)_2](ClO_4)_2$ is comprised of monomeric $[Ni(dap)_2(MeCN)_2]^{2+}$ cations that show an octahedral geometry about the nickel(II) centre, with the two bidentate diaminopropane ligands coordinated in a square-planar fashion to the nickel centre and two solvent acetonitrile molecules coordinated in the axial positions. This can be seen in the ORTEP diagram presented in figure 3.14.

Reproduced with permission of the copyright owner. Further reproduction prohibited without permission.

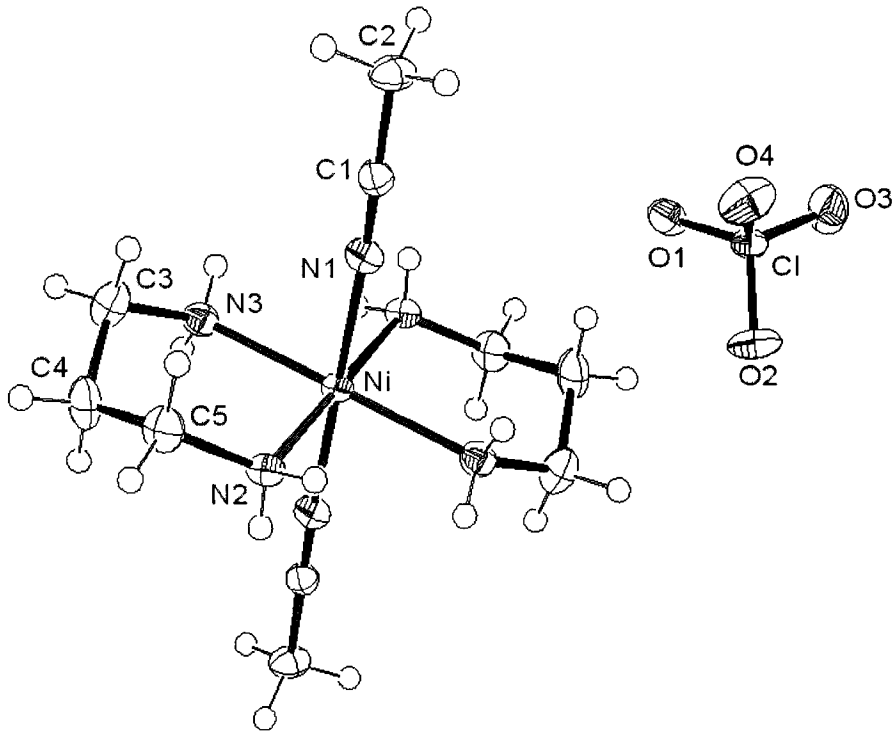

Figure 3.14 ORTEP diagram of $[Ni(dap)_2(MeCN)_2](ClO_4)_2$. Only one ClO_4^- is shown for clarity.

The perchlorate anions associated with the complex take up tetrahedral geometries with all bond angles close to the expected 109.5° common for tetrahedral complexes. Three of the bonds in the perchlorate ion are approximately of equal length (Cl-O(2) - 1.4304(17)Å, Cl-O(3) - 1.4320(19)Å and Cl-O(4) - 1.4265(17)Å) while the Cl-O(1) - 1.4389(16)Å is elongated slightly. It is interesting to note that the bond angles involving the elongated bond vary slightly from the 109.5° expected bond angle while the bond angles that exclude this bond are all very close to the expected value. Inspection of the unit cell packing diagram in Figure 3.15 indicates that hydrogen bonding exists between the O(1) of the perchlorate and the N-H of the complex which

Reproduced with permission of the copyright owner. Further reproduction prohibited without permission.

accounts for the variations in both the bond length and the bond angle involving the O(1) oxygen.

The N-Ni-N bond of the metal centre with the two axial acetonitrile units is linear at 180° but the Ni-N-C bond and the N-C-C bond angles within the acetonitrile units are slightly offset at 176.19(18)Å and 179.4(2)Å respectively.

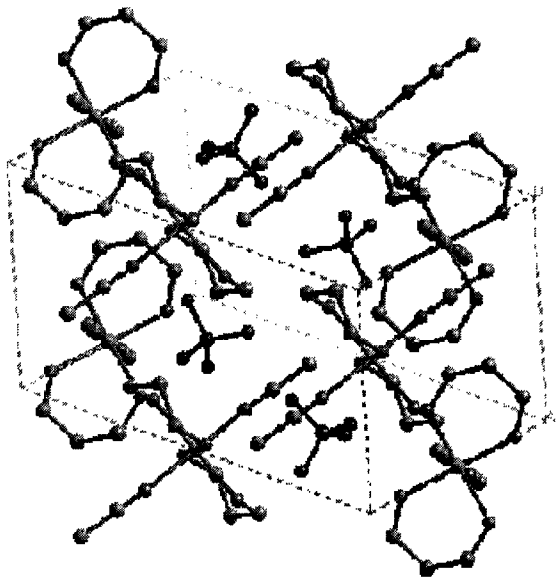

Figure 3.15 Unit cell for $[Ni(dap)_2(MeCN)_2](ClO_4)_2$

In a perfect square-planar molecule there are four 90° angles formed, however in this case, angles around the nickel centre involving the nitrogens of the two diaminopropane ligands are not equal. The N(2)-Ni-N(3) bond angle, that of the formed chelate ring, is 87.15(7)° while the bond angle between the N(3)-Ni-N(2)#1, where there is no chelate ring, is 92.85(7)°. As expected, the above bond angles of the nitrogens must total 180° which is the bond angle between N(3)-Ni-N(3)#1 as dictated by the centre of symmetry centred around the Ni centre. However, the smaller bond angle associated with the nitrogens that are part of the chelate ring indicates that the chelate

Reproduced with permission of the copyright owner. Further reproduction prohibited without permission.

ring acts to lessen this angle for the formation of the ring which does lead to some ring strain with N-C-C angles of 121.44(15)° and C-C-C bond angles of 112.0(2)°. The ligands take up the most thermodynamically favourable chair conformation which is common for metal complexes containing six-membered chelate rings.

There is also some slight distortion within the angle formed between N(axial)-Ni-N(equatorial) bonds. The N(2)-Ni-N(1) bond angle of 91.01(7)° matches the N(2)#1-Ni-N(1) bond angle of 88.99(7)° in the requirement that the sum to 180° based on the centre of symmetry about the nickel centre.

Comparing the angles formed in the chelate ring in the $[Ni(dap)_2(MeCN)_2]^{2+}$ complex to other complexes with similar chelate ring structures the bite angle formed in the six-membered chelate ring of $[Ni(2,3,2\text{-tet})]^{2+}$ has been reported as 94.5(2)° which is significantly larger than the similar angle observed for the $[Ni(dap)_2(MeCN)_2]^{2+}$ compound, however, the $[Ni(2,3,2\text{-tet})]^{2+}$ is different in that each of the nitrogen atoms that are part of the six-membered chelate are also part of separate five-membered chelate rings which have less flexibility with less atoms. As a result, the two five-membered rings pull their corresponding nitrogen atoms together to form the ring thus decreasing the angle. The decrease in this angle then results in an increased bite angle for the six-membered ring.

A better complex for comparison is $[Cu(dap)_2](NO_2)_2$ [81] which is structurally similar to the $[Ni(dap)_2(MeCN)_2]^{2+}$ complex. The only differences are the metal centre and the different axial coordinated molecules. The bite angle formed in the $[Cu(dap)_2]^{2+}$ complex is 86.8(2)° which compares very well to 87.15(7)° bite angle observed in the $[Ni(dap)_2(MeCN)_2]^{2+}$ complex. The six-membered chelate ring in the $[Cu(dap)_2]^{2+}$ complex takes the same *trans-III* chair

Reproduced with permission of the copyright owner. Further reproduction prohibited without permission.

conformation as seen in this $[Ni(dap)_2(MeCN)_2]^{2+}$ complex, further indicating the increased stability accorded to such conformations.

Comparing the bond lengths formed between the metal centre and the coordinated nitrogens of the chelate rings of the two compounds discussed and presented here, it should be noted that the bond lengths for the $[Ni(dap)_2(MeCN)_2]^{2+}$ complex (2.1017(17)Å, 2.1017(17)Å, 2.1042(17)Å, 2.1042(17)) are longer than those formed for the $[Ni(2,3,2\text{-tet})]^{2+}$ complex (1.907(5)Å, 1.928(5)Å, 1.934(5)Å, 1.916(5)Å). This is a direct function of the axial ligands that are present on the $[Ni(dap)_2(MeCN)_2]^{2+}$ complex but absent on the $[Ni(2,3,2\text{-tet})]^{2+}$ complex. This is known as Jahn-Teller distortion which describes the effect that axial ligands have on the planar ligands. As the axial ligands are moved further away from the centre, the planar ligands are consequently pulled closer and *vice versa*. The $[Ni(2,3,2\text{-tet})]^{2+}$ molecule represents the extreme case where there are no axial ligands, thus the bond lengths of the planar ligands are shorter. Comparing these bond lengths to those found for the previously discussed $[NiL_8]^{2+}$ cation, which has no axial ligands, the Ni-N bond lengths of the $[Ni(dap)_2(MeCN)_2]^{2+}$ complex are significantly longer than those for the $[NiL_8]^{2+}$ cation, as expected.

3.5 THF - Water Solubility Properties of $[NiL_{4,8,12}]^{2+}$

The study of mixed solvents and their effects on their solutes is not uncommon. In this case the effect of aqueous THF mixtures on the solubility of the $[NiL_{8,12}]^{2+}$ complexes was studied as a function of increasing THF mole fraction in the solvent mixture. This particular solvent combination does not appear to be all that common as there is very little literature on the subject. The results obtained for the solubility of the $[NiL_{8,12}]^{2+}$ complexes in the varying THF - water

Reproduced with permission of the copyright owner. Further reproduction prohibited without permission.

solvent mixtures are interesting.

Figure 3.16 below shows the absorbance at 450 nm of saturated solutions of $[NiL_8]^{2+}$ and $[NiL_{12}]^{2+}$ *versus* an increasing THF to water mole ratio. Unfortunately, the $[NiL_4]^{2+}$ complex was determined to be too soluble to complete the studies.

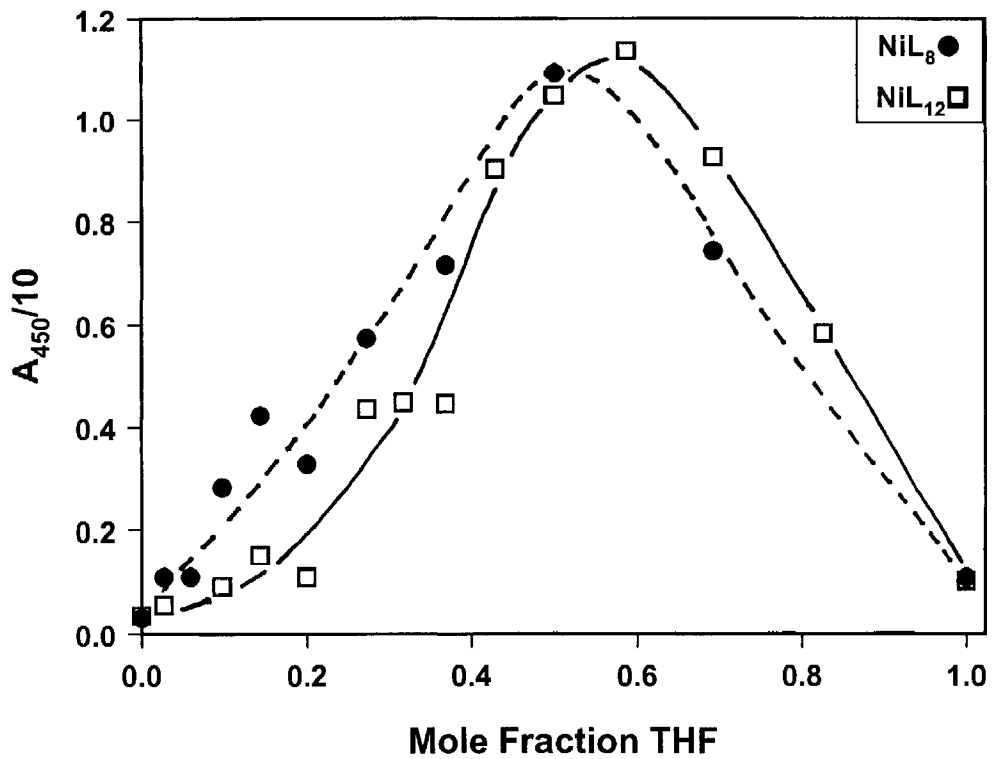

Figure 3.16 Absorbance versus THF mole fraction for $[NiL_8]^{2+}$ and $[NiL_{12}]^{2+}$ at 298K.

The graph shows that the compounds have extremely low solubility in pure water as well as in low THF compositions. The solubility does increase slightly as the THF composition moves to the 0.14 to 0.20 mole fraction range, but the compounds are still only sparingly soluble. There is a large increase in solubility at a mole fraction of approximately 0.5 - 0.6. This

Reproduced with permission of the copyright owner. Further reproduction prohibited without permission.

maximum in solubility is then followed by a steady decrease from about mole fraction 0.6 THF through to pure THF solvent. Overall, the compounds appear to be equally sparingly soluble in pure THF and water but fairly soluble in a one-to-one mixture of the two solvents. The graph also indicates that the solubility for the $[NiL_8]^{2+}$ is generally greater that for $[NiL_{12}]^{2+}$ at low THF mole fractions.

This behaviour is not unknown for such nickel(II) azacompounds in the THF - water mixtures. Very similar results have previously been observed in this lab using similar nickel(II) macrocycles bearing either one or two pendant-arms.[105]

The most probable explanation for the observed solubility behaviour is that it is a result of the dual hydrophobic/hydrophilic nature of the $[NiL_{8,12}]^{2+}$ compounds. The charged metal centre, or head group, represents the hydrophilic nature of the compounds while the alkyl pendant-arms comprise the hydrophobic character of the compounds. In pure water these compounds have low solubility and the solubility decreases as the length of the pendant-arm increases adding further hydrophobic character to the compounds. The $[NiL_{12}]^{2+}$ compound had such low solubility that it was not possible to obtain a sufficiently concentrated solution for any of the studies without the use of cyclodextrin to increase its solubility. As the THF component of the solvent mixture is increased, the solubilities of the compounds start to increase slightly but the increased THF component does not appear to have much effect in the low to mid mole fraction regions. It is only when the molar fraction is increased to about 0.5 - 0.6 that the solubilities of the compounds increase greatly. If this was simply a matter of the compound having a much higher solubility in the THF solvent than in the water solvent, there would be a clear explanation. However, for each compound the solubility is approximately equal in pure THF and pure water.

Reproduced with permission of the copyright owner. Further reproduction prohibited without permission.

As a result of the dual hydrophobic/hydrophilic nature of the compounds, each compound will be comprised of parts that favour one of the two solvents. The charged head group will prefer the water solvent while the alkyl pendant-arm will be more stable in the less polar THF solvent. Thus, while either pure solvent does not solubilize the compound significantly, optimum mixtures of the two solvents do.

The occurrence of the maximum solubility at close to equimolar amounts suggest that this solvent composition strikes the optimum balance between the hydrophobic and the hydrophilic components of the compound. The low solubility in any mixed ratio other than that close to one-to-one also suggests that the affinity of the hydrophobic tail for THF and the hydrophilic head group for water are approximately equal. Had this peak occurred at higher mole fraction, it could be suggested that the tail had a higher affinity for the THF than the head-group for the water and *vice versa,* had the optimum mole fraction occurred at a lower mole fraction.

The point of maximum solubility was approximately equal for both the $[NiL_8]^{2+}$ and $[NiL_{12}]^{2+}$ however the $[NiL_8]^{2+}$ was more soluble in the lower THF mole fractions. In both compounds, there is no difference in the hydrophilic head group but the $[NiL_{12}]^{2+}$ compound should have slightly more hydrophobic character in its tail due to the increased length. This would suggest that the $[NiL_8]^{2+}$ would be increasingly soluble in the more hydrophilic solvent mixtures. While the opposite may be true for the more hydrophobic mixtures, it is inconclusive from the chart. The higher solubility of the $[NiL_4]^{2+}$ compound in the low THF mole fractions also supports this observation as it has the least hydrophobic character

The solvation properties in THF - water mixtures were used to attempt to grow crystals of the compounds. A solution with a THF mole fraction of approximately 0.6 was used to dissolve

Reproduced with permission of the copyright owner. Further reproduction prohibited without permission.

the compound. The solution was then left standing to allow the THF to evaporate by effusion. As the THF evaporates the mole fraction of THF decreases resulting in reduced solubility of the compound causing it to precipitate out. This process is relatively slow, allowing crystals to form. This slow precipitation does occur, but the resulting solid compound does not produce crystals suitable for X-Ray analysis. While this process did not produce the desired results for this compound, there is the potential that other compounds of similar dual hydrophobic/hydrophilic character may also display similar characteristics in the mixed solvent which may allow for facile crystal growth.

3.6 Future Work

There are a number of directions that can be taken to further complement the work presented in this thesis. Any further work can be categorized as work to continue studying the supramolecular complexes that are formed between the pendant-arms of the macrocyclic complexes and the host cyclodextrin molecules, or as work to further develop macrocycles that could be used as heavy metal sensors.

3.6.1 Supramolecular Complexes

The work presented here has shown that there is a supramolecular complex formed between the macrocycle and the cyclodextrin molecules. However, the difficulties encountered in quantifying the stability of such complexes, *via* binding constant determination, indicate that the system could be modified.

The binding constants could only be estimated on a kinetic basis and thus could not be repeated by a second method. One method that may allow for the estimation of a second set of

Reproduced with permission of the copyright owner. Further reproduction prohibited without permission.

binding constants is NMR. Recalling that the difficulty encountered with the NMR technique was largely due to the paramagnetic line broadening associated with the nickel(II), it will require the development of a system that is not paramagnetic, such as palladium(II).

NMR may also be more useful if the solubility of the nickel(II) macrocycle was increased. While this would not eliminate the line broadening, the increased solubility would allow for more concentrated $[NiL_{4,8,12}]^{2+}$ solutions. This may make it possible to measure the change in the NMR by following the better defined peaks associated with the cyclodextrins – recall that the chemical shift of the compound not in excess is studied. This may be done by using a counter-ion other than perchlorate. Perchlorate is chosen as it is known to be non-coordinating and thus does not affect the electrochemistry at the metal centre, nor the outer-sphere nature of the redox kinetics. Any other counter-ion would need to be of similar character.

Another possibility is to have a nickel(II) macrocycle that has a fluorescent marker. This potentially would make it possible to study the binding constants from both kinetic and fluorescence methods. There are a number of examples where macrocyclic compounds contain aromatic pendant-arms. 2,2,4,9,9,11-Hexamethyl-1,5,8,12-hexamethylcyclotetradecane copper(II) perchlorate with two naphthalene pendant-arms (attached at N5 and N12) has been synthesized in this lab. While free naphthalene is known to fluoresce, it would have to be determined if this remains true when part of a part metal ion - macrocyclic system. It may also be possible to use complexes similar to those studied here but with aniline pendant-arms replacing the alkyl chains used here.

Once a system is established to determine the binding constants on the one-armed macrocycles, it follows that this system should be expanded to study two-armed macrocyclic complexes. This would return us to where this path of study originated.

Reproduced with permission of the copyright owner. Further reproduction prohibited without permission.

3.6.2 Macrocycles for Larger Metal Binding

The work on this topic is far from complete and in fact was only a secondary aspect within this thesis. The requirements for a macrocyclic compound to form stable complexes with different metal ions have already been outlined.

To form macrocyclic ligands that have the ability to form complexes with larger metal ions, where the ligand is somewhat selective will be mostly based on the size of the macrocycle itself. The closeness of the fit between the cavity and the metal ion will determine the stability. Therefore, future attempts to synthesize the larger macrocycles will probably benefit from using a larger metal ion. However, some preliminary work using palladium has been done in this lab and the process is more complex than expected where simply using a palladium ion in place of nickel in the synthesis does not provide great results. Thus there is work to be done to determine the best method for the larger ring sizes.

It may also be possible to change the binding characteristics of the macrocycle by changing the nature of the pendant-arms to include amines that provide additional coordinating atoms, similar to the addition of carboxylate groups. Any of these change may provide macrocycles that bind preferentially to specific groups of metals.

From this point the specificity can potentially be increased in several ways. The rigidity of a macrocycle can be increased by the addition of bridges between the donor atoms. The increased rigidity will increase the specificity based on the size of the metal ion. As well the nature of the donor atoms within the macrocycle can be altered to preferentially bind one metal over another.

Reproduced with permission of the copyright owner. Further reproduction prohibited without permission.

Chapter 5 - Conclusions

The work completed here has shown that the use of oxidation kinetics is a viable method for determining association constants with cyclodextrins. The $[NiL_{4,8,12}]^{2+}$ compounds have been shown to form supramolecular complexes with α- and β-cyclodextrins. Evidence of the formation of the complexes was observed through ESMS and NMR titrations but the association constants could not be quantified.

The kinetics of oxidation of the $[NiL_{4,8,12}]^{2+}$ by $[Ni(hmca)(OH_2)]^{2+}$ produced rate constants and activation parameters that were consistent with those of typical outer-sphere systems. Results indicated that length of the pendant-arm tail had minimal effects on the oxidation rate. Similarly, electrochemical measurements showed that the redox potential of the nickel(II/III) centre was unaffected by the length of the tail or the presence of cyclodextrin in solution. The latter, coupled with the well behaved oxidation kinetics observed, allowed for the association constants to be estimated based on the oxidation kinetics. The rate of oxidation was significantly slowed by the

Reproduced with permission of the copyright owner. Further reproduction prohibited without permission.

presence of cyclodextrin in solution. The derived rate expression for the oxidation kinetics in the presence of cyclodextrin produced estimated association constants. The association constants were dependent on both the length of the tail of each complex and the size of the cylodextrin and were generally similar to association constants for cyclodextrins with other alkyl chains.

The unsuccessful synthesis of larger azamacrocycles using nickel as a template ion indicated the nickel is too small and that these complexes are probably more accessible using a larger template ion. However, the attempted synthesis of a sixteen-membered ring with four butyl group pendant-arms did produce $[Ni(dap)_2(MeCN)_2](ClO_4)_2$, for which a crystal structure was obtained.

Reproduced with permission of the copyright owner. Further reproduction prohibited without permission.

References

1. House, D.A.; Curtis, N.F. *J.Am. Chem. Soc.* **1962**, *84*, 3248; Blight, M.M.; Curtis, N.F. *J. Chem. Soc.* **1962**, 1204; House, D.A.; Curtis, N.F. *J. Chem. Soc.* **1964**, 223.

2. Thompson, M.C.; Busch, D.H. *J. Am. Chem. Soc.* **1964**, *86*, 3651; Melson, G.A. Busch, D.H. *J. Am. Chem. Soc.* **1965**, *87*, 1706; Taylor, L.T.; Vergez, S.C. Busch, D.H. *J. Am. Chem. Soc.* **1966**, *88*, 3170.

3. Gerbeleu, N.V.; Arion, V.B.; Burgess, J. "Template Synthesis of Macrocyclic Compounds", Wiley-VHC, New York, **1999**.

4. Melson, G.A. "Coordination Chemistry of Macrocyclic Compounds", Plenum Press, New York, **1979**, p 2.

5. Bosnich, B.; Poon, C.K.; Tobe, M.L. *Inorg. Chem.* **1965**, *4*, 1102.

6. Bosnich, B.; Tobe, M.L.; Webb, G.A. *Inorg. Chem.* **1965**, *4*, 1109.

7. Lindoy, L.F.; "The Chemistry of Macrocyclic Ligand Complexes", Cambridge University Press, Cambridge, **1989**, p 2.

8. Byriel, K.; Dunster, K. R.; Gahan, L.R.; Kennard, C.H.L.; Latten, J.L.; Swann, I.L.; Duckworth, P.A. *Polyhedron*, **1992**, *11*, 1205.

9. Lindoy, L.F.; "The Chemistry of Macrocyclic Ligand Complexes", Cambridge University Press, Cambridge, **1989**, p 235.

10. Ghosh, A.; Wondigmagegn, T; Ryeng, H. *Curr. Opin. in Chem. Biol.* **2001**, *5*, 744.

11. Schroder, F.C.;Farmer, J.J.; Smedley, S.R.; Eisner, T.; Meinwald, J. *Tetrahedron Lett.* **1998**, *39*, 6625.

12. Cabbiness, D.K.; Margerum, D.W. *J. Am. Chem. Soc.* **1969**, *91*, 6540.

13. Kodama. M.; Kimera, E. *J. Chem. Soc., Chem. Com.* **1975**, 326; Kodama. M.; Kimera, E. *J. Chem. Soc., Dalton Trans.* **1976**, 116.

14. Hinz, F.P.; Margerum, D.W. *Inorg. Chem.* **1974**, *13*, 2941.

15. Frensdorff, H.K. *J. Am. Chem. Soc.* **1971**, *93*, 600.

16. Melson, G.A. "Coordination Chemistry of Macrocyclic Compounds", Plenum Press, New York, **1979**, p 166.

Reproduced with permission of the copyright owner. Further reproduction prohibited without permission.

17. Haines, R.I.; McAuley, A. *Coord. Chem. Rev.*, **1981,** 39, 77.

18. Bernard, B.R.; Haines, R.I.; Rowley, J.E. *Transition Met. Chem.* **2001**, *26*, 164.

19. Fabbrizzi, L.; Lari, A.; Poggi, A.; Seghi, ,B. *Inorg. Chem*, **1982**, *21*, 2083.

20. Koek, J.H.; Kohlen, E.W.M.J.; Russel, S.W.; van der Wolf, L.; ter Steeg, P.F.; Hellemons, J.C. *Inorg. Chim. Acta* **1999**, *295*, 189.

21. Lindoy, L.F.; "The Chemistry of Macrocyclic Ligand Complexes", Cambridge University Press, Cambridge, **1989**, p 51.

22. Haines, R.I.; Hutchings. D.R.; Lucas, R.J.; Miller, D. *Can. J. Chem.* **2001**, *79*, 54.

23. Korybut-Daszkiewicz, B.; Gluzinski, P. Kajewski, J.; Kremme, A.; Misnev, A. *Eur. J. Inorg. Chem.* **1999**, 263.

24. Davis, P.J.; Wainright, K.P. *Inorg. Chim. Acta* **1999**, *294*, 103.

25. Freeman, G.M.; Barfield, E.K.; Van Derveer, D.G. *Inorg. Chem.* **1984**, *23*, 3092.

26. Bu, X.H.; An, Y.T. Chen, M.; Shionoya, M. Kimura, E. *J. Chem. Soc., Dalton Trans.* **1995**, 2289.

27. Wong, E.H.; Weisman, G.R.; Hill, D.C.; Reed, D.P.; Rogers, M.E.; Condon, J.S.; Fagan, M.A.; Calabreses, J.C.; Lam, K-C.; Guzie, I.A.; Rheingold, A.L. *J. Am. Chem. Soc.* **2000**, *122*, 10561.

28. Odom, D.; Gramer, C.J., Young Jr., V.G.; Hilderbrand, S.A.; Sherman, S.E. *Inorg. Chim. Acta* **2000**, *297*, 404.

29. Lindoy, L.F.; "The Chemistry of Macrocyclic Ligand Complexes", Cambridge University Press, Cambridge, **1989**, p 13-20; Atkinson, I.M.; Byriel, K.A.; Chia, P.S.K,; Kennard, C.H.L.; Leong, A.J.; Lindoy, L.F.; Lowe, M.P., Mahendran, S.; Smith, G.; Wei, G. *Aust. J. Chem.* **1998**, *51*, 985; Fenton, R.R.; Lindoy, L.F.; Luckay, R.C.; Turville, F.R.; Wei, G. *Aust. J. Chem.* **2001**, *54*, 59.

30. Melson, G.A. "Coordination Chemistry of Macrocyclic Compounds", Plenum Press, New York, **1979**, p .155-157.

31. Effendy; Fenton, R.R.; Lindoy, L.F.; Price, J.R.; Skelton, B.W.; Strixner, T.; Wei, G.; White, A.H. *J. Incl. Phenom. Macro. Chem.* **2001**, *41*, 185.

32. Bang, H.; Lee, E.L.; Lee, E.Y.; Suh, J.; Suh, M.P. *Inorg. Chim. Acta* **2000**, *308*, 150.

Reproduced with permission of the copyright owner. Further reproduction prohibited without permission.

33. Richman, J.E.; Atkins, T,J. *J. Am. Chem. Soc.* **1974**, *96*, 2268-70; Atkins, T.J.; Richman, J.E.; Oettle, W.F. *Org. Synth.* **1978**, *58*, 86.

34. Lindoy, L.F.; "The Chemistry of Macrocyclic Ligand Complexes", Cambridge University Press, Cambridge, **1989**, p 27.

35. Curtis, N.F. *J. Chem. Soc.* **1960**, 4409.

36. House, D.A.; Curtis, N.F.; *Chem. Ind.* **1961**, 1708.

37. Curtis, N.F.; Curtis, Y.M.; Powel, H.K.J. *J. Chem. Soc., A* **1966**, 1015.

38. Thompson, M.C.; Busch, D.H. *J. Am. Chem. Soc.* **1964**, *86*, 3651.

39. Lehn, J.-M. *Science* **1993**, *260*, 1762.

40. Steed, J.W.; Atwood, J.L.; "Supramolecular Chemistry", John Wiley & Sons, New York, **2000**, p 2.

41. Lehn, J.-M. *Angew. Chem. Int. Ed. Engl.* **1988**, *27*, 90.

42. Lehn, J.-M. *Science* **1985**, *227*, 849.

43. Jones, J.W.; Zakharov, L.N.; Rheingold, A.L.; Gibson, H.W.; *J. Am. Chem. Soc.* **2002**, *124*, 13378.

44. Akutagawa, T.; Hasegawa, T.; Nakamura, T.; Inabe, T. *J. Am. Chem. Soc.* **2002**, *124*, 8903.

45. Wagner, B.D.; Stojanovic, N.; Day, A.I.; Blanch, R.J. *J. Phys. Chem. B* **2003**, *107*, 10741.

46. Harada, A. *Acc. Chem. Res.* **2001**, *34*, 456.

47. Szejtli, J. *Chem. Rev.* **1998**, *98*, 1743.

48. Li, S.; Purdy, W.C. *Chem. Rev.* **1992**, *92,* 1457.

49. Atwood, J.L.; Cavies, J.E.D,; Macnicol, D.D.; Vogtle, F. "Comprehensive Supramolecular Chemistry", Pergamon, New York, **1996**, p 8, 193.

50. Steed, J.W.; Atwood, J.L.; "Supramolecular Chemistry", John Wiley & Sons, New York, **2000**, p 323.

51. Uekama, K.; Hirahama, F.; Irie, T.; *Chem. Rev.* **1998**, *98*, 2045.

Reproduced with permission of the copyright owner. Further reproduction prohibited without permission.

52. Atwood, J.L.; Cavies, J.E.D,; Macnicol, D.D.; Vogtle, F. "Comprehensive Supramolecular Chemistry", Pergamon, New York, **1996**, p 483-499.

53. Hedges, A.R. *Chem. Rev.* **1998**, **98**, 2035.

54. Smith, A.C.; Macarney, D.H.; *J. Org. Chem.* **1998**, *63*, 9243.

55. Schneider, H.-J.; Hacket, F.; Rudiger, V.; Ikeda, H. *Chem. Rev.* **1998**, *98*, 1755.

56. Griffiths, T.R.; Anderson, R.A. *J. Chem .Soc., Faraday Trans.1* **1984**, *80*, 2361.

57. Wagner, B.D.; MacDonald, P.J. *J. Photochem. Photobiol. A; Chem.* **1998**, *114*, 151.

58. Wilkins, R.G. "Kinetics and Mechanism of Reactions of Transition Metal Complexes", VCH Publishers Inc., New York, **1991**, p 165.

59. Connors, A.C.; "Chemical Kinetics", VCH Publishers Inc., New York, **1990**, p 1-2.

60. Jordan, R.B. "Reaction Mechanisms of Inorganic and Organometallic Systems 2nd Edition", Oxford University Press, New York, **1998**, p 15.

61. Taube, H.; Myers, H.; Rich, R.L. *J. Am. Chem. Soc.* **1953**, *75*, 4118; Taube, H.; Myers, H. *J. Am. Chem. Soc.* **1954**, *76*, 2103.

62. Connors, A.C.; "Chemical Kinetics", VCH Publishers Inc., New York, **1990**, p 179.

63. Wilkins, R.G. "Kinetics and Mechanism of Reactions of Transition Metal Complexes", VCH Publishers Inc., New York, **1991**, p 154-70.

64. Marcus, R.A. *Ann. Rev. Phys. Chem.*, **1964**, *15*, 155; Hush, N.S. *Trans. Faraday Soc.* **1961**, *57*, 557; Sutin, N. *Acc. Chem. Res.* **1982**, *15*, 275; Marcus, R.A.; Sutin, N. *Biochim. Biophys. Acta* **1985**, *811*, 265.

65. Jordan, R.B. "Reaction Mechanisms of Inorganic and Organometallic Systems 2nd Edition", Oxford University Press, New York, **1998**, p 200.

66. Wainright, K.P. *Coord. Chem Rev.* **1997**, *167*, 35; Haines, R.I. *Rev. Inorg. Chem.* **2002**, *21*, 165.

67. McAuley, A.; Subramanian, S.; Zaworotko, M.J.; Atencio, R. *Inorg. Chem.* **1998,** 37, 4607; McAuley, A.; Subramanian, S.; Zaworotko, M. J.; Biradha, K.; *Inorg. Chem.* **1999**, *38*, 5078; McAuley, A.; Subramanian, S. *Inorg. Chem.* **1997**, *36*, 5376; Rodopoulos, M.; Rodopoulos, T.; Bridson, J.N.; Elding, L.I.; Rettig, S.J.; McAuley, A. *Inorg. Chem.* **2001** *40*, 2737.

Reproduced with permission of the copyright owner. Further reproduction prohibited without permission.

68. Davis, K.; Haines, R.I. *Unpublished observations*

69. Haines, R.I.; Northcott, S.J. *Can. J. Chem.* **1992**, *70*, 2785.

70. Baer, A.J.; Macartney, D.H. *Inorg. Chem.* **2000**, *39*, 1410.

71. Davis, K.; Haines, R.I.; Tran, P. *Unpublished observations*

72. Suh, M.P.; Kang, S-G. *Inorg. Chem.* **1988**, *27*, 2544.

73. Brodovitch, J.C.; McAuley, A. *Inorg. Chem.* **1981**, *20*, 1667.

74. Wilson, L.D.; Verral, R.E. *Can. J. Chem.* **1998,** *76*, 25.

75. Wylie, S.R.; Macartney, D.H. *Inorg. Chem.* **1993**, *32*, 1830.

76. SADABS v2.02: Area-Detector Absorption Correction. (1996) Siemens Industrial Automation, Inc.: Madison, WI.

77. SHELXTL 6.1, Bruker AXS Inc., Madison, WI 2001

78. Choi, H.J.; Suh, M.P. *Inorg. Chem.* **2003**, *42*, 1151.

79. Curtis, N.F. *Coord. Chem. Rev.* **1968**, *3*, 3.

80. Hay,R.W.; Danby, A.; Lightfoot, P.; Lampeka, Y.D. *Polyhedron* **1997**, *16*, 2777; Suh, M.P.; Choi, J.; Kang, S-G.; Shin, W. *Inorg. Chem.* **1989,** *28*, 1763; Fabbrizzi, L.; Lanfredi, A.M.; Pelavicini, P.; Perotti, A.; Taglietti, A.; Ugozzoli,F. *J. Chem. Soc., Dalton Trans.* **1991**, 3263.

81. Fawcett, T.G.; Rudich, S.M.; Toby, B.H.; Lalancette, R.A.; Potenza, J.A.; Schugar, H.J. *Inorg. Chem.* **1980**, *19*, 940.

82. Lovecchio, F.V.; Gore, E.S.; Busch, D.H. *J. Am. Chem. Soc.* **1974**, *96*, 3109; Buttafaza, A.; Fabbrizzi, L.; Perotti, A.; Poggi, A.; Poli, G.; Seghi, B. *Inorg. Chem.* **1986**, *25*, 1456.

83. Macartney, D.H.; Personal communication.

84. Wilson, L.D.; Verral, R.E.; *J. Phys. Chem. B* **2000**, *104*, 1880.

85. Lampeka, Y.D.; Gavrish, S.P.; Hay, R.W.; Eisenblatter, T.; Lightfoot, P. *J. Chem. Soc., Dalton Trans.* **2000**, 2023. Abba, F.; De Santis, G.; Fabrizzi, L.; Licchelli, M.; Lanfredi, A.M.M.; Pallavicini, P.; Poggi, A. Ugozzoli, F. *Inorg. Chem.* **1994**, *33*, 1366.

86. Scatchard, G. *Ann. N.Y. Acad. Sci.* **1949**, *51*, 660.

Reproduced with permission of the copyright owner. Further reproduction prohibited without permission.

87. Mirzoian, A.; Kaifer, A.E. *Chem. Eur. J.* **1997**, *3*, 1052.

88. Wang, Y.; Menoza, S.; Kaifer, A.E. *Inorg. Chem.* **1998**, *37*, 317.

89. Gonzalez, B.; Casado, C.M.; Alonso, B.; Cuadrado, I.; Moran, M.; Wang, Y.; Kaifer, A.E.; *Chem. Commun.* **1998**, 2569.

90. McAuley, A.; Norman, P.R., Olubuyide, O. *Inorg. Chem.* **1984**, *23*, 1938; McAuley, A.; Xu, C. *Inorg. Chem.* **1988**, *27*, 1204.

91. Fairbank, N.G.; McAuley, A.; Norman, P.R., Olubuyide, O. *Can. J. Chem.* **1985**, *63*, 2983.

92. Haines, R.I.; Hutchings, D.R. *Can. J. Chem.* **2003**, *81*, 186.

93. McAuley, A.; Olubuyide, O.; Spencer, L.; West, P.R. *Inorg. Chem.* **1984**, *23*, 2594; Macartney, D.H.; McAuley, A., Olubuyide, O.A. *Inorg. Chem.* **1985**, *24*, 307.

94. Zhang, X.; Gramlich, G.; Wang, X.; Nau, W.M. *J. Am. Chem. Soc.* **2002**, *124*, 254.

95. Park, J.W.; Song, H.J. *J. Phys. Chem.* **1989**, *93*, 6454.

96. Wilson, L.D.; Verrall, R.E. *J. Phys. Chem. B* **1997**, *101*, 9270.

97. Macartney, D.H.; Waddling, C.A. *Inorg. Chem.* **1994**, *33*, 5912.

98. Wilson, L.D.; Siddall, S.R.; Verrall, R.E. *Can. J. Chem.* **1997**, *75*, 927.

99. Funasaki, N.; Ishikawa. S.; Neya, S. *J. Phys. Chem. B* **2003**, *107*, 10094.

100. Rekharsky, M.V.; Mayhew, M.P.; Goldberg, R.N.; Ross, P.D.; Yamashoji, Y.; Yoshihisa, I. *J. Phys. Chem. B* **1997**, *101*, 87.

101. Lampeka, Y.D.; Gavrish, S.P.; Maloshtan, I.M.; Dalley, N.K.; Lamb, J.D.; Nazarenko, A.Y. *Inorg. Chim. Acta* **1998**, *282*, 142.

102. Fabbrizzi, L. J. *Chem. Soc. Dalton Trans.* **1979**, 1857.

103. Amaral, S.; Turnbull, M.M. *J. Chem. Cryst.* **2002**, *32*, 11.

104. Anichini, A.; Fabbrizzi, L.; Paoletti, P. *Inorg. Chim. Acta* **1977**, L21.

105. Davis, K.; Haines, R.I.; Murnaghan, A.M.; Park, M. *Unpublished observations*

Reproduced with permission of the copyright owner. Further reproduction prohibited without permission.

Appendix A - Tables of Chemicals and Solvents

Chemical Name	Supplier	Purity
α-Cyclodextrin	Aldrich	
β-Cyclodextrin	Aldrich	
1,3-diaminopropane	Sigma	98 %
1,4,8,11-tetraazaaundecane	Strem Chemicals	97 %
1,5,8,12-tetraazadodecane	Strem Chemicals	97 %
2-chloroethyl ether	Fluka	99%
Butylmethyl ketone	Fluka	99%
Formaldehyde	Anachemia	37 %
n-butylamine	Aldrich	99 %
n-dodecylamine	Sigma	99%
n-octylamine	Aldrich	99 %
Nickel(II) Chloride	Anachemia	Reagent Grade
Nickel(II) Perchlorate	Alfa	
Perchloric acid	AnalaR	60 %
Sodium hydroxide	BDH	ACS
Sodium Perchlorate	Fisher	HPLC
Trifluromethanesulphonic acid	Aldrich	98 %

Reproduced with permission of the copyright owner. Further reproduction prohibited without permission.

Solvent Name	Supplier	Purity
Acetone	Fisher	HPLC
Acetonitrile	Caledon	ACS
Deuterium oxide	CDN Isotopes	99.9 %
Dichloromethane	Caledon	ACS
Diethyl ether	Caledon	ACS
Ethanol	Commercial Alcohols INC	
Methanol	BDH	ACS
Tetrahydrofuran	Aldrich	ACS

Reproduced with permission of the copyright owner. Further reproduction prohibited without permission.

Appendix B - Labelled Ball and Stick Diagram for $[NiL_8](ClO_4)$

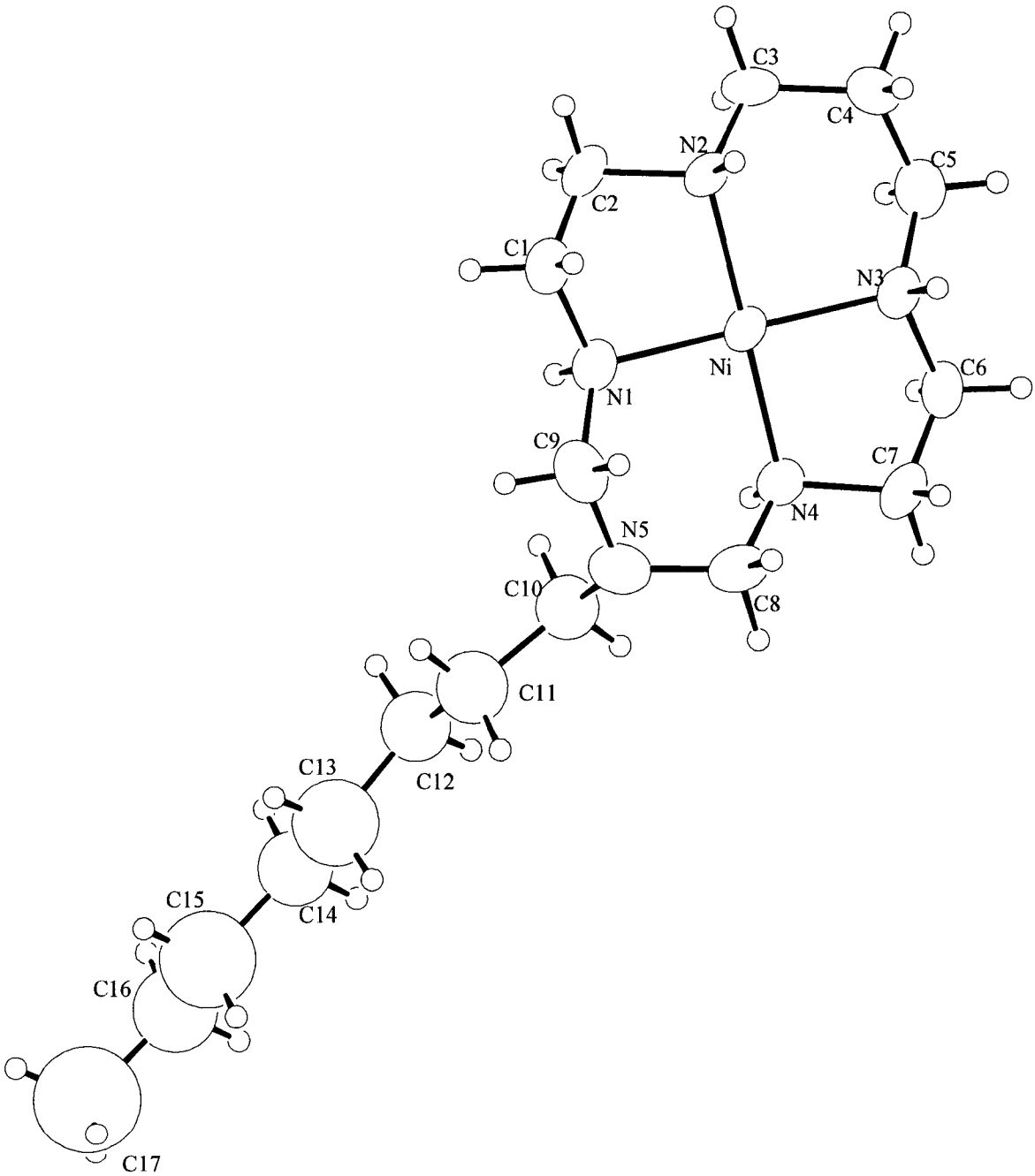

Reproduced with permission of the copyright owner. Further reproduction prohibited without permission.

Appendix C - Law of Mass Balance

$$NiL + CD \overset{K}{\rightleftharpoons} NiL(CD)$$

$$K = \frac{[NiL(CD)]}{[NiL][CD]} \quad (1)$$

so $[NiL(CD)] = K[NiL][CD]$ (2)

and $[NiL_{tot}] = [NiL(CD)] + [NiL]$ (3)

substituting (2) into (3) gives:

$$[NiL_{tot}] = K[NiL][CD] + [NiL] = [NiL](1 + K[CD]) \quad (4)$$

$$\text{so } [NiL] = \frac{[NiL_{tot}]}{1+K[CD]} \quad (5)$$

similarly $$K = \frac{[NiL(CD)]}{[NiL][CD]}$$

$$\text{so } [NiL] = \frac{[NiL(CD)]}{K[CD]} \quad (6)$$

substituting (6) into (3) gives:

$$[NiL_{tot}] = [NiL(CD)] + \frac{[NiL(CD)]}{K[CD]} = [NiL(CD)](1 + (1/K[CD])) \quad (7)$$

$$\text{so } [NiL(CD)] = \frac{K[NiL_{tot}][CD]}{1 + K[CD]} \quad (8)$$

Reproduced with permission of the copyright owner. Further reproduction prohibited without permission.

Appendix D - X-Ray Crystallographic Data

Compound	$[NiL_4](ClO_4)_2$	*trans*-$[Ni(dap)_2(MeCN)_2](ClO_4)_2$
Empirical Formula	$C_{17}H_{39}Cl_2N_5O_8Ni$	$C_{10}H_{26}Cl_2N_6O_8Ni$
Formula Weight	571.13	487.98
Crystal Colour, Habit	orange, plates	purple, blocks
Crystal Dimensions (mm)	0.08 x 0.22 x 0.40	0.4 x 0.1 x 0.1
Crystal System	triclinic	monoclinic
Lattice type	Primitive	
No. of Reflections Used for Unit Cell Determination(2θ range)		2.58 to 28.27°
Omega Scan Peak Width at Half-height		
Lattice Parameters	a = 8.2751(13)Å b = 8.3691(13)Å c = 22.916(5)Å α = 97.078(10)° β = 90.573(13)° γ = 115.494(10)° V = 1418.1(5)Å^3	a = 7.6484(7)Å b = 9.5925(9)Å c = 14.0290(14)Å α = 90° β = 97.572(2)° γ = 90° V = 1020.29(17)Å^3
Space Group	P-1 (#2)	P2(1)/C
Z value	2	2
Density	1.337 g/cm^3	1.588 g/cm^3
F_{000}	604	508
μ(MoKα)	9.17 cm^{-1}	1.261 cm^{-1}

Table D.1 Crystal Data

Reproduced with permission of the copyright owner. Further reproduction prohibited without permission.

Compound	$[NiL_4](ClO_4)_2$	*trans*-$[Ni(dap)_2(MeCN)_2](ClO_4)_2$
Diffractometer	Rigaku AFC8	Bruker - AXS SMART APEX/CCD
Radiation	MoKα (λ = 0.71069Å) graphite monochromated	λ = 0.71073Å
Detector Aperture	70.0 mm x 70.0 mm	
Crystal to Detector Distance	26.09 mm	
Voltage Current		
Temperature	296 (1) K	293(2)K
$2\theta_{max}$	60.7°	
Number of Reflections Measured	Total: 13910	Total: 6327
	Unique 6687 (R_{int} = 0.025)	Unique 2370 (R_{int}=0.0486)
Corrections	Lorentz-polarization Absorption (trans. factor: 0.7434-1.0009) Secondary Extinction (coefficient: 1.75800 x 10^{-2})	

Table D.2 Intensity Measurements

Reproduced with permission of the copyright owner. Further reproduction prohibited without permission.

Compound	$[NiL_4](ClO_4)_2$	*trans*-$[Ni(dap)_2(MeCN)_2](ClO_4)_2$
Structure Solution	Direct Methods(SHELXS86)	
Refinement	Full-matrix lest-squares on F^2	Full-matrix lest-squares on F^2
Function Minimized	$\Sigma w (Fo^2 - Fc^2)^2$	
Least Squares Weights	$w = 1/[\sigma^2(Fo^2) + (0.1000 \cdot P)^2 + 0.000 \cdot P]$	
Anomalous Dispersion	All non-hydrogen atoms	
No. Observations (I.8.00σ(I))	6127	
No. Variables	259	
Reflection/Parameter Ratio	23.66	
Residuals: R1; wR2	0.082; 0.284	0.0407; 0.0892
Goodness of Fit Indicator	2.84	0.999
Max Shift/Error in Final Cycle	0.00	
Maximum Peak in Final Diff. Map	0.95 $e^-/Å^3$	0.726 $e^-/Å^3$
Minimum Peak in Final Diff. Map	-0.94 $e^-/Å^3$	-0.419 $e^-/Å^3$

Table D.3 Structure Solution and Refinement

Reproduced with permission of the copyright owner. Further reproduction prohibited without permission.

Atom	x	y	z	Beq
Ni(1)	0.3871	-0.1606	0.1614	4.310
Cl(1)	0.1651	0.0850	.01001	5.641
Cl(2)	0.6036	0.5886	0.2218	7.051
O(1)	0.2887	0.0298	0.0747	18.963
O(2)	0.1291	0.1907	0.0641	9.512
O(3)	0.2366	0.1850	0.1555	27.118
O(4)	0.0063	-0.0648	0.1067	21.458
O(5)	0.6179	0.4486	0.2454	10.190
O(6)	0.6169	0.5667	0.1608	18.116
O(7)	0.7420	0.7514	0.2472	20.725
O(8)	0.4379	0.5880	0.2336	12.674
N(1)	0.5016	0.0493	0.2216	5.062
N(2)	0.6169	-0.0741	0.1256	4.813
N(3)	0.2709	-0.3730	0.1018	5.142
N(4)	0.1615	-0.2441	0.1985	4.836
N(5)	0.2677	-0.0469	0.2933	6.686
C(1)	0.6991	0.1244	0.2153	6.185
C(2)	0.7204	0.1155	0.1525	5.932
C(3)	0.6130	-0.0927	0.0602	5.462
C(4)	0.5081	-0.2827	0.0327	6.465
C(5)	0.3151	-0.3605	0.0395	6.457
C(6)	0.0801	-0.4470	0.1082	5.789
C(7)	0.0512	-0.4322	0.1723	6.282
C(8)	0.1647	-0.2273	0.2638	6.754
C(9)	0.4563	0.0219	0.2837	6.872
C(10)	0.1761	0.0634	0.2860	8.325
C(11)	0.1923	0.1840	0.3444	13.024

Reproduced with permission of the copyright owner. Further reproduction prohibited without permission.

C(12)	0.0860	0.2932	0.3356	11.136
C(13)	0.0664	0.3889	0.3954	18.241
C(14)	-0.0615	0.4757	0.3850	12.083
C(15)	-0.0829	0.5825	0.4381	33.174
C(16)	-0.2036	0.6621	0.4222	16.541
C(17)	-0.2431	0.7513	0.4764	44.908

Table D.4 Atomic coordinates and B_{iso}/B_{eq} of $[NiL_8](ClO_4)_2$ where $B_{eq} = 8/s\ \pi^2(U_{11}(aa^*)^2 + U_{22}(bb^*)^2 + U_{33}(cc^*)^2 + 2U_{12}(aa^*bb^*)\cos\gamma + 2U_{13}(aa^*cc^*)\cos\beta + 2U_{23}(bb^*cc^*)\cos\alpha)$

Reproduced with permission of the copyright owner. Further reproduction prohibited without permission.

Atom	Atom	Distance	Atom	Atom	Distance
Ni1	N4	1.936(5)	Ni1	N2	1.951(5)
Ni1	N3	1.963(6)	Ni1	N1	1.957(6)
Cl1	O1	1.39(1)	Cl1	O2	1.397(10)
Cl1	O4	1.39(1)	Cl1	O3	1.399(10)
Cl2	O8	1.39(1)	Cl2	O5	1.397(10)
Cl2	O7	1.398(10)	Cl2	O6	1.398(10)
N1	C9	1.495(11)	N1	C1	1.493(10)
N2	C2	1.486(9)	N2	C3	1.486(10)
N3	C6	1.443(9)	N3	C5	1.483(11)
N4	C7	1.480(9)	N4	C8	1.485(11)
N5	C8	1.446(12)	N5	C9	1.442(12)
N5	C10	1.448(3)	C1	C2	1.447(13)
C3	C4	1.495(12)	C4	C5	1.461(13)
C6	C7	1.489(13)	C10	C11	1.541(7)
C11	C12	1.543(8)	C12	C13	1.546(9)
C13	C14	1.551(9)	C14	C15	1.479(12)
C15	C16	1.484(12)	C16	C17	1.481(12)

Table D.5 Bond Lengths(Å) of $[NiL_8](ClO_4)_2$

Reproduced with permission of the copyright owner. Further reproduction prohibited without permission.

Atom	Atom	Atom	Angle	Atom	Atom	Atom	Angle
N4	Ni1	N2	178.8(3)	N4	Ni1	N3	86.8(2)
N2	Ni1	N3	94.2(2)	N4	Ni1	N1	92.7(2)
N2	Ni1	N1	86.3(2)	N3	Ni1	N1	179.3(2)
O1	Cl1	O2	109.77(14)	O1	Cl1	O4	109.53(14)
O2	Cl1	O4	109.69(14)	O1	Cl1	O3	109.32(15)
O2	Cl1	O3	109.24(14)	O4	Cl1	O3	109.26(15)
O8	Cl2	O5	109.61(14)	O8	Cl2	O7	109.54(14)
O5	Cl2	O7	109.49(14)	O8	Cl2	O6	109.43(14)
O5	Cl2	O6	109.41(14)	O7	Cl2	O6	109.35(15)
C9	N1	C1	112.1(7)	C9	N1	Ni1	116.5(5)
C1	N1	Ni1	107.2(4)	C2	N2	C3	111.2(6)
C2	N2	Ni1	106.2(4)	C3	N2	Ni1	117.5(4)
C6	N3	C5	112.5(7)	C6	N3	Ni1	107.7(4)
C5	N3	Ni1	119.5(5)	C7	N4	C8	110.1(6)
C7	N4	Ni1	107.6(4)	C8	N4	Ni1	118.8(5)
C8	N5	C9	112.9(6)	C8	N5	C10	110.9(7)
C9	N5	C10	118.9(8)	C2	C1	N1	105.8(7)
C1	C2	N2	107.5(6)	N2	C3	C4	111.7(6)
C5	C4	C3	116.0(6)	C4	C5	N3	112.8(7)
N3	C6	C7	108.2(7)	N4	C7	C6	107.5(6)
N5	C8	N4	114.0(6)	N5	C9	N1	115.1(7)
N5	C10	C11	109.9(5)	C10	C11	C12	108.5(4)
C11	C12	C13	110.7(7)	C12	C13	C14	108.4(4)
C15	C14	C13	114.2(8)	C14	C15	C16	109.0(5)
C15	C16	C17	109.3(5)				

Table D.6 Bond angles(°) of $[NiL_8](ClO_4)_2$

Reproduced with permission of the copyright owner. Further reproduction prohibited without permission.

Atom	x	y	z	U(eq)
Ni	0	5000	0	17(1)
Cl	7715(1)	9164(1)	1685(1)	23(1)
N(1)	1429(2)	3269(2)	605(1)	23(1)
N(2)	1369(3)	6333(2)	1029(1)	22(1)
N(3)	-1827(3)	4688(2)	983(1)	22(1)
O(1)	6490(2)	9482(2)	2350(1)	33(1)
O(2)	7077(3)	9700(2)	753(1)	43(1)
O(3)	9383(3)	9787(2)	2023(2)	53(1)
O(4)	7902(3)	7687(2)	1631(1)	47(1)
C(1)	2159(3)	2350(2)	977(2)	21(1)
C(2)	3108(3)	1182(2)	1458(2)	27(1)
C(3)	-2960(3)	3434(3)	938(2)	32(1)
C(4)	-3786(3)	3113(3)	-79(2)	33(1)
C(5)	2562(3)	7435(2)	736(2)	28(1)

Table D.7 Atomic coordinates (x 10^4) and equivalent isotropic displacement parameters (A^2 x 10^3) for *trans*-$[Ni(MeCN)_2(dap)_2](ClO_4)_2$. U(eq) is defined as one third of the trace of the orthogonalized Uij tensor

Reproduced with permission of the copyright owner. Further reproduction prohibited without permission.

Atoms	Distance	Atoms	Distance
Ni-N(2)	2.1017(17)	Cl-O(1)	1.4389(16)
Ni-N(2)#1	2.1017(17)	N(1)-C(1)	1.134(3)
Ni-N(1)	2.1042(17)	N(2)-C(5)	1.471(3)
Ni-N(1)#1	2.1042(17)	N(3)-C(3)	1.479(3)
Ni-N(3)#1	2.1098(19)	C(1)-C(2)	1.452(3)
Ni-N(3)	2.1098(19)	C(3)-C(4)	1.513(3)
Cl-O(4)	1.4265(17)	C(4)-C(5)#1	1.513(3)
Cl-O(3)	1.4304(17)	C(5)-C(4)#1	1.513(3)
Cl-O(2)	1.4320(19)		

Table D.8 Bond Lengths(Å) of *trans*-$[Ni(dap)_2(MeCN)_2](ClO_4)_2$

Atoms	Angle	Atoms	Angle
N(2)-Ni-N(2)#1	180.0	N(3)#1-Ni-N(3)	180.0
N(2)-Ni-N(1)	91.01(7)	O(4)-Cl-O(2)	109.45(11)
N(2)#1-Ni-N(1)	88.99(7)	O(4)-Cl-O(3)	109.92(13)
N(2)-Ni-N(1)#1	88.99(7)	O(2)-Cl-O(3)	109.53(12)
N(2)#1-Ni-N(1)#1	91.01(7)	O(4)-Cl-O(1)	108.89(11)
N(1)-Ni-N(1)#1	180.0	O(2)-Cl-O(1)	110.08(11)
N(2)-Ni-N(3)#1	92.85(7)	O(3)-Cl-O(1)	108.96(11)
N(2)#1-Ni-N(3)#1	87.15(7)	C(1)-N(1)-Ni	176.19(18)
N(1)-Ni-N(3)#1	91.28(7)	C(5)-N(2)-Ni	120.57(14)
N(1)#1-Ni-N(3)#1	88.72(7)	C(3)-N(3)-Ni	121.44(15)
N(2)-Ni-N(3)	87.15(7)	N(1)-C(1)-C(2)	179.4(2)
N(2)#1-Ni-N(3)	92.85(7)	N(3)-C(3)-C(4)	112.0(2)
N(1)-Ni-N(3)	88.72(7)	C(5)#1-C(4)-C(3)	115.1(2)
N(1)#1-Ni-N(3)	91.28(7)	N(2)-C(5)-C(4)#1	112.04(19)

Table C.9 Bond angles(°) of *trans*-$[Ni(dap)_2(MeCN)_2](ClO_4)_2$

Reproduced with permission of the copyright owner. Further reproduction prohibited without permission.